Practical Deployment and Evolution of Intelligent Metasurfaces

Jiancheng An (安建成)

School of Electrical and Electronics Engineering
Nanyang Technological University, Singapore

2025.05.28

Outline

- Background
- Codebook Solution for RIS-Aided Wireless Systems
- SIM-Enabled Electromagnetic Domain Signal Processing
- FIM-Enhanced Wireless Communication and Sensing
- Future Directions

Outline

- **Background**
- Codebook Solution for RIS-Aided Wireless Systems
- SIM-Enabled Electromagnetic Domain Signal Processing
- FIM-Enhanced Wireless Communication and Sensing
- Future Directions

➢ Background – Intelligent Metasurfaces

Programmable Metasurface

Cui *et al.*, LSA, 2014

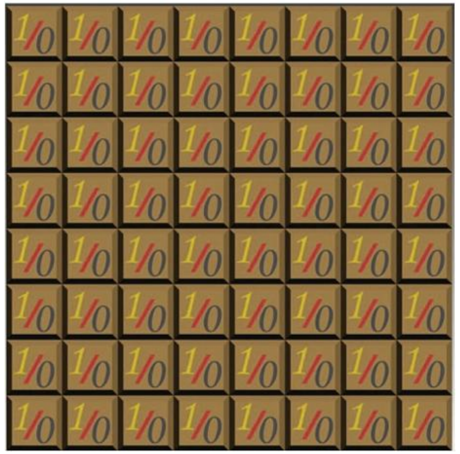

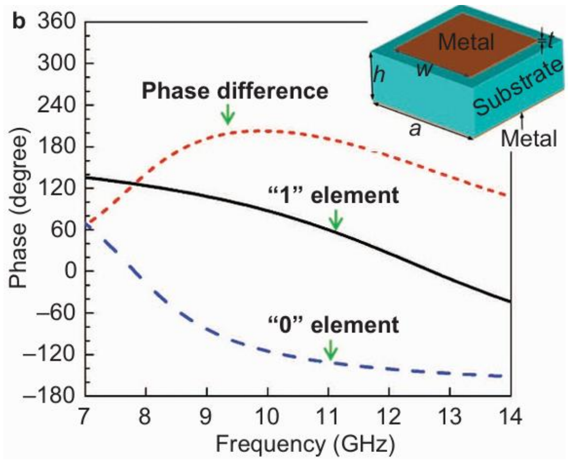

Transparent Metasurface

DOCOMO, 2020

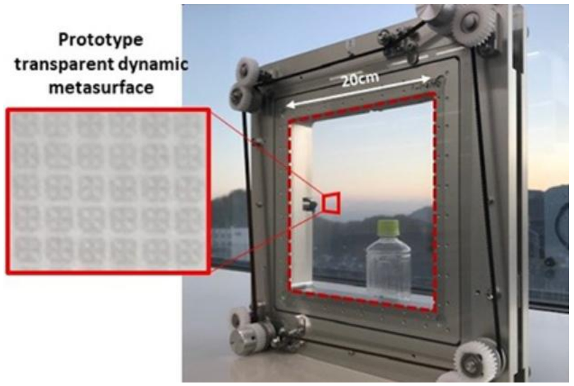

Waveguide-Fed Metasurface

D. R. Smith *et al.*, PRA, 2017

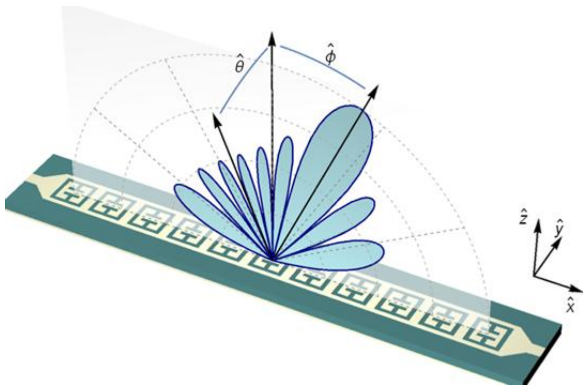

Q1: How to Deploy RIS in Practical Wireless Systems?

➢ Background – Evolution of MIMO

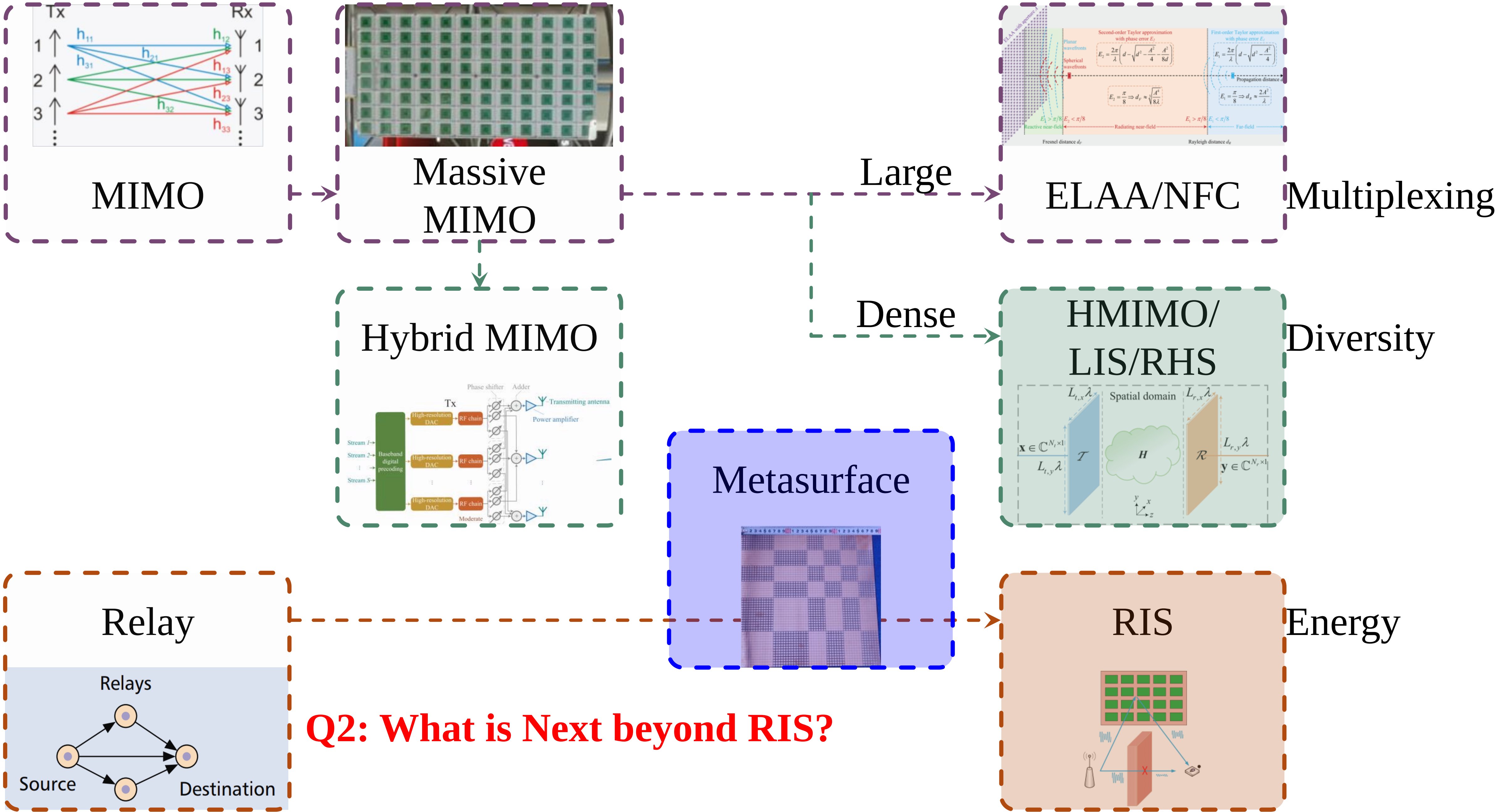

➢ Background – Rigid vs Flexible

Wall

Billboard

Outer Window

Car Window

Curtain

Clothing

Schoolbag

Balloon

Q3: Is It Possible to Deploy RIS on Flexible Objects?

Outline

- Background
- **Codebook Solution for RIS-Aided Wireless Systems (Q1)**
  - § Why Adopt the Codebook Solution
  - § Performance Analysis
  - § Effective Codebook Design
- SIM-Enabled Electromagnetic Domain Signal Processing
- FIM-Enhanced Wireless Communication and Sensing
- Future Directions

Q1: How to Deploy RIS in Practical Wireless Systems?

Outline

- Background
- Codebook Solution for RIS-Aided Wireless Systems (Q1)
  - **Why Adopt the Codebook Solution**
  - Performance Analysis
  - Effective Codebook Design
- SIM-Enabled Electromagnetic Domain Signal Processing
- FIM-Enhanced Wireless Communication and Sensing
- Future Directions

➢ Why Adopt the Codebook Solution

Channel

Estimation

+

Joint

Optimization

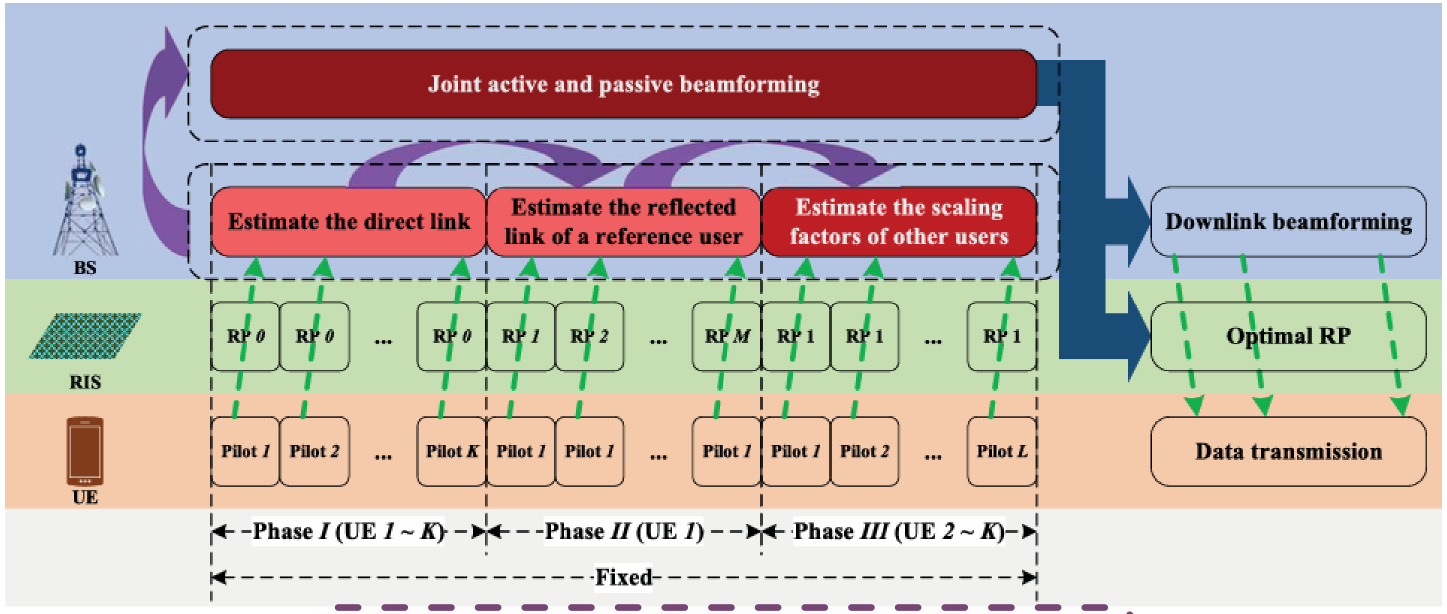

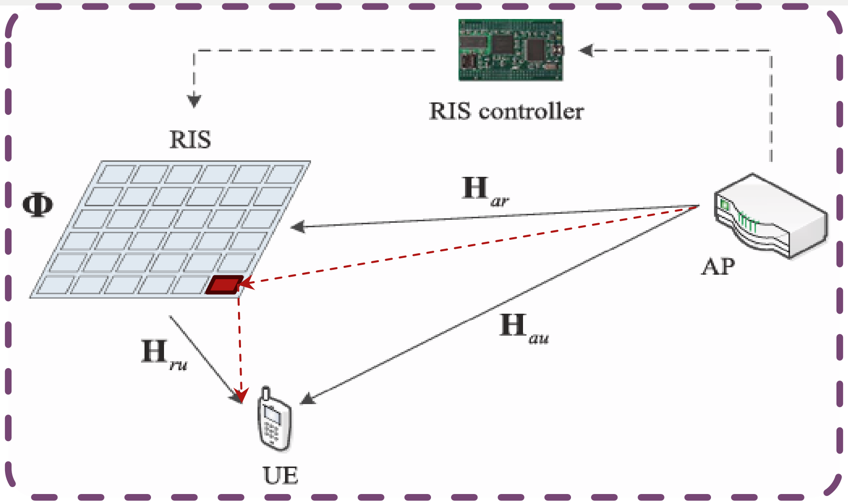

J. An, C. Xu, Q. Wu, D. W. K. Ng, M. Di Renzo, C. Yuen, and L. Hanzo, "Codebook-Based Solutions for Reconfigurable Intelligent Surfaces and Their Open Challenges," *IEEE Wireless Commun.*, vol. 31, no. 2, pp. 134-141, April 2024. (**Highly Cited Paper**)

➢ Why Adopt the Codebook Solution

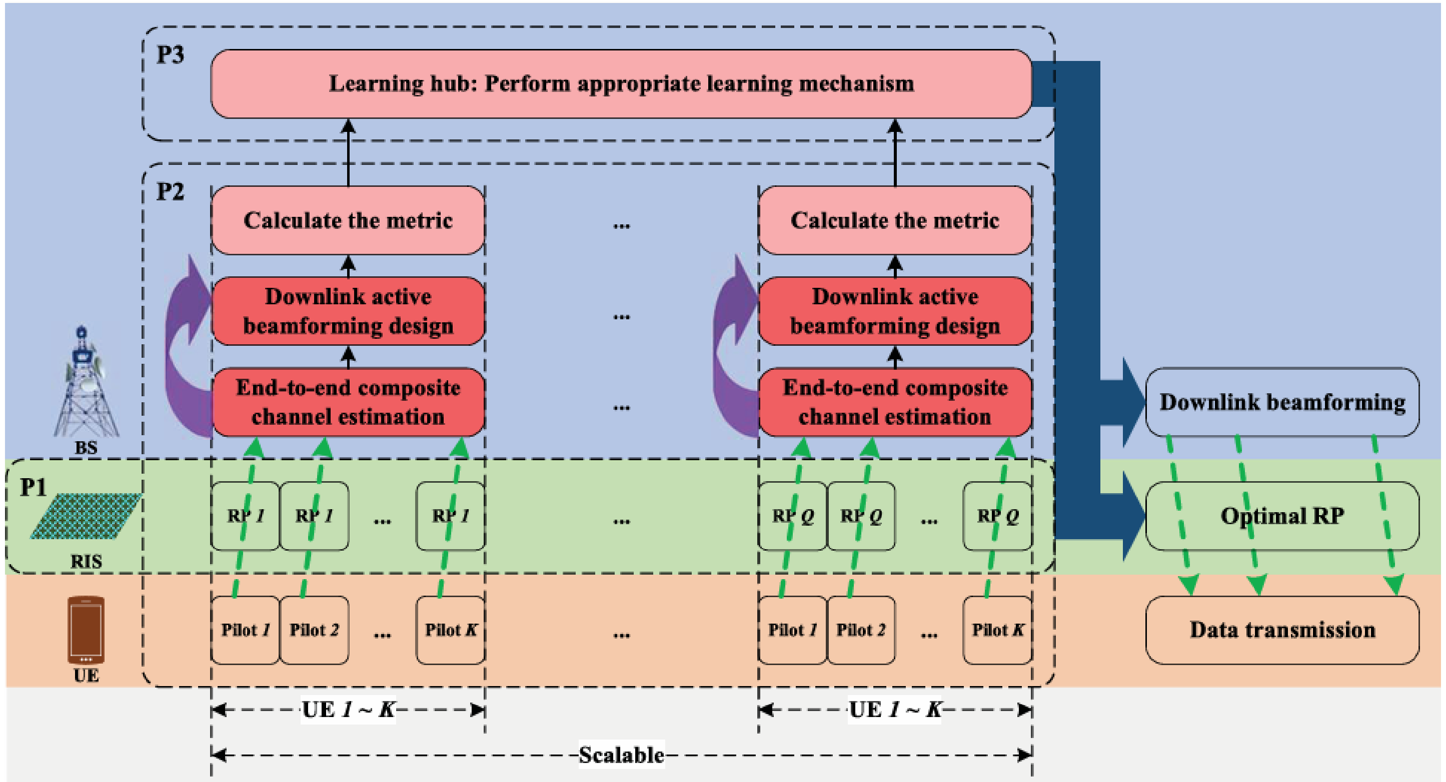

- Backward Compatibility
- Reduced Error Propagation
- Scalable Pilot Overhead
- Reduced Control Signaling
- Reduced Computational Complexity
- Stronger Robustness

J. An, C. Xu, Q. Wu, D. W. K. Ng, M. Di Renzo, C. Yuen, and L. Hanzo, "Codebook-Based Solutions for Reconfigurable Intelligent Surfaces and Their Open Challenges," *IEEE Wireless Commun.*, vol. 31, no. 2, pp. 134-141, April 2024. (**Highly Cited Paper**)

Outline

- Background
- Codebook Solution for RIS-Aided Wireless Systems (Q1)
  - § Why Adopt the Codebook Solution
  - **§ Performance Analysis**
  - § Effective Codebook Design
- SIM-Enabled Electromagnetic Domain Signal Processing
- FIM-Enhanced Wireless Communication and Sensing
- Future Directions

➢ Performance Analysis – Power vs Overhead

Received power — Pilot overhead

$$P_r \to P_{DL}\rho_{ar}^2\rho_{ru}^2 M\left(\log Q + C\right)$$

Number of elements

❖ Case I

$Q = 1$ → $P_r = M P_{DL}\rho_{ar}^2\rho_{ru}^2$

❖ Case II

$Q_{\max} = B^M$ → $P_r \to M^2 P_{DL}\rho_{ar}^2\rho_{ru}^2 \log B$ → **Number of phase shifts**

Received Power vs Overhead

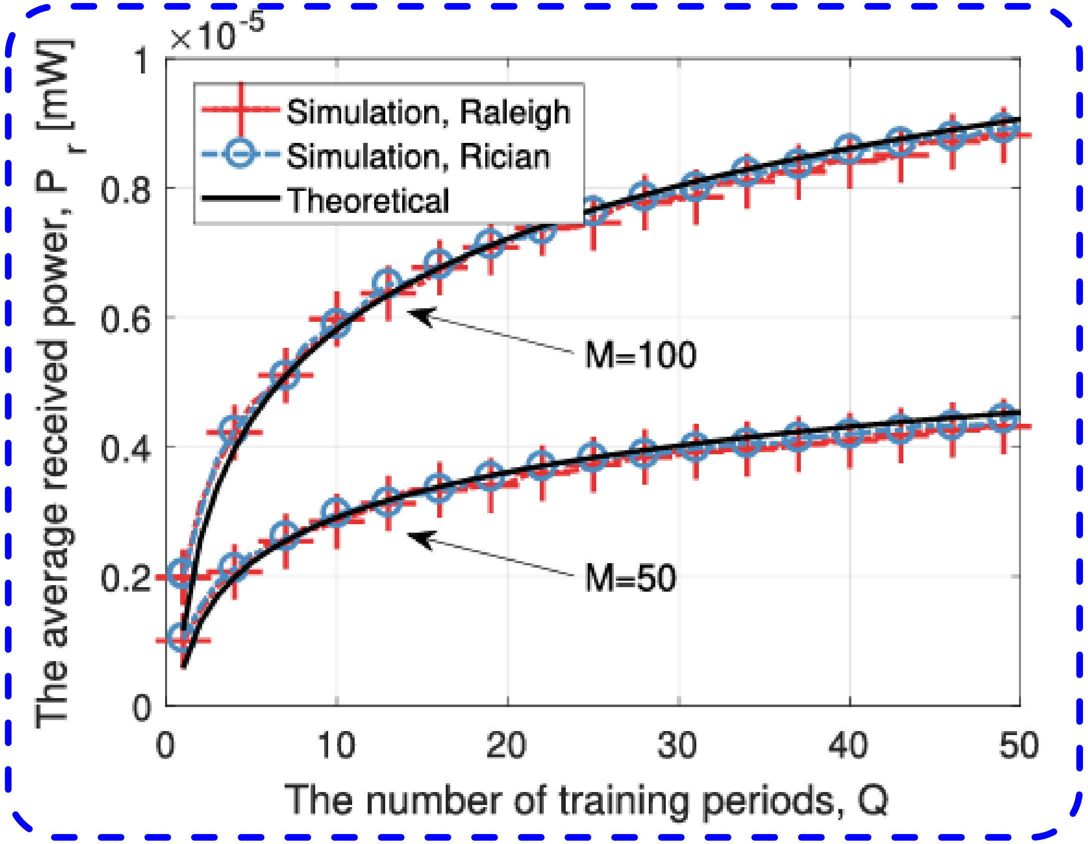

J. An, et al., "Low-complexity channel estimation and passive beamforming for RIS-assisted MIMO systems relying on discrete phase shifts," *IEEE Trans. Commun.*, vol. 70, no. 2, pp. 1245-1260, Feb. 2022. (**Highly Cited Paper**)

➢ Performance Analysis – Effect of Channel Estimation Errors

❖ Perfect CSI

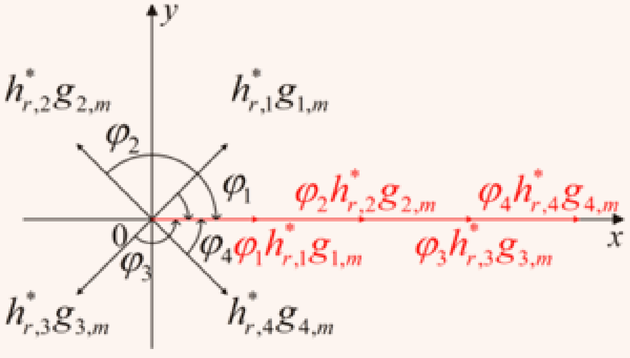

❖ Perfect CSI

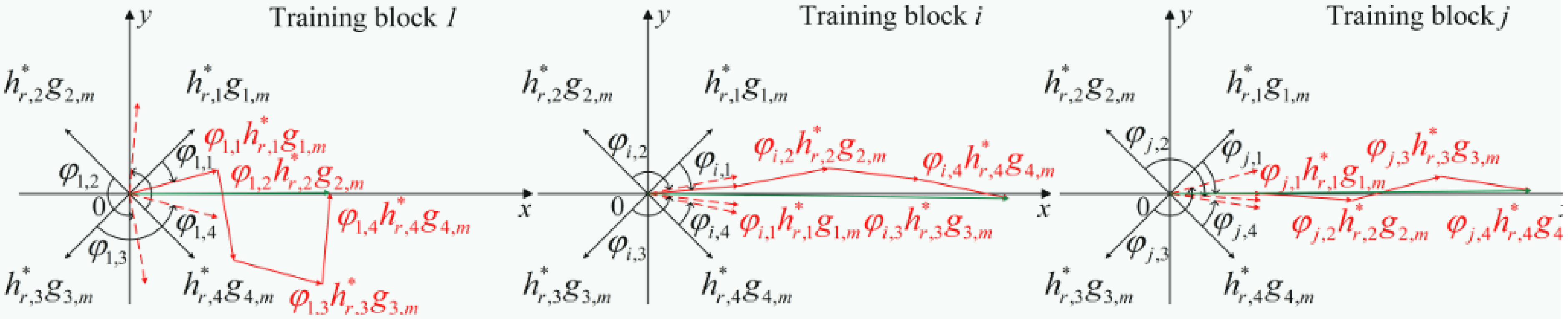

❖ Imperfect CSI

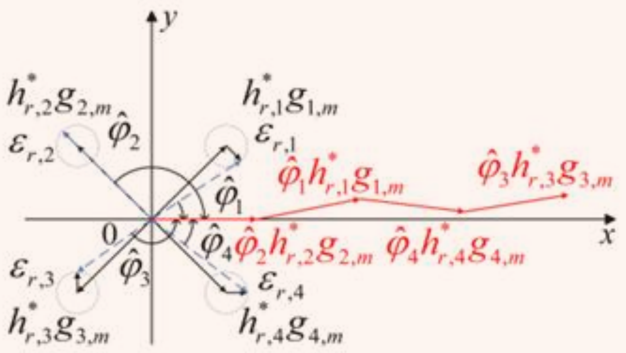

❖ Imperfect CSI

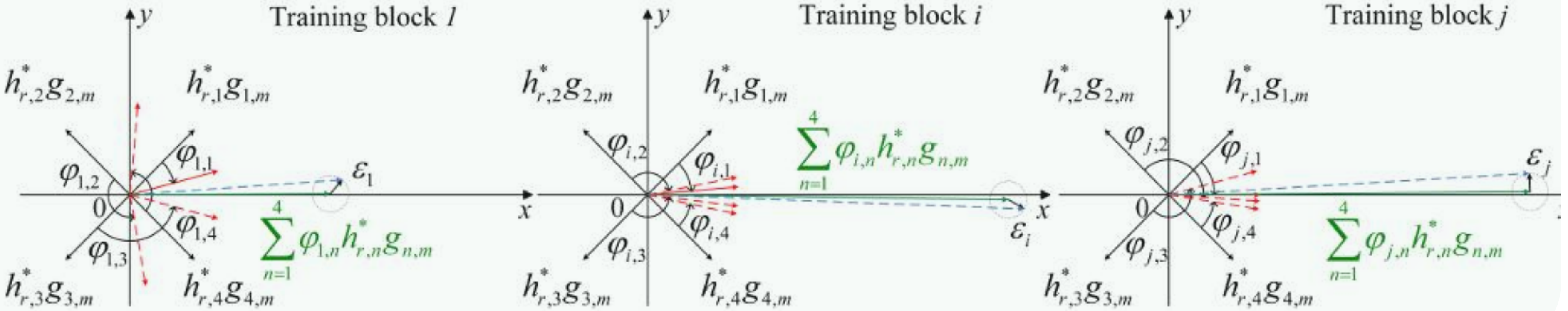

Conventional

Codebook Solution

Z. Yu, J. An, E. Basar, L. Gan and C. Yuen, "Environment-Aware Codebook Design for RIS-Assisted MU-MISO Communications: Implementation and Performance Analysis," *IEEE Trans. Commun.*, vol. 72, no. 12, pp. 7466-7479, Dec. 2024.

➢ Performance Analysis

Rate vs Overhead

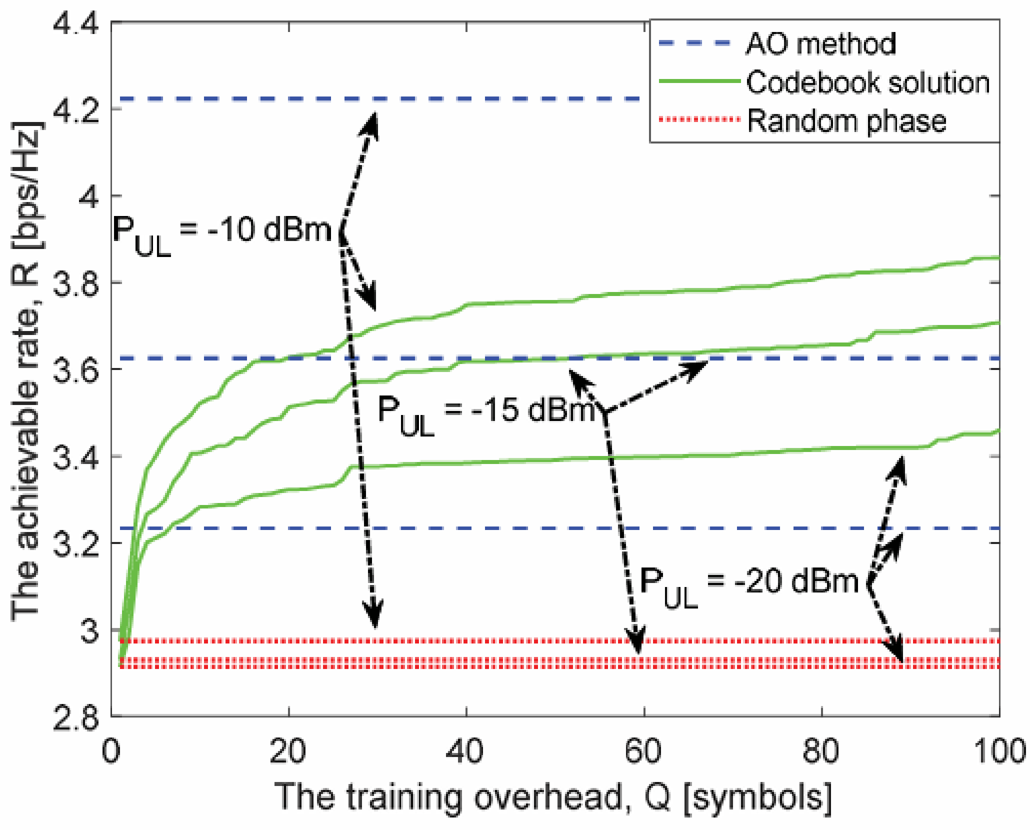

Effective Rate vs Coherence Time

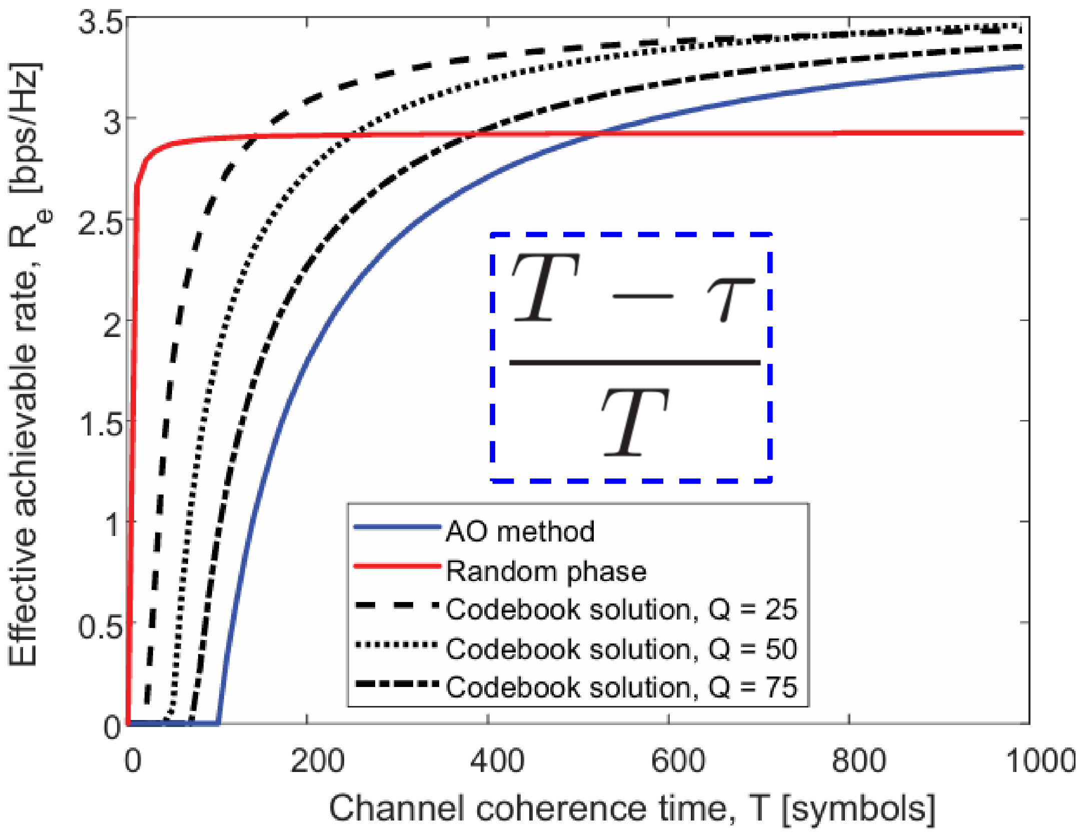

J. An, C. Xu, Q. Wu, D. W. K. Ng, M. Di Renzo, C. Yuen, and L. Hanzo, "Codebook-Based Solutions for Reconfigurable Intelligent Surfaces and Their Open Challenges," *IEEE Wireless Commun.*, vol. 31, no. 2, pp. 134-141, April 2024. (**Highly Cited Paper**)

Outline

- Background
- Codebook Solution for RIS-Aided Wireless Systems (Q1)
  - § Why Adopt the Codebook Solution
  - § Performance Analysis
  - **§ Effective Codebook Design**
- SIM-Enabled Electromagnetic Domain Signal Processing
- FIM-Enhanced Wireless Communication and Sensing
- Future Directions

➢ Effective Codebook Design – Environment-Aware Codebook

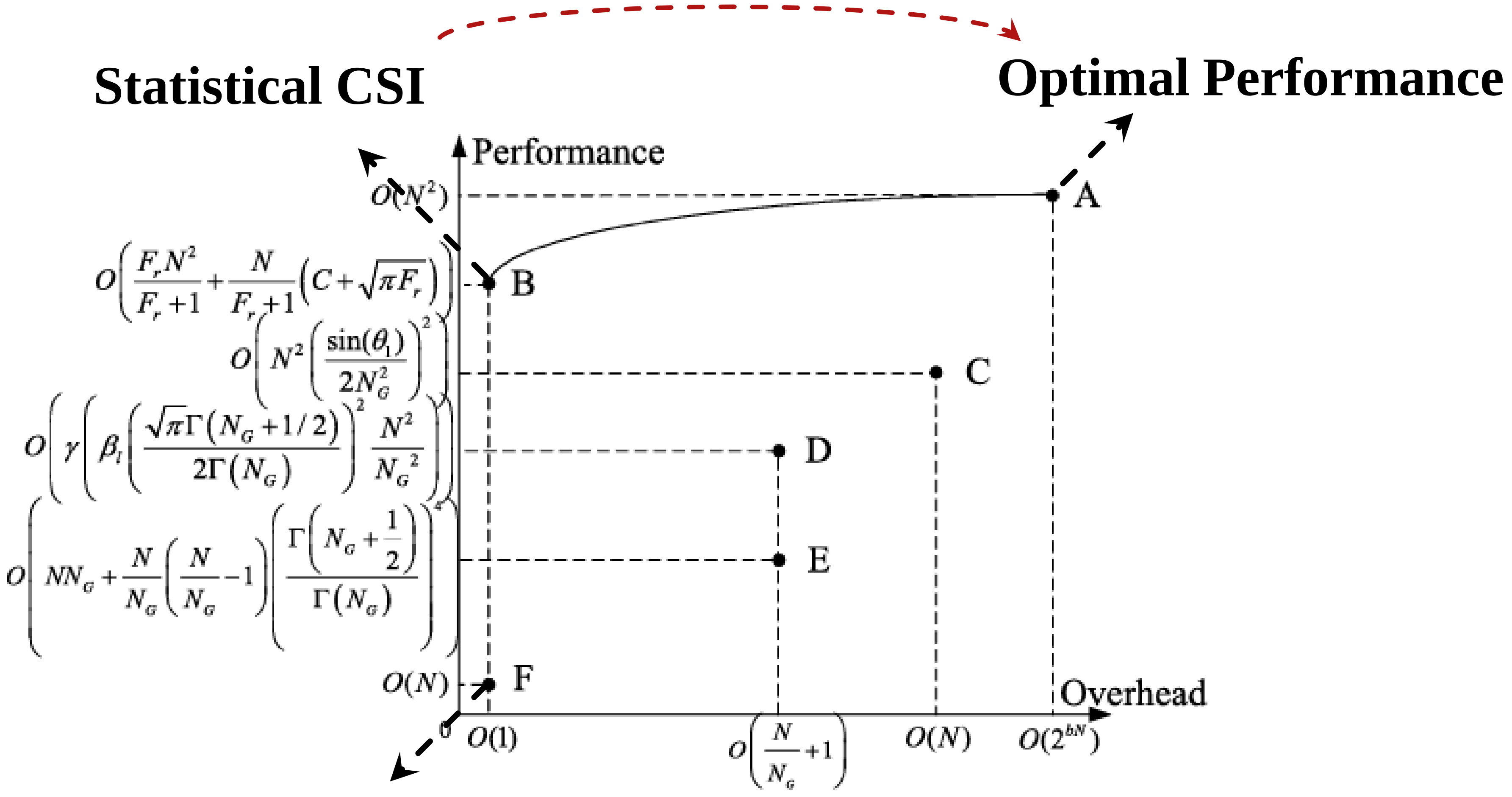

Z. Yu, J. An, E. Basar, L. Gan and C. Yuen, "Environment-Aware Codebook Design for RIS-Assisted MU-MISO Communications: Implementation and Performance Analysis," *IEEE Trans. Commun.*, vol. 72, no. 12, pp. 7466-7479, Dec. 2024.

➢ Effective Codebook Design – Weighted Codebook

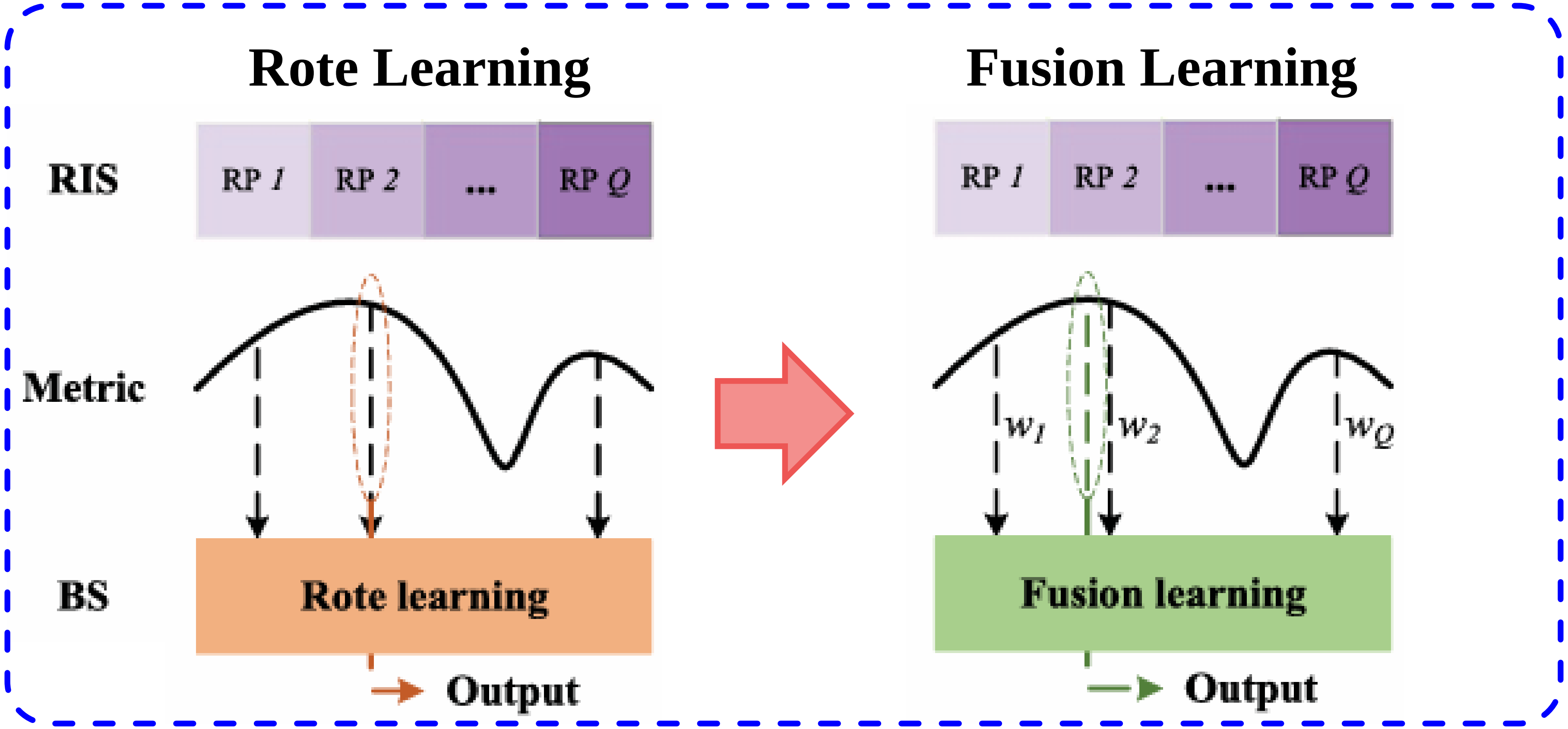

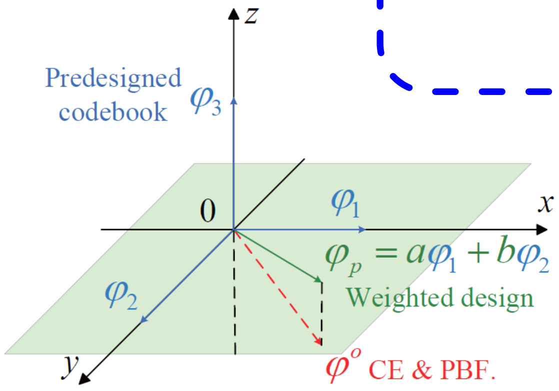

Scheme	Reference	Overhead	Complexity	RIS RC solution
CE & PBF	[7], [8], [16]	$N+1$	High	$\boldsymbol{\varphi} \in \mathbb{C}^N$
PC	[1], [9]–[14]	Q	Low	$\boldsymbol{\varphi} \in \{\boldsymbol{\varphi}_1, \boldsymbol{\varphi}_2, \cdots, \boldsymbol{\varphi}_Q\}$
Proposed	✓	Q	Moderate	$\boldsymbol{\varphi} \in \text{span}\{\boldsymbol{\varphi}_1, \cdots, \boldsymbol{\varphi}_Q\}$

Z. Yu, J. An, L. Gan, H. Li and S. Chatzinotas, “Weighted Codebook Scheme for RIS-Assisted Point-to-Point MIMO Communications,” *IEEE Wireless Commun. Lett.*, vol. 14, no. 5, pp. 1571-1575, May 2025.

Outline

- ➢ Background
- ➢ Codebook Solution for RIS-Aided Wireless Systems
- ➢ **SIM-Enabled Electromagnetic Domain Signal Processing (Q2)**
  - § MIMO Precoding
  - § DOA Estimation
  - § Semantic Encoding
- ➢ FIM-Enhanced Wireless Communication and Sensing
- ➢ Future Directions

Q2: What is Next beyond RIS?

➢ What is Stacked Intelligent Metasurface (SIM)

Stacked Intelligent Metasurface (SIM)

- ➢ **Physical entity**: Have the capability of reconfiguring the EM behavior.
- ➢ **Capability**: Achieve artificial intelligence via a physical neural network.
- ➢ **Architecture**: Multi-layer structure to mimic a neural network in the wave domain.

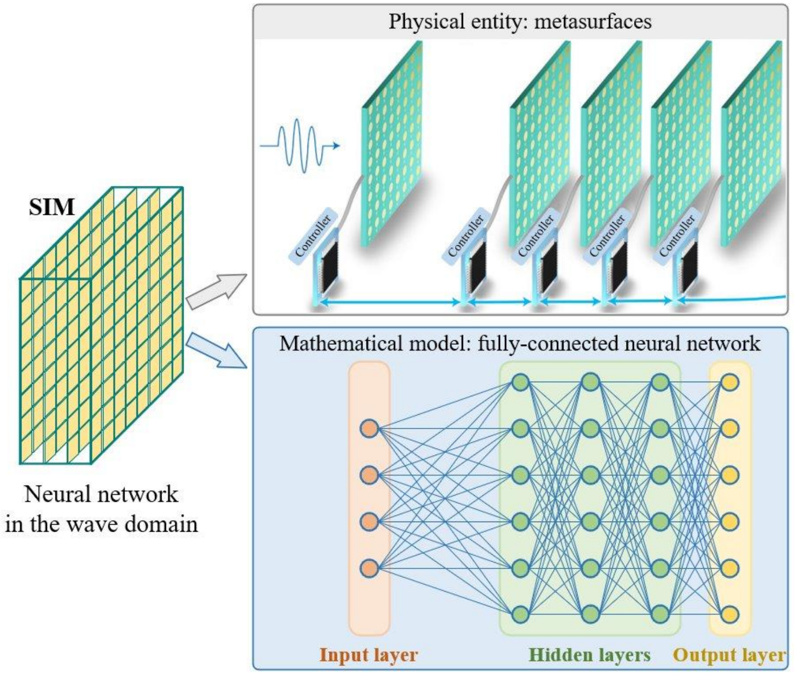

- □ **Function**: Carry out various signal processing and computing tasks in the wave domain.

➢ Hardware Foundation – SIM Prototype

	H-S	H-P	H-A
Feature	**Static**	**Programmable & Passive**	**Programmable & Active**
Prototype	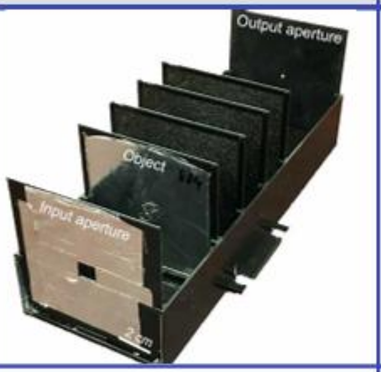		
Authors	J. Li et al. [3]	Z. Wang et al. [4]	C. Liu et al. [5]
Operating frequency	206~300 GHz	5.8 GHz	5.4 GHz
Function	Image classification	Dual-functional beamforming	Multi-beam focusing
# of meta-atoms per layer	$40\times 40 = 1600$	$16\times 16 = 256$	$8\times 8 = 64$
# of layers	3	2	5
Quantization bits	4 bits	1 bit	9 bits
Layer spacing	0.03 m	0.15 m	0.1 m
Material	VeroBlackPlus RGD875	Copper	F4B, prepreg

Outline

- Background
- Codebook Solution for RIS-Aided Wireless Systems
- SIM-Enabled Electromagnetic Domain Signal Processing (Q2)
  - § **MIMO Precoding**
  - § DOA Estimation
  - § Semantic Encoding
- FIM-Enhanced Wireless Communication and Sensing
- Future Directions

➢ A Comparison of Conventional MIMO and SIM-aided MIMO

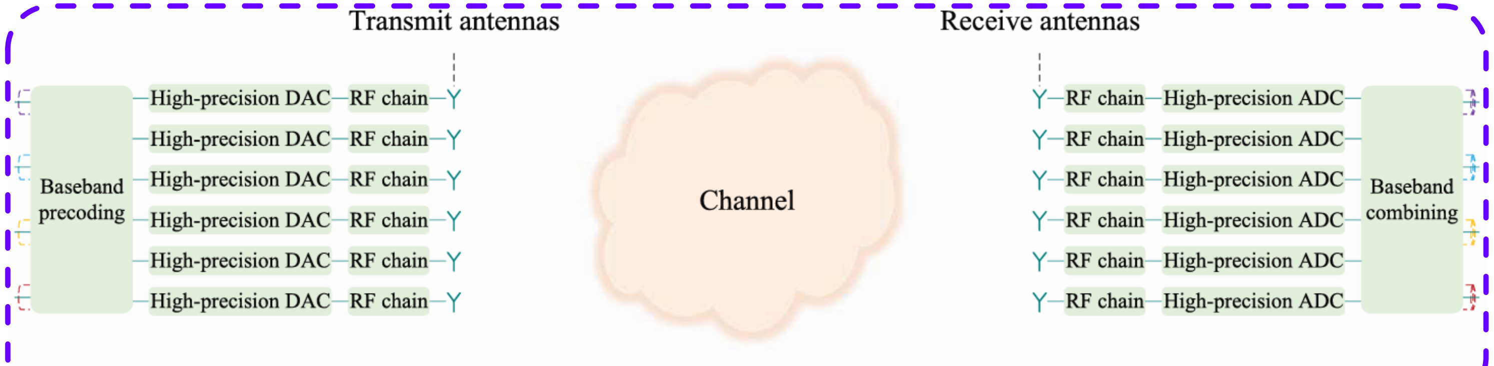

(a) Conventional MIMO transmission: Parallel subchannels in the eigenspace.

- ❑ Number of active RF chains: **Large**
- ❑ Precision of DACs/ADCs: **High**
- ❑ Energy consumption: **High**

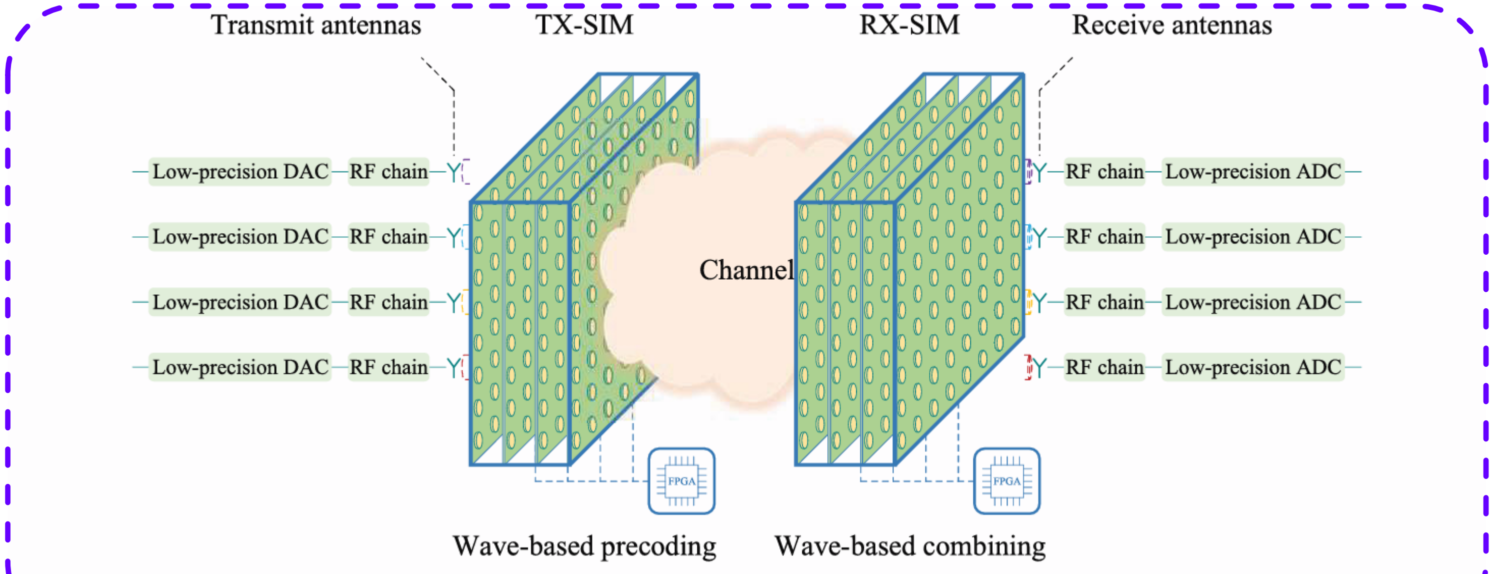

(b) SIM-aided HMIMO transmission: Parallel subchannels in the physical space.

- ❑ Number of active RF chains: **Small**
- ❑ Precision of DACs/ADCs: **Low**
- ❑ Energy consumption: **Low**

J. An et al., "**Stacked intelligent metasurfaces** for efficient holographic MIMO communications in 6G," IEEE J. Sel. Areas Commun., vol. 41, no. 8, pp. 2380–2396, Aug. 2023. (**Highly Cited Paper**)

➢ SIM-aided HMIMO System Model

- ❑ $\mathbf{\Phi}^l$: Transmission coefficient matrix of the l-th transmit layer;
- ❑ $\mathbf{\Psi}^k$: Transmission coefficient matrix of the k-th receive layer;
- ❑ $\mathbf{W}^l$: Propagation coefficient matrix from the (l - 1)-st transmit layer to the l-th transmit layer;
- ❑ $\mathbf{U}^k$: Propagation coefficient matrix from the k-th receive layer to the (k - 1)-st receive layer.

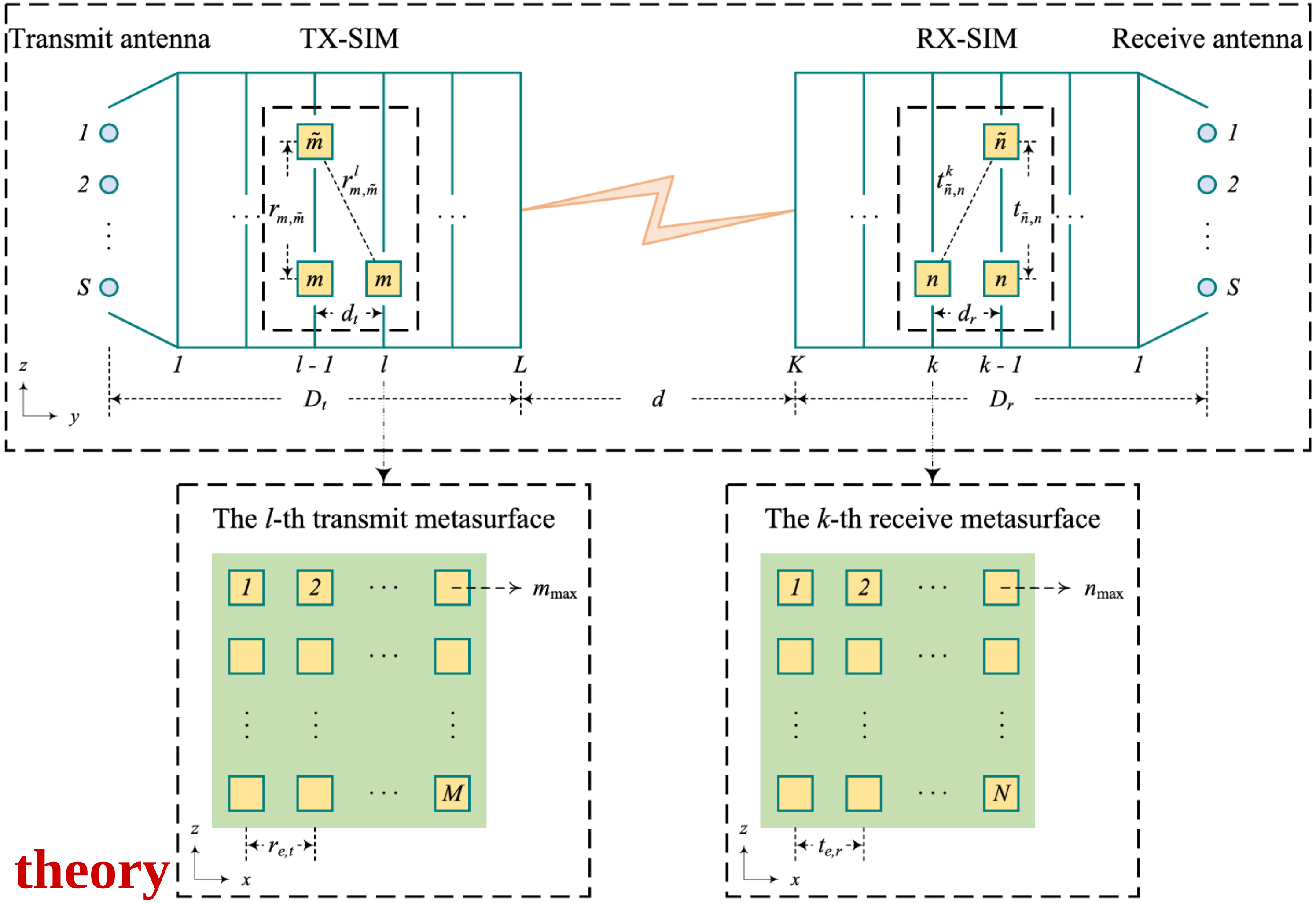

○ **Rayleigh-Sommerfeld diffraction theory**

J. An et al., "**Stacked intelligent metasurfaces** for efficient holographic MIMO communications in 6G," IEEE J. Sel. Areas Commun., vol. 41, no. 8, pp. 2380–2396, Aug. 2023. (**Highly Cited Paper**)

➢ SIM-aided HMIMO System Model

- The EM response of the TX-SIM is

$$\mathbf{P} = \mathbf{\Phi}^L \mathbf{W}^L \cdots \mathbf{\Phi}^2 \mathbf{W}^2 \mathbf{\Phi}^1 \mathbf{W}^1 \in \mathbb{C}^{M \times S}.$$

- The EM response of the RX-SIM is

$$\mathbf{Q} = \mathbf{U}^1 \mathbf{\Psi}^1 \mathbf{U}^2 \mathbf{\Psi}^2 \cdots \mathbf{U}^K \mathbf{\Psi}^K \in \mathbb{C}^{S \times N}.$$

- The spatially-correlated HMIMO channel is

$$\mathbf{G} = \mathbf{R}_{\mathrm{Rx}}^{1/2} \tilde{\mathbf{G}} \mathbf{R}_{\mathrm{Tx}}^{1/2} \in \mathbb{C}^{N \times M}$$

Spatial correlation matrix at the RX-SIM

Spatial correlation matrix at the TX-SIM

i.i.d. Rayleigh fading channel

J. An et al., "**Stacked intelligent metasurfaces** for efficient holographic MIMO communications in 6G," IEEE J. Sel. Areas Commun., vol. 41, no. 8, pp. 2380–2396, Aug. 2023. (**Highly Cited Paper**)

➢ Problem Formulation

- Utilize two SIMs to perform the MIMO precoding and combining in the wave domain. The optimization problem is formulated as

$$\underset{\phi_m^l,\,\psi_n^k,\,\alpha}{\text{minimize}}\ \Gamma = \left\| \alpha \mathbf{QGP} - \boldsymbol{\Lambda}_{1:S,1:S} \right\|_F^2$$

The singular values of $\mathbf{G}$

$$\begin{aligned}
\text{subject to}\ \mathbf{P} &= \boldsymbol{\Phi}^L \mathbf{W}^L \cdots \boldsymbol{\Phi}^2 \mathbf{W}^2 \boldsymbol{\Phi}^1 \mathbf{W}^1, \\
\mathbf{Q} &= \mathbf{U}^1 \boldsymbol{\Psi}^1 \mathbf{U}^2 \boldsymbol{\Psi}^2 \cdots \mathbf{U}^K \boldsymbol{\Psi}^K, \\
\boldsymbol{\Phi}^l &= \text{diag}\left(\left[\phi_1^l, \phi_2^l, \cdots, \phi_M^l\right]^T\right),\ l \in \mathcal{L}, \\
\boldsymbol{\Psi}^k &= \text{diag}\left(\left[\psi_1^k, \psi_2^k, \cdots, \psi_N^k\right]^T\right),\ k \in \mathcal{K}, \\
\left|\phi_m^l\right| &= 1,\ m \in \mathcal{M},\ l \in \mathcal{L}, \\
\left|\psi_n^k\right| &= 1,\ n \in \mathcal{N},\ k \in \mathcal{K}, \\
\alpha &\in \mathbb{C},
\end{aligned}$$

scaling factor

➢ Challenges

- The non-convex constant modulus constraint on each transmission coefficient;
- The highly coupled variables in the objective function

J. An et al., "**Stacked intelligent metasurfaces** for efficient holographic MIMO communications in 6G," IEEE J. Sel. Areas Commun., vol. 41, no. 8, pp. 2380–2396, Aug. 2023. (**Highly Cited Paper**)

➢ The Proposed Gradient Descent Algorithm

Step 1: Calculate the partial derivatives

$$\frac{\partial \Gamma}{\partial \theta_m^l} = 2\sum_{s=1}^{S}\sum_{\tilde{s}=1}^{S} \Im\left[\left(\alpha \phi_m^l x_{m,s,\tilde{s}}^l\right)^* \left(\alpha h_{s,\tilde{s}} - \lambda_{s,\tilde{s}}\right)\right],$$

$$\frac{\partial \Gamma}{\partial \xi_n^k} = 2\sum_{s=1}^{S}\sum_{\tilde{s}=1}^{S} \Im\left[\left(\alpha \psi_n^k y_{n,s,\tilde{s}}^k\right)^* \left(\alpha h_{s,\tilde{s}} - \lambda_{s,\tilde{s}}\right)\right],$$

Step 2: Normalize the partial derivatives

$$\frac{\partial \Gamma}{\partial \theta_m^l} \leftarrow \frac{\pi}{\varrho_l} \cdot \frac{\partial \Gamma}{\partial \theta_m^l}, \quad m \in \mathcal{M},\ l \in \mathcal{L},$$

$$\frac{\partial \Gamma}{\partial \xi_n^k} \leftarrow \frac{\pi}{\varepsilon_k} \cdot \frac{\partial \Gamma}{\partial \xi_n^k}, \quad n \in \mathcal{N},\ k \in \mathcal{K},$$

Step 3: Update the phase shifts

$$\theta_m^l \leftarrow \theta_m^l - \eta \frac{\partial \Gamma}{\partial \theta_m^l}, \quad m \in \mathcal{M},\ l \in \mathcal{L},$$

$$\xi_n^k \leftarrow \xi_n^k - \eta \frac{\partial \Gamma}{\partial \xi_n^k}, \quad n \in \mathcal{N},\ k \in \mathcal{K},$$

Step 4: Update the scaling factor and the learning rate

$$\alpha = \left(\mathbf{h}^H \mathbf{h}\right)^{-1} \mathbf{h}^H \boldsymbol{\lambda},$$

$$\eta \leftarrow \eta \beta,$$

J. An et al., "**Stacked intelligent metasurfaces** for efficient holographic MIMO communications in 6G," IEEE J. Sel. Areas Commun., vol. 41, no. 8, pp. 2380–2396, Aug. 2023. (**Highly Cited Paper**)

➢ Simulation Setups

- The thicknesses of both the TX-SIM and RX-SIM are **0.05 m**.
- The SIM-aided HMIMO system operates at **28 GHz**.
- The propagation distance is **250 m**, with path loss exponent of **3.5**.
- The total power available at the transmitter is **20 dBm**.
- The average noise power is **−110 dBm**.

➢ Performance Metrics

- The **NMSE** between the actual channel matrix and the target diagonal one is

$$\Delta = \mathbb{E}\left(\frac{\left\|\alpha\mathbf{QGP}-\mathbf{\Lambda}_{1:S,1:S}\right\|_{\mathrm{F}}^{2}}{\left\|\mathbf{\Lambda}_{1:S,1:S}\right\|_{\mathrm{F}}^{2}}\right)$$

- The **channel capacity** of the SIM-assisted HMIMO system is

$$C = \sum_{s=1}^{S}\log_2\left(1+\frac{p_s\left|\alpha h_{s,s}\right|^2}{\sum_{\tilde{s}\neq s}^{S} p_{\tilde{s}}\left|\alpha h_{s,\tilde{s}}\right|^2+\sigma^2}\right)$$

J. An et al., "**Stacked intelligent metasurfaces** for efficient holographic MIMO communications in 6G," IEEE J. Sel. Areas Commun., vol. 41, no. 8, pp. 2380–2396, Aug. 2023. (**Highly Cited Paper**)

➢ Performance versus the Number of Metasurface Layers

○ 4 data streams, 100 elements per layer, half-wavelength element spacing

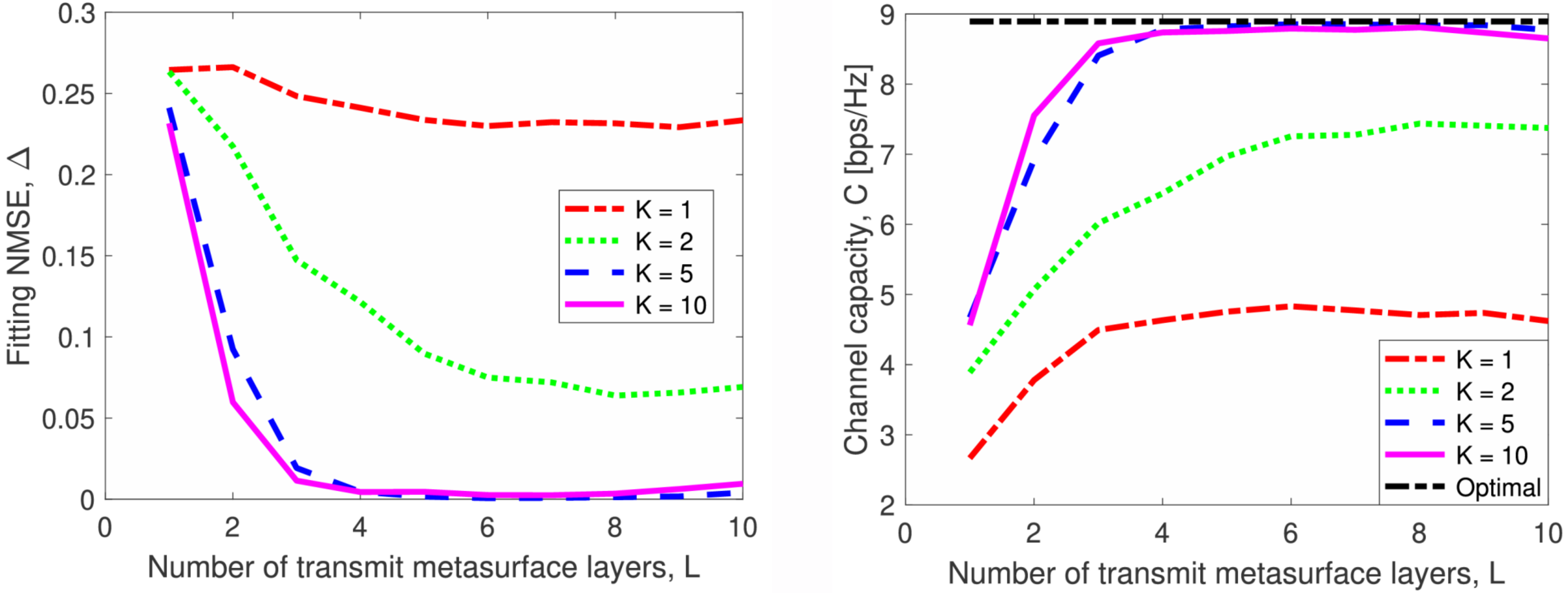

- ❑ Channel fitting NMSE and channel capacity approach their optimal values when using $L = 7$ metasurface layers.
- ❑ Further increasing the number of metasurface layers fail to improve the performance.

J. An et al., "**Stacked intelligent metasurfaces** for efficient holographic MIMO communications in 6G," IEEE J. Sel. Areas Commun., vol. 41, no. 8, pp. 2380–2396, Aug. 2023. (**Highly Cited Paper**)

➢ Performance versus the Number of Meta-atoms per Layer

○ 4 data streams, 7 metasurface layers, half-wavelength element spacing

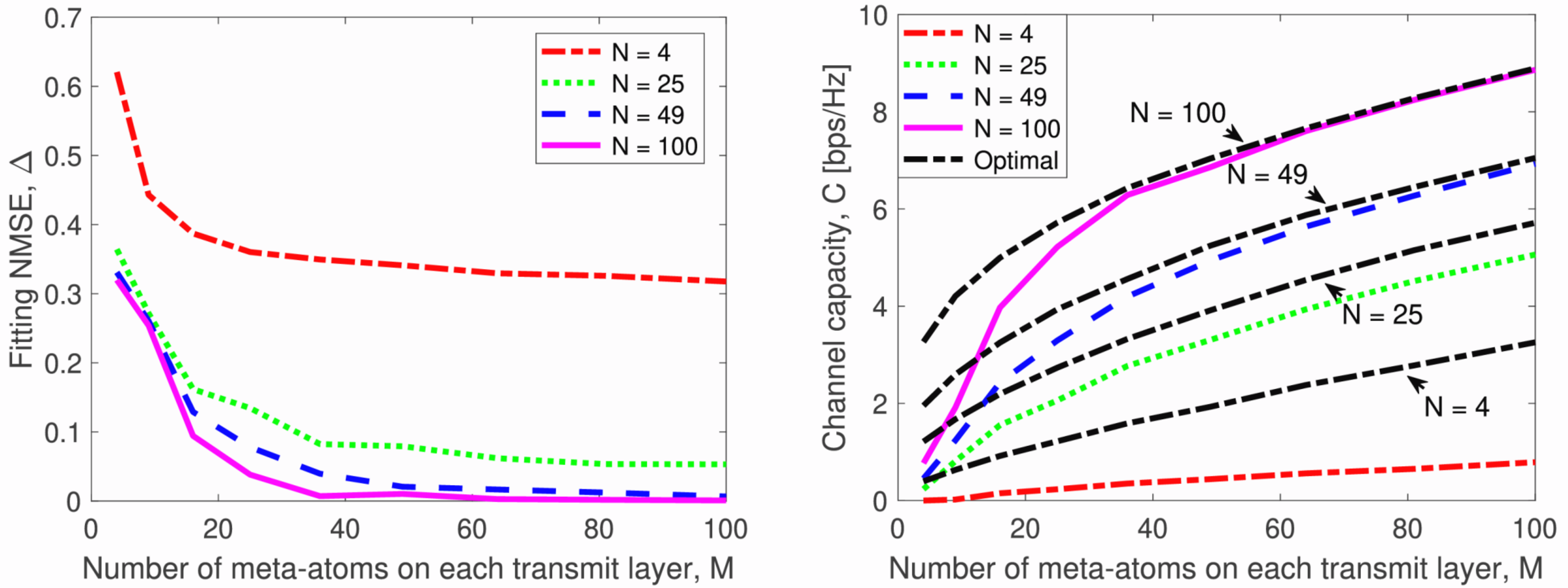

❑ The fitting NMSE decreases monotonically as the number of meta-atoms per layer increases.

❑ The channel capacity is improved as the number of meta-atoms increases, albeit the number of data streams is fixed. **(Selection gain)**

J. An et al., "**Stacked intelligent metasurfaces** for efficient holographic MIMO communications in 6G," IEEE J. Sel. Areas Commun., vol. 41, no. 8, pp. 2380–2396, Aug. 2023. (**Highly Cited Paper**)

➢ Performance versus the Number of Data Streams

○ **100 meta-atoms per layer, 7 metasurface layers, half-wavelength element spacing**

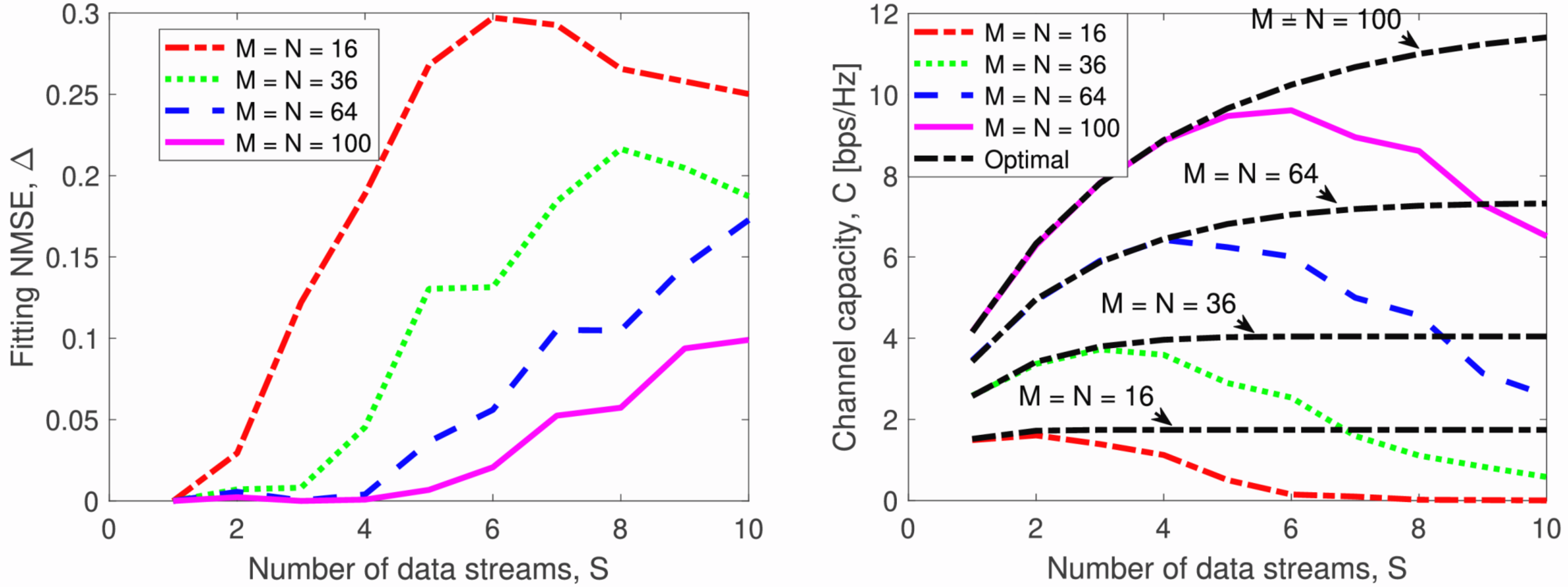

❑ The increasing number of data streams offers a proportional multiplexing gain. **(Tradeoff)**

❑ It is more challenging to acquire a low channel fitting NMSE for a growing number of data streams. Hence, channel capacity achieves its maximum for a certain number of data streams.

J. An et al., "**Stacked intelligent metasurfaces** for efficient holographic MIMO communications in 6G," IEEE J. Sel. Areas Commun., vol. 41, no. 8, pp. 2380–2396, Aug. 2023. (**Highly Cited Paper**)

➢ The visualization of the end-to-end spatial channel matrix

○ 4 data streams, 100 elements per layer, half-wavelength element spacing

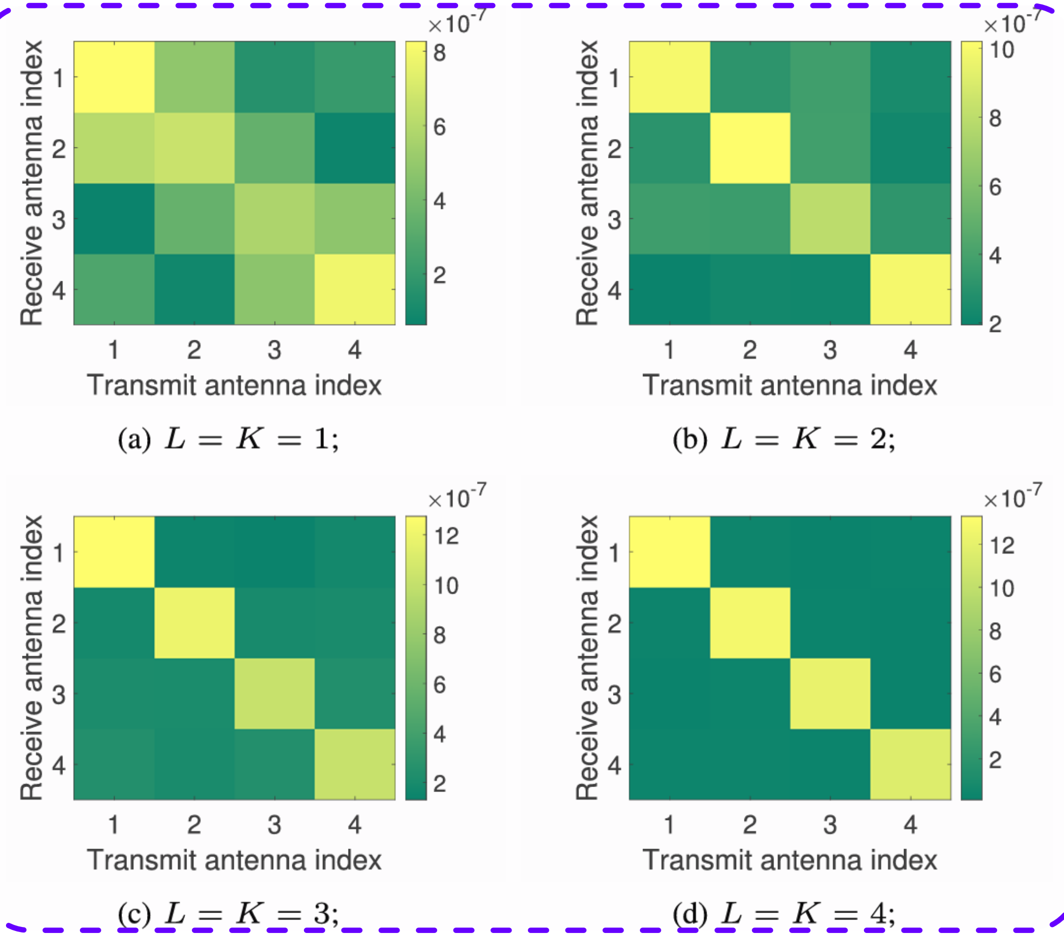

- ❑ For a small number of metasurface layers, the TX-SIM and RX-SIM struggle to form a diagonal end-to-end channel matrix.
- ❑ As the number of metasurface layers increases, the TX-SIM and RX-SIM attain a stronger inference capability.
- ❑ The TX-SIM and RX-SIM having **four metasurface layers** respectively succeed in forming an almost perfectly diagonal channel matrix.

J. An et al., "**Stacked intelligent metasurfaces** for efficient holographic MIMO communications in 6G," IEEE J. Sel. Areas Commun., vol. 41, no. 8, pp. 2380–2396, Aug. 2023. (**Highly Cited Paper**)

➢ Conclusions

- ❑ We proposed a SIM-aided HMIMO communication paradigm, which attains substantial spatial gains while **performing the precoding and combining directly in the native EM regime at the speed of light**.
- ❑ A **7-layer SIM having half-wavelength element spacing** achieved an excellent channel fitting performance and approached the maximum channel capacity.
- ❑ Both our theoretical analysis and simulation results have shown the **quadratic channel gain when doubling the number of meta-atoms**.
- ❑ A **150% capacity gain** was attained over its conventional massive MIMO and RIS-assisted counterparts.

J. An et al., "**Stacked intelligent metasurfaces** for efficient holographic MIMO communications in 6G," IEEE J. Sel. Areas Commun., vol. 41, no. 8, pp. 2380–2396, Aug. 2023. (**Highly Cited Paper**)

➢ SIM-aided Multiuser MISO System Model

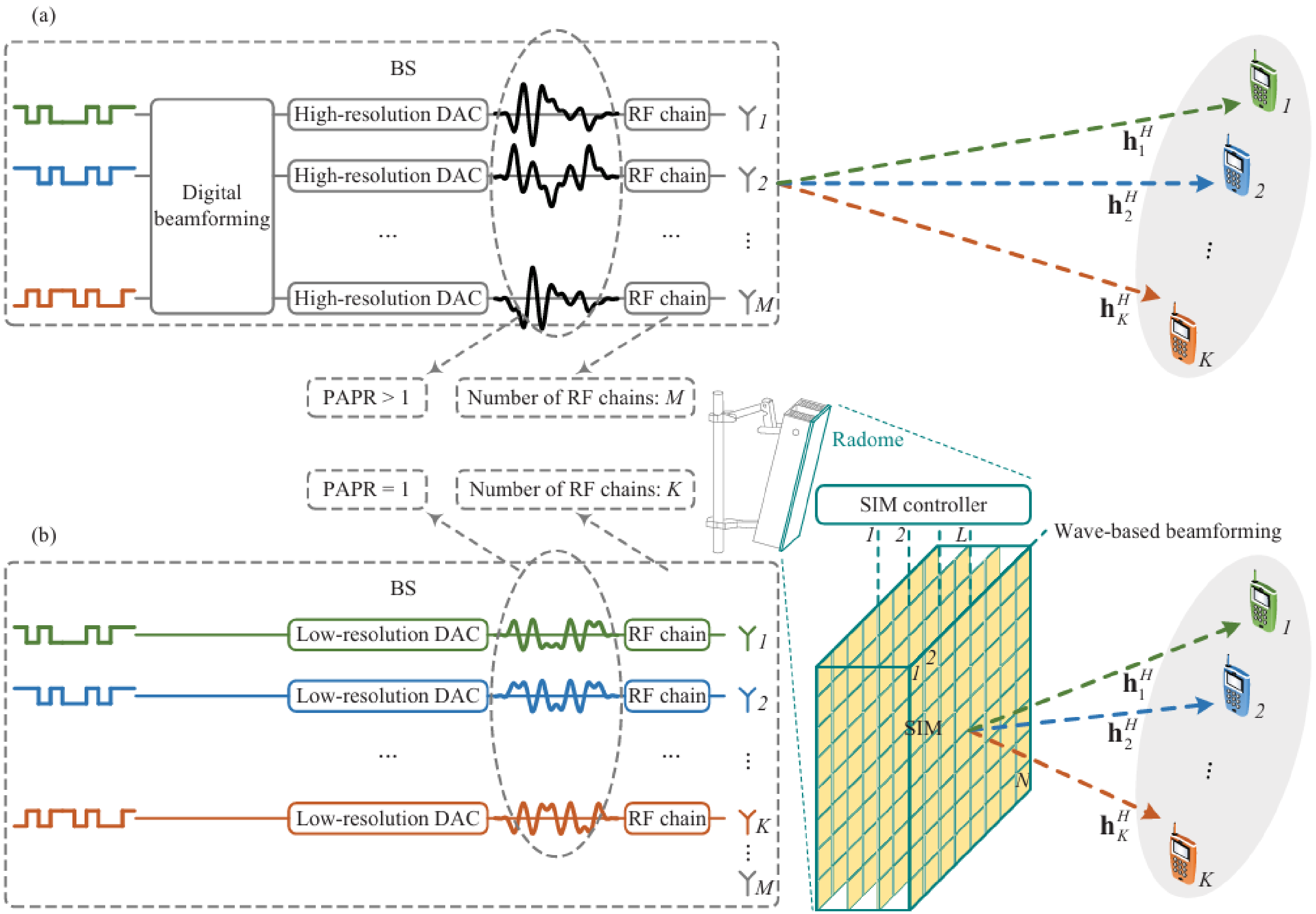

J. An, M. Di Renzo, M. Debbah, and C. Yuen, "**Stacked intelligent metasurfaces** for multiuser beamforming in the wave domain," Proc. IEEE Int. Conf. Commun. (ICC), Rome, Italy, May 2023, pp. 2834 – 2839. **(ICC 2023 Best Paper Award)**

J. An, M. Di Renzo, M. Debbah, H. V. Poor, and C. Yuen. "**Stacked intelligent metasurfaces** for multiuser downlink beamforming in the wave domain," *IEEE Trans. Wireless. Commun.*, 2025, Early Access.

➢ SIM-aided Multiuser MISO System Model

- L: The number of metasurface layers
- N: The number of meta-atoms on each layer
- K: The number of single-antenna users
- M: The number of antennas at the BS

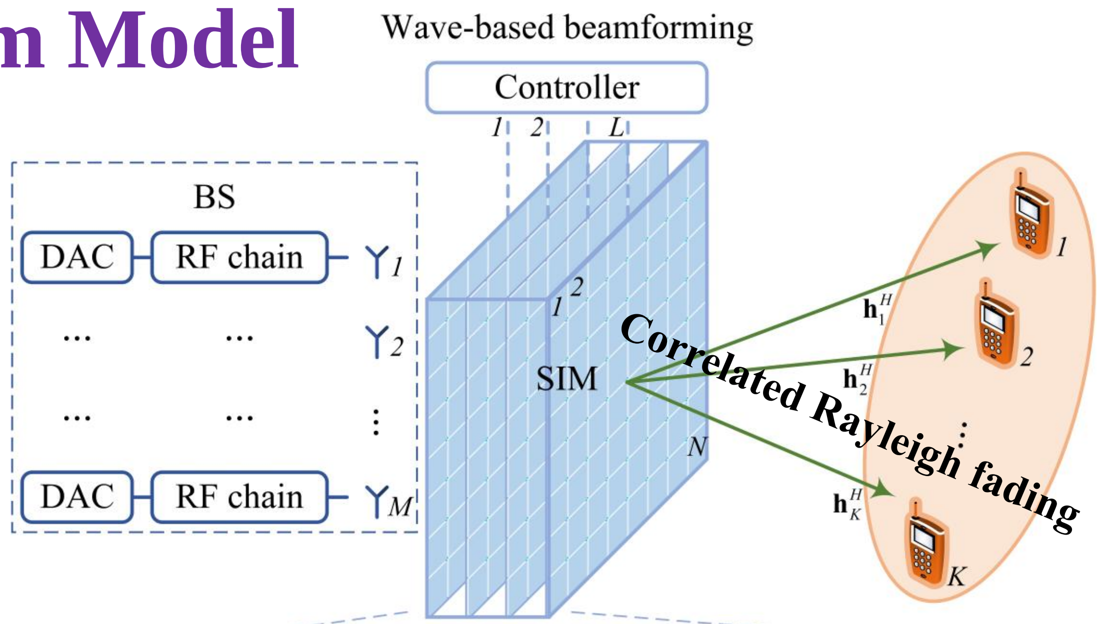

➢ Objective & Challenge

➢ Use SIM to mitigate multiuser interference in the EM wave domain.

❖ The optimization of SIM involves configuring a large number of phase shift values!

❑ The BS first selects K antennas for transmitting K independent data streams. **(M = K in this paper)**

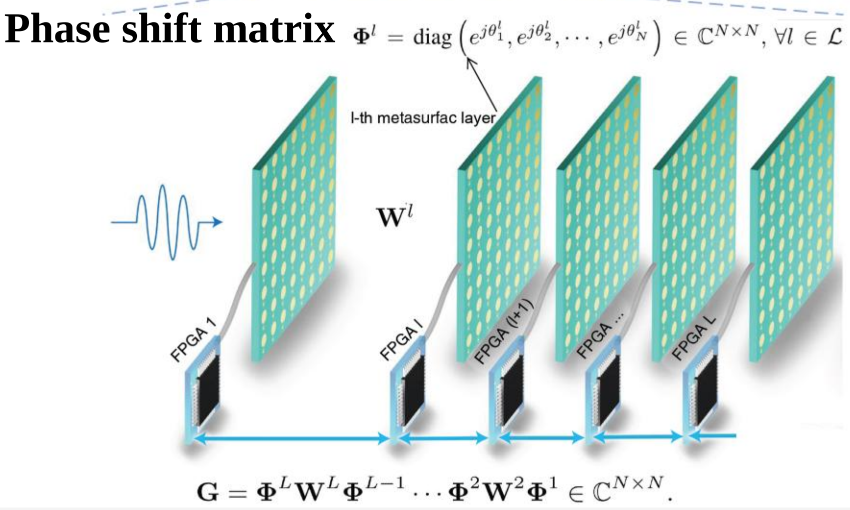

J. An, M. Di Renzo, M. Debbah, and C. Yuen, "**Stacked intelligent metasurfaces** for multiuser beamforming in the wave domain," Proc. IEEE Int. Conf. Commun. (ICC), Rome, Italy, May 2023, pp. 2834 – 2839. **(ICC 2023 Best Paper Award)**

J. An, M. Di Renzo, M. Debbah, H. V. Poor, and C. Yuen. "**Stacked intelligent metasurfaces** for multiuser downlink beamforming in the wave domain," *IEEE Trans. Wireless. Commun.*, 2025, Early Access.

➢ SIM-aided Multiuser MISO System Model

➢ The inter-layer propagation coefficient is

$$w_{n,n'}^{l} = \frac{d_x d_y \cos \chi_{n,n'}^{l}}{d_{n,n'}^{l}} \left(\frac{1}{2\pi d_{n,n'}^{l}} - j\frac{1}{\lambda} \right) e^{j2\pi d_{n,n'}^{l}/\lambda}$$

➢ The wave-domain beamforming matrix is

$$\mathbf{G} = \mathbf{\Phi}^{L}\mathbf{W}^{L}\mathbf{\Phi}^{L-1}\cdots\mathbf{\Phi}^{2}\mathbf{W}^{2}\mathbf{\Phi}^{1} \in \mathbb{C}^{N\times N}$$

➢ The signal received at the *k*-th user is

$$y_k = \mathbf{h}_k^H \mathbf{G} \sum_{k'=1}^{K} \mathbf{w}_{k'}^{1} \sqrt{p_{k'}} s_{k'} + n_k, \ \forall k \in \mathcal{K},$$

➢ The SINR at the *k*-th user is

$$\gamma_k = \frac{\left|\mathbf{h}_k^H \mathbf{G} \mathbf{w}_k^1\right|^2 p_k}{\sum_{k'\neq k}^{K} \left|\mathbf{h}_k^H \mathbf{G} \mathbf{w}_{k'}^1\right|^2 p_{k'} + \sigma_k^2}, \ \forall k \in \mathcal{K}$$

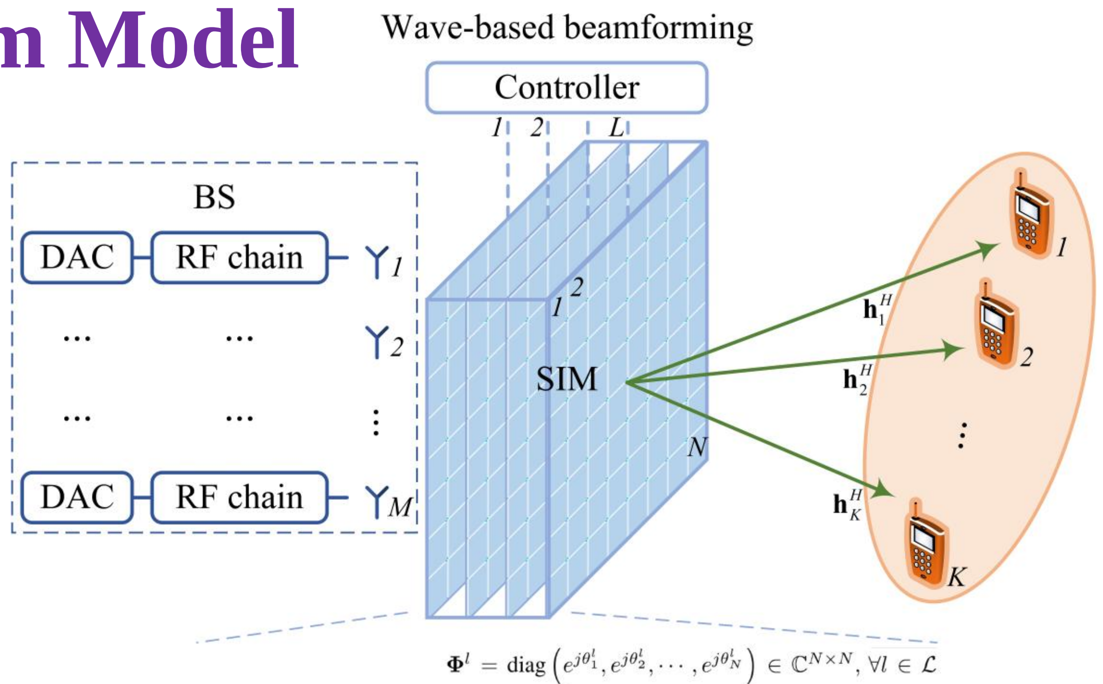

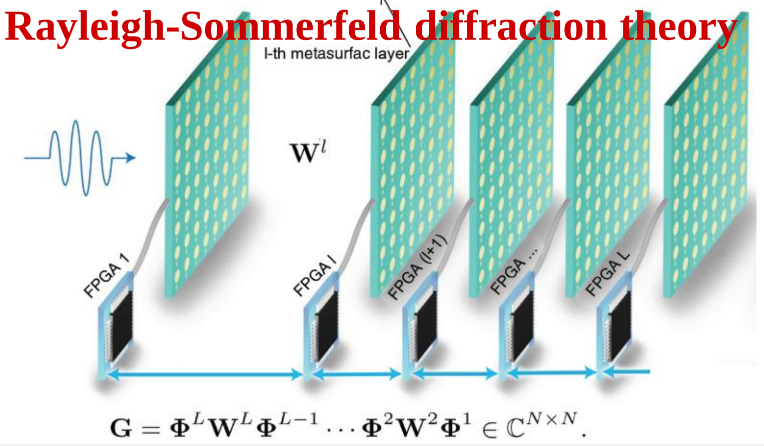

J. An, M. Di Renzo, M. Debbah, and C. Yuen, "**Stacked intelligent metasurfaces** for multiuser beamforming in the wave domain," Proc. IEEE Int. Conf. Commun. (ICC), Rome, Italy, May 2023, pp. 2834 – 2839. **(ICC 2023 Best Paper Award)**

J. An, M. Di Renzo, M. Debbah, H. V. Poor, and C. Yuen. "**Stacked intelligent metasurfaces** for multiuser downlink beamforming in the wave domain," *IEEE Trans. Wireless. Commun.*, 2025, Early Access.

➢ Problem Formulation

➢ **Optimization objective**: Maximizing the sum rate of all the users.

➢ **Optimization variables**: Transmit power allocation at the BS, SIM phase shifts.

➢ **Assumption**: The CSI of all the channels is perfectly known by the BS, i.e., h_k.

The k-th user's channel

❖ **Optimization problem:**

$$\begin{aligned} \max_{\mathbf{p},\, \boldsymbol{\vartheta}} \quad & R = \sum\nolimits_{k=1}^{K} \log_2 \left(1 + \gamma_k\right) \\ \text{s.t.} \quad & \sum\nolimits_{k=1}^{K} p_k \leq P_T, \\ & p_k \geq 0, \ \forall k \in \mathcal{K}, \\ & \theta_n^l \in \left[0, 2\pi\right), \ \forall n \in \mathcal{N}, \ \forall l \in \mathcal{L}. \end{aligned}$$

- Objective function
- Sum power constraint at the BS
- Individual power constraint at the BS
- Phase shift constraint at the SIM

J. An, M. Di Renzo, M. Debbah, and C. Yuen, "**Stacked intelligent metasurfaces** for multiuser beamforming in the wave domain," Proc. IEEE Int. Conf. Commun. (ICC), Rome, Italy, May 2023, pp. 2834 – 2839. **(ICC 2023 Best Paper Award)**

J. An, M. Di Renzo, M. Debbah, H. V. Poor, and C. Yuen. "**Stacked intelligent metasurfaces** for multiuser downlink beamforming in the wave domain," *IEEE Trans. Wireless. Commun.*, 2025, Early Access.

➢ Alternating Optimization Algorithm

➢ Given the SIM phase shifts $\boldsymbol{\vartheta}$, the power allocation is solved by using the iterative water-filling algorithm.

$$p_k = \left(p_o - \frac{\sum_{k' \neq k}^{K} \left| \mathbf{h}_k^H \mathbf{G} \mathbf{w}_{k'}^1 \right|^2 p_{k'} + \sigma_k^2}{\left| \mathbf{h}_k^H \mathbf{G} \mathbf{w}_k^1 \right|^2} \right)^+$$

Add a damping term to enhance the robustness

I

➢ Given the power allocation $\mathbf{p}$, the phase shift optimization subproblem is solved by applying the gradient ascent algorithm.

$$\theta_n^l \leftarrow \theta_n^l + \mu \frac{\partial R}{\partial \theta_n^l}, \ \forall n \in \mathcal{N}, \ \forall l \in \mathcal{L}$$

Partial derivative

$$\frac{\partial R}{\partial \theta_n^l} = 2 \log_2 e \sum_{k=1}^{K} \delta_k \left(p_k \eta_{k,k} - \gamma_k \sum_{k' \neq k}^{K} p_{k'} \eta_{k,k'} \right)$$

II

J. An, M. Di Renzo, M. Debbah, and C. Yuen, "**Stacked intelligent metasurfaces** for multiuser beamforming in the wave domain," Proc. IEEE Int. Conf. Commun. (ICC), Rome, Italy, May 2023, pp. 2834 – 2839. **(ICC 2023 Best Paper Award)**

J. An, M. Di Renzo, M. Debbah, H. V. Poor, and C. Yuen. "**Stacked intelligent metasurfaces** for multiuser downlink beamforming in the wave domain," *IEEE Trans. Wireless. Commun.*, 2025, Early Access.

➢ Simulation Results

Carrier frequency: 28 GHz, transmit power: 10 dBm, noise power: -104 dBm

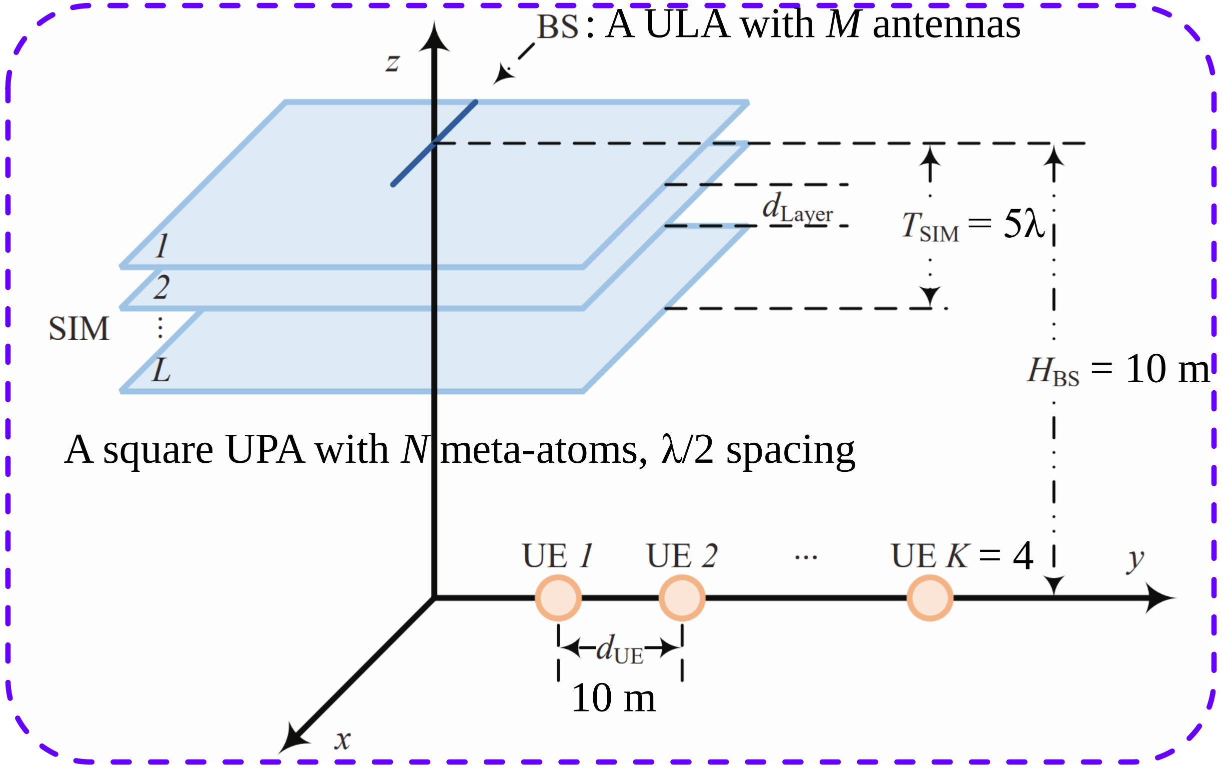

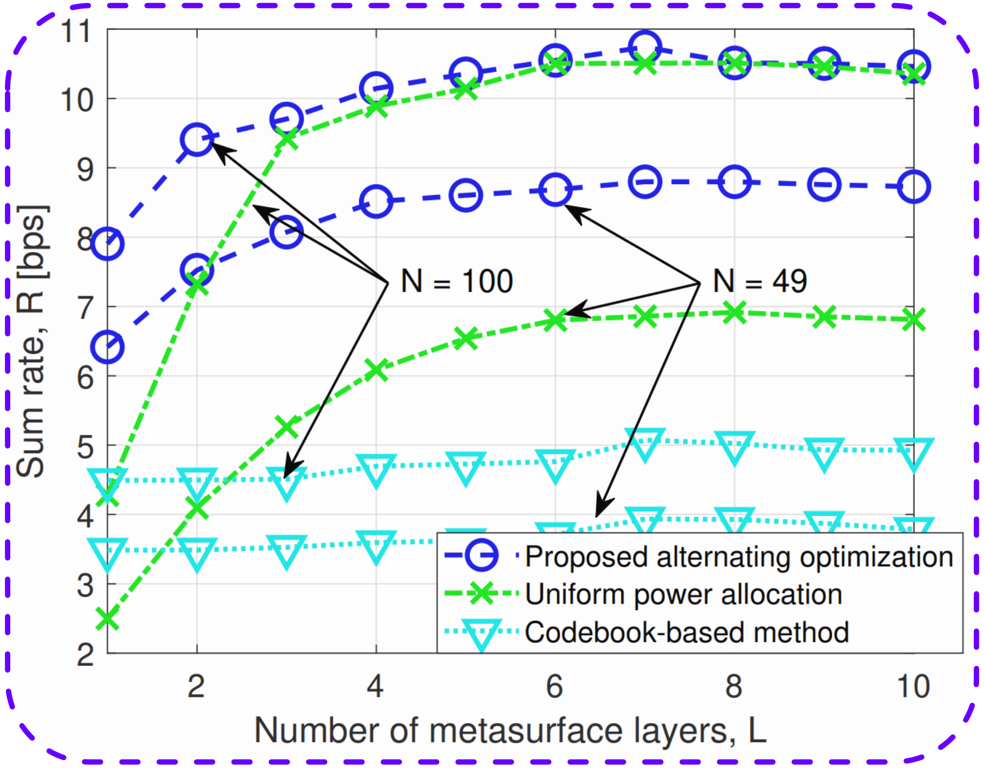

R increases as *L* increases and reaches the maximum at approximately *L* = 7.

J. An, M. Di Renzo, M. Debbah, and C. Yuen, "**Stacked intelligent metasurfaces** for multiuser beamforming in the wave domain," Proc. IEEE Int. Conf. Commun. (ICC), Rome, Italy, May 2023, pp. 2834 – 2839. **(ICC 2023 Best Paper Award)**

J. An, M. Di Renzo, M. Debbah, H. V. Poor, and C. Yuen. "**Stacked intelligent metasurfaces** for multiuser downlink beamforming in the wave domain," *IEEE Trans. Wireless. Commun.*, 2025, Early Access.

➢ Conclusions

- ❑ A SIM-enabled wave-domain beamforming design was proposed, which substantially **reduces the precoding delay and hardware cost compared to its digital counterpart**.
- ❑ A joint transmit power allocation and phase shift optimization problem has been formulated to maximize the sum rate. The former has been tackled by applying the **modified iterative water-filling algorithm**, while the latter have been optimized by leveraging the **gradient ascent algorithm**.
- ❑ Simulation results have demonstrated that the wave-domain beamforming design achieves **significant performance gains** compared to the state-of-the-art benchmarks.

J. An, M. Di Renzo, M. Debbah, and C. Yuen, "**Stacked intelligent metasurfaces** for multiuser beamforming in the wave domain," Proc. IEEE Int. Conf. Commun. (ICC), Rome, Italy, May 2023, pp. 2834 – 2839. **(ICC 2023 Best Paper Award)**

J. An, M. Di Renzo, M. Debbah, H. V. Poor, and C. Yuen. "**Stacked intelligent metasurfaces** for multiuser downlink beamforming in the wave domain," *IEEE Trans. Wireless. Commun.*, 2025, Early Access.

Outline

- Background
- Codebook Solution for RIS-Aided Wireless Systems
- SIM-Enabled Electromagnetic Domain Signal Processing (Q2)
    - § MIMO Precoding
    - **§ DOA Estimation**
    - § Semantic Encoding
- FIM-Enhanced Wireless Communication and Sensing
- Future Directions

➢ SIM as a Diffractive Neural Network

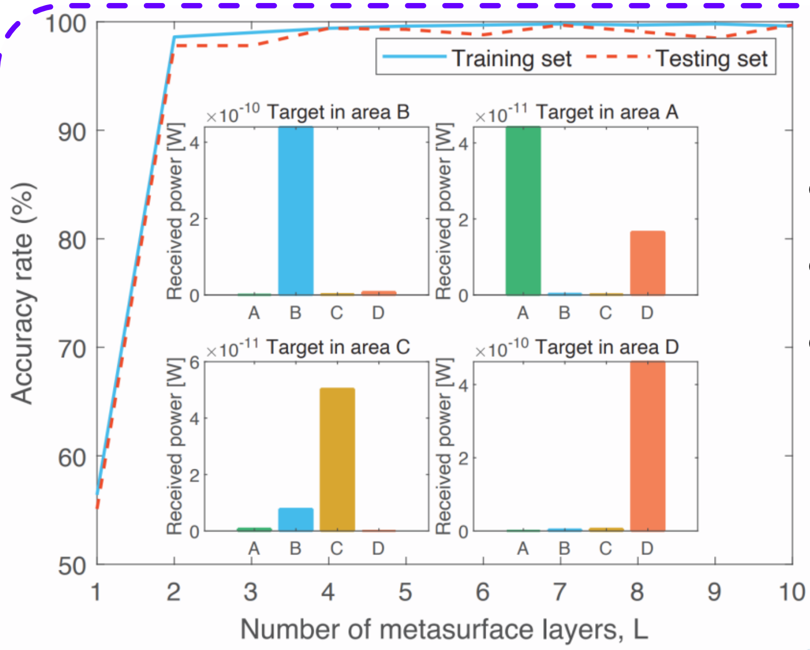

- 100 meta-atoms per layer
- Signal power: 20 dBm
- Noise power: -140 dBm

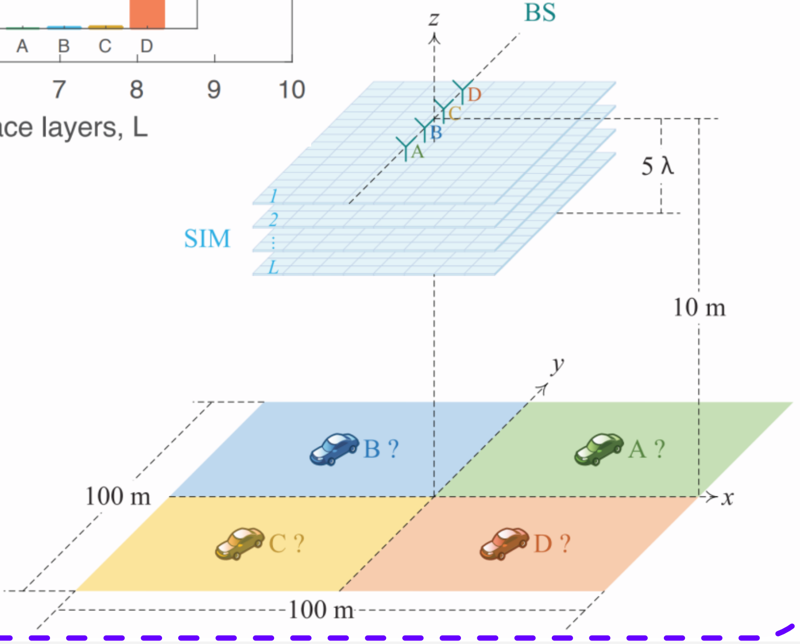

- 1000 training samples
- 100 testing samples
- Loss function: MSE
- Reinforcement learning

- ❑ A 4-layer SIM is capable of correctly estimating the DOA of a target of interest with a detection success rate of 99.5% in the training set and 99% in the testing set, as the EM wave propagates through it.
- ❑ The EM waves radiated from the target would be focused on the corresponding receive antenna with the aid of a well-trained SIM.

J. An, C. Yuen, C. Xu, H. Li, D. W. K. Ng, M. Di Renzo, M. Debbah, and L. Hanzo, "**Stacked intelligent metasurface**-aided MIMO transceiver design," *IEEE Wireless Commun.*, vol. 31, no. 4, pp. 123-131, Aug. 2024. (**Highly Cited Paper**)

➢ SIM-aided Array System Model

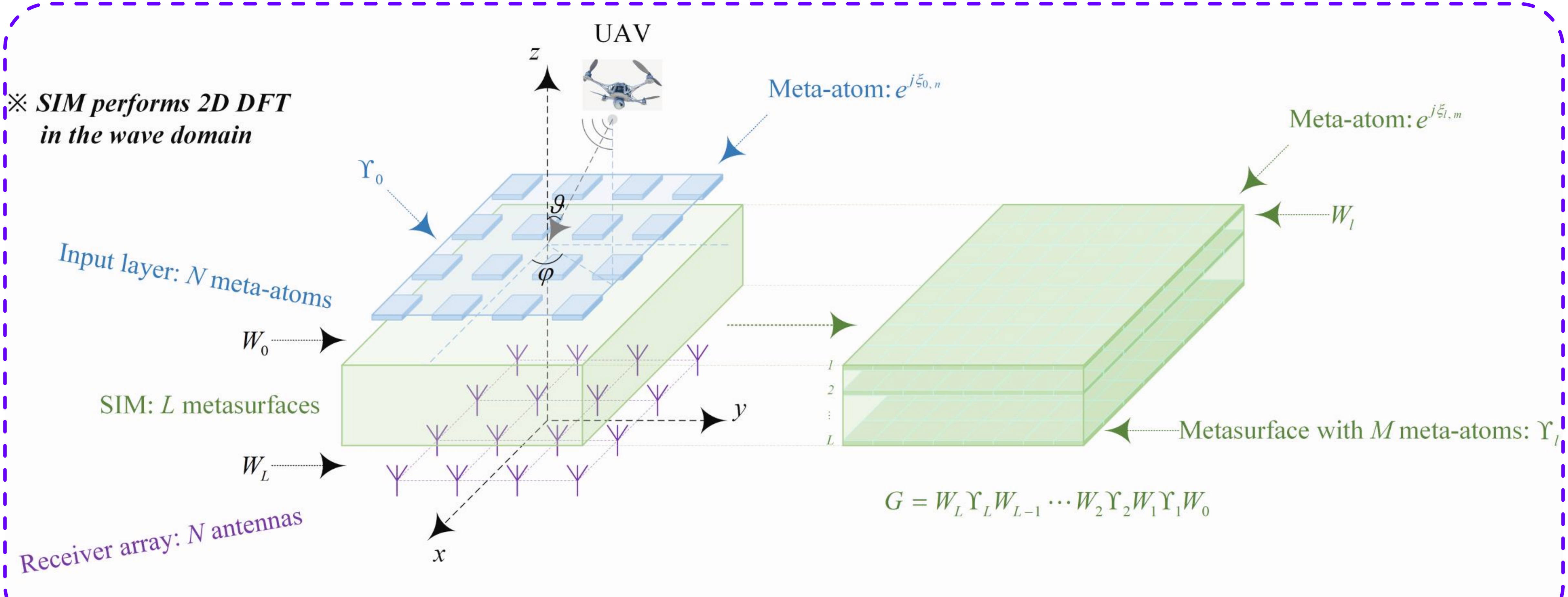

(a) Array layout. (b) A schematic of SIM.

J. An, C. Yuen, Y. Guan, M. Di Renzo, M. Debbah, H. V. Poor, and L. Hanzo, "Two-dimensional direction-of-arrival estimation using **stacked intelligent metasurfaces**," *IEEE J. Sel. Areas Commun.*, vol. 42, no. 10, pp. 2786-2802, Oct. 2024.

➢ SIM-aided Array System Model

➢ The electrical angles in the *x*- and *y*-directions are

$$\psi_{\mathrm{x}} = \kappa d_{\mathrm{x}} \sin(\vartheta) \cos(\varphi)$$
$$\psi_{\mathrm{y}} = \kappa d_{\mathrm{y}} \sin(\vartheta) \sin(\varphi)$$

➢ The steering vector *w.r.t.* the input layer of the SIM

$$\boldsymbol{a}(\psi_{\mathrm{x}}, \psi_{\mathrm{y}}) = \boldsymbol{a}_{\mathrm{y}}(\psi_{\mathrm{y}}) \otimes \boldsymbol{a}_{\mathrm{x}}(\psi_{\mathrm{x}})$$

$$[\boldsymbol{a}_{\mathrm{x}}(\psi_{\mathrm{x}})]_{n_{\mathrm{x}}} \triangleq e^{j\psi_{\mathrm{x}}(n_{\mathrm{x}}-1)}$$
$$[\boldsymbol{a}_{\mathrm{y}}(\psi_{\mathrm{y}})]_{n_{\mathrm{y}}} \triangleq e^{j\psi_{\mathrm{y}}(n_{\mathrm{y}}-1)}$$

➢ The signal being incident upon the input layer is

$$\boldsymbol{x} = \boldsymbol{a}(\psi_{\mathrm{x}}, \psi_{\mathrm{y}}) s$$

- ❖ A single source
- ❖ Continuous phase tunning

➢ The inter-layer propagation coefficient is

$$[\boldsymbol{W}_l]_{m,\breve{m}} = \frac{A_{\text{meta-atom}} \cos \epsilon_{m,\breve{m}}}{2\pi d_{m,\breve{m}}^2} (1 - j\kappa d_{m,\breve{m}}) e^{j\kappa d_{m,\breve{m}}}$$

➢ The transfer function matrix of the SIM is

$$\boldsymbol{G} = \boldsymbol{W}_L \boldsymbol{\Upsilon}_L \boldsymbol{W}_{L-1} \cdots \boldsymbol{W}_2 \boldsymbol{\Upsilon}_2 \boldsymbol{W}_1 \boldsymbol{\Upsilon}_1 \boldsymbol{W}_0$$

Transmission coefficient matrix

➢ The complex signal received at the array is

$$\boldsymbol{r} = \sqrt{\varrho} \boldsymbol{G} \boldsymbol{\Upsilon}_0 \boldsymbol{x} + \boldsymbol{u} = \sqrt{\varrho} \boldsymbol{G} \boldsymbol{\Upsilon}_0 \boldsymbol{a}(\psi_{\mathrm{x}}, \psi_{\mathrm{y}}) s + \boldsymbol{u}$$

SNR Normalized noise

J. An, C. Yuen, Y. Guan, M. Di Renzo, M. Debbah, H. V. Poor, and L. Hanzo, “Two-dimensional direction-of-arrival estimation using **stacked intelligent metasurfaces**,” *IEEE J. Sel. Areas Commun.*, vol. 42, no. 10, pp. 2786-2802, Oct. 2024.

➢ Problem Formulation & Solution

$$\min_{\{\xi_{l,m}\}} \quad \mathcal{L} = \|\beta \boldsymbol{G} - \boldsymbol{F}\|_F^2$$

$$\text{s.t.} \quad \boldsymbol{G} = \boldsymbol{W}_L \boldsymbol{\Upsilon}_L \boldsymbol{W}_{L-1} \cdots \boldsymbol{W}_2 \boldsymbol{\Upsilon}_2 \boldsymbol{W}_1 \boldsymbol{\Upsilon}_1 \boldsymbol{W}_0,$$

$$\boldsymbol{\Upsilon}_l = \text{diag}\left(\left[e^{j\xi_{l,1}}, e^{j\xi_{l,2}}, \cdots, e^{j\xi_{l,M}}\right]^T\right),$$

$$\xi_{l,m} \in [0, 2\pi), \ m = 1, \cdots, M, \ l = 1, \cdots, L,$$

$$\beta \in \mathbb{C}.$$

- Objective function
- The EM response of the SIM
- Transmission coefficient matrix of the *l*-th layer
- Individual phase shift constraint
- Scaling factor for normalization

$$f_{n,\breve{n}} = [\boldsymbol{F}]_{n,\breve{n}} \triangleq e^{-j2\pi \frac{(n_x-1)(\breve{n}_x-1)}{N_x}} e^{-j2\pi \frac{(n_y-1)(\breve{n}_y-1)}{N_y}}$$

- 2D DFT matrix

Gradient Calculation

$$\nabla_{\boldsymbol{\xi}_l} \mathcal{L} = 2 \sum_{n=1}^{N} \Im\left\{\beta^* \boldsymbol{\Upsilon}_l^H \boldsymbol{P}_{l,n}^H (\beta \boldsymbol{g}_n - \boldsymbol{f}_n)\right\}$$

Parameter Update

$$\boldsymbol{\xi}_l \leftarrow \boldsymbol{\xi}_l - \eta \nabla_{\boldsymbol{\xi}_l} \mathcal{L}$$

SIM phase shifts

$$\eta \leftarrow \eta\zeta$$

Learning rate

$$\beta = \left(\boldsymbol{g}^H \boldsymbol{g}\right)^{-1} \boldsymbol{g}^H \boldsymbol{f}$$

Scaling factor

J. An, C. Yuen, Y. Guan, M. Di Renzo, M. Debbah, H. V. Poor, and L. Hanzo, "Two-dimensional direction-of-arrival estimation using **stacked intelligent metasurfaces**," *IEEE J. Sel. Areas Commun.*, vol. 42, no. 10, pp. 2786-2802, Oct. 2024.

➢ DOA Estimation Protocol

➢ Tuning the phase shifts of the input layer to generate the angular spectrum with fine granularity.

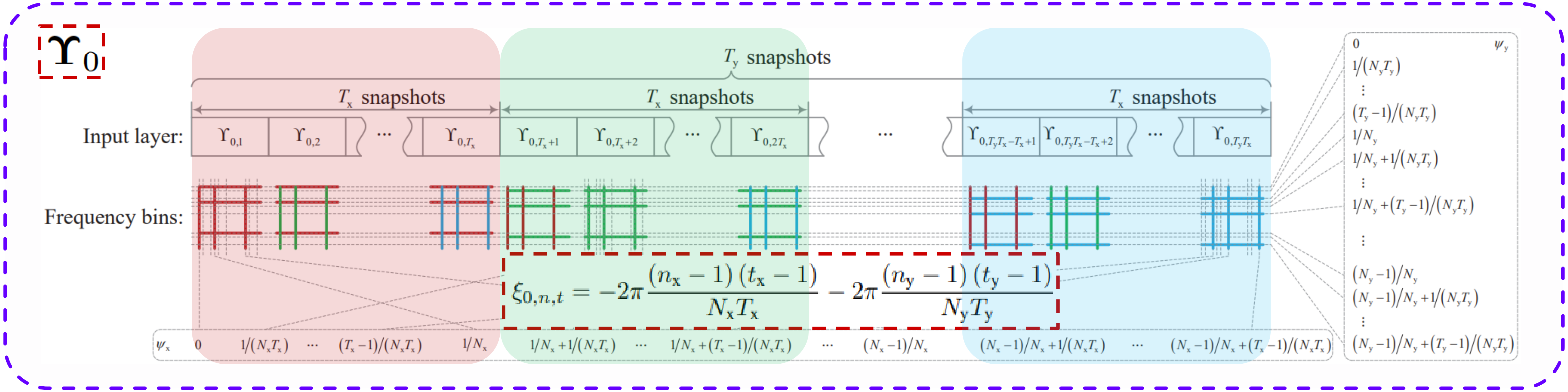

The 2D index of the peak

Received signal

$$[\hat{n}, \hat{t}] = \arg \max_{\substack{n=1,\cdots,N,\\ t=1,\cdots,T}} |r_{n,t}|^2$$

Antenna Snapshot

The estimated electrical angles

$$\hat{\psi}_x = \mathrm{mod}\left[2\left(\frac{\hat{n}_x - 1}{N_x} + \frac{\hat{t}_x - 1}{N_x T_x}\right) + 1, 2\right] - 1$$

$$\hat{\psi}_y = \mathrm{mod}\left[2\left(\frac{\hat{n}_y - 1}{N_y} + \frac{\hat{t}_y - 1}{N_y T_y}\right) + 1, 2\right] - 1$$

The estimated azimuth and elevation angles

$$\hat{\varphi} = \arctan\left(\frac{\hat{\psi}_y d_x}{\hat{\psi}_x d_y}\right),$$

$$\hat{\vartheta} = \arcsin\left(\frac{1}{\kappa}\sqrt{\frac{\hat{\psi}_x^2}{d_x^2} + \frac{\hat{\psi}_y^2}{d_y^2}}\right)$$

J. An, C. Yuen, Y. Guan, M. Di Renzo, M. Debbah, H. V. Poor, and L. Hanzo, "Two-dimensional direction-of-arrival estimation using **stacked intelligent metasurfaces**," *IEEE J. Sel. Areas Commun.*, vol. 42, no. 10, pp. 2786-2802, Oct. 2024.

➢ Simulation Setup

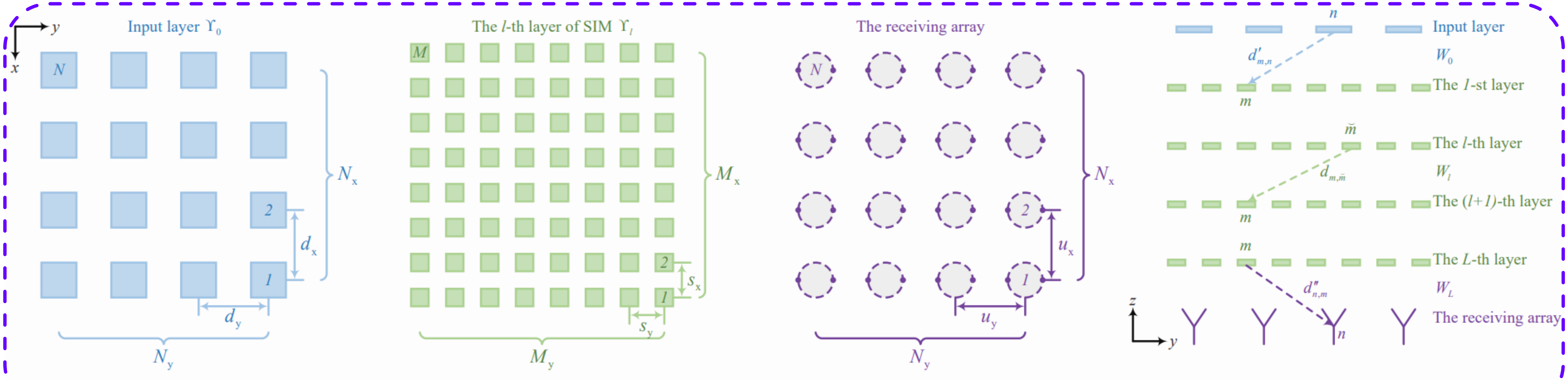

(a) The top view.
(b) The front view.

- The receiver has N probes arranged on (N_x, N_y) grids.
- The system operates at 60 GHz.
- The receiver antenna array is arranged in the same way as the input layer of the SIM, both with λ/2 element spacing.

J. An, C. Yuen, Y. Guan, M. Di Renzo, M. Debbah, H. V. Poor, and L. Hanzo, "Two-dimensional direction-of-arrival estimation using **stacked intelligent metasurfaces**," *IEEE J. Sel. Areas Commun.*, vol. 42, no. 10, pp. 2786-2802, Oct. 2024.

➢ Ablation Study

➢ Three rounds

The first-round experiment with coarse granularity

M	T_{SIM}	$s_x = s_y = 2\lambda/3$			$s_x = s_y = 2\lambda/6$			$s_x = s_y = 2\lambda/9$		
		$L=3$	$L=6$	$L=9$	$L=3$	$L=6$	$L=9$	$L=3$	$L=6$	$L=9$
9	3λ	−9.04	−9.22	−5.10	−2.34	−3.10	−3.82	−1.40	−2.67	−1.28
	6λ	−3.72	−15.39	−10.59	−1.33	−1.39	−1.75	−1.10	−1.25	−1.25
	9λ	−2.03	−5.34	−12.16	−1.22	−1.27	−1.25	−0.91	−1.25	−1.25
36	3λ	−21.40	−17.70	−6.44	−19.89	−27.84	−14.24	−4.98	−4.64	−3.00
	6λ	−16.43	−51.35	−77.43	−3.98	−7.35	−3.94	−2.12	−2.42	−1.29
	9λ	−12.16	−21.44	−45.99	−2.11	−2.44	−3.88	−1.40	−1.36	−1.25
81	3λ	−32.90	−19.59	−5.42	−20.93	−15.51	−32.51	−11.39	−8.93	−4.22
	6λ	−34.65	**−186.34**	**−174.09**	−11.17	−21.12	−11.03	−4.02	−6.64	−5.23
	9λ	−20.34	**−183.78**	−149.94	−4.40	−7.17	−11.21	−1.80	−3.32	−2.81

The second-round experiment with moderate granularity

M	T_{SIM}	$s_x = s_y = 2\lambda$			$s_x = s_y = 2\lambda/3$			$s_x = s_y = 2\lambda/5$		
		$L=4$	$L=6$	$L=8$	$L=4$	$L=6$	$L=8$	$L=4$	$L=6$	$L=8$
49	4λ	−1.58	−0.56	−0.38	−38.69	−27.79	−19.27	−22.74	−67.44	−19.13
	6λ	−8.24	−2.11	−0.83	−21.11	−64.99	−41.89	−13.64	−13.34	−41.31
	8λ	−23.36	−13.06	−2.18	−21.03	−39.62	−50.57	−6.39	−10.69	−15.80
81	4λ	−1.66	−0.52	−0.38	−39.88	−27.21	−28.59	−39.46	−49.97	−143.56
	6λ	−9.47	−2.48	−0.96	−40.76	**−186.34**	−55.88	−23.20	**−176.10**	−20.38
	8λ	−21.78	−5.61	−3.37	−31.07	−71.25	**−182.64**	−11.90	−33.63	−9.54
121	4λ	−1.28	−0.54	−0.36	−32.92	−74.72	−16.65	**−183.27**	−115.42	**−182.88**
	6λ	−10.29	−2.46	−1.40	−62.48	**−179.98**	**−179.26**	−45.93	−96.94	**−199.67**
	8λ	−24.44	−8.73	−3.35	−61.87	**−199.91**	**−192.93**	−28.65	**−194.52**	−35.18

The third-round experiment with fine granularity

M	T_{SIM}	$s_x = s_y = 2\lambda/2$			$s_x = s_y = 2\lambda/3$			$s_x = s_y = 2\lambda/4$		
		$L=5$	$L=6$	$L=7$	$L=5$	$L=6$	$L=7$	$L=5$	$L=6$	$L=7$
100	7λ	−34.33	−31.57	−40.62	−52.49	**−183.68**	**−185.46**	−78.29	**−174.16**	−65.66
	8λ	**−181.78**	−141.26	−65.18	−47.77	**−190.77**	−100.66	**−194.17**	−114.11	**−182.10**
	9λ	−75.05	**−186.58**	−28.49	−52.09	−59.48	**−188.36**	−40.13	−68.04	**−192.96**
121	7λ	−43.44	−36.41	−17.11	−66.08	**−188.02**	**−181.77**	**−194.05**	**−188.23**	**−187.96**
	8λ	−72.48	−82.82	**−180.05**	−78.40	**−199.91**	**−194.52**	−93.94	**−192.73**	**−177.78**
	9λ	−165.68	−103.64	**−185.65**	−39.28	−78.45	**−183.62**	−117.50	**−183.12**	**−208.78**
144	7λ	−35.95	−163.67	−34.67	**−195.45**	**−191.91**	**−192.13**	**−186.43**	**−188.46**	**−179.55**
	8λ	−84.74	**−181.21**	−91.63	−72.60	**−183.46**	**−201.35**	−52.73	**−183.36**	**−178.34**
	9λ	**−183.27**	−105.71	**−186.88**	−111.27	**−174.52**	**−199.73**	−44.56	**−180.33**	**−178.95**

A four-tuple (T_{SIM}, L, M, s_x)

i) T_{SIM}: Thickness of the SIM;

ii) L: Number of metasurface layers;

iii) M: Number of meta-atoms per layer;

iv) $s_x = s_y$: Element spacing.

❑ $u_x = u_y = \lambda/2$.

❑ (2, 2) grids.

J. An, C. Yuen, Y. Guan, M. Di Renzo, M. Debbah, H. V. Poor, and L. Hanzo, "Two-dimensional direction-of-arrival estimation using **stacked intelligent metasurfaces**," *IEEE J. Sel. Areas Commun.*, vol. 42, no. 10, pp. 2786-2802, Oct. 2024.

➢ Fundamental Trade-Offs

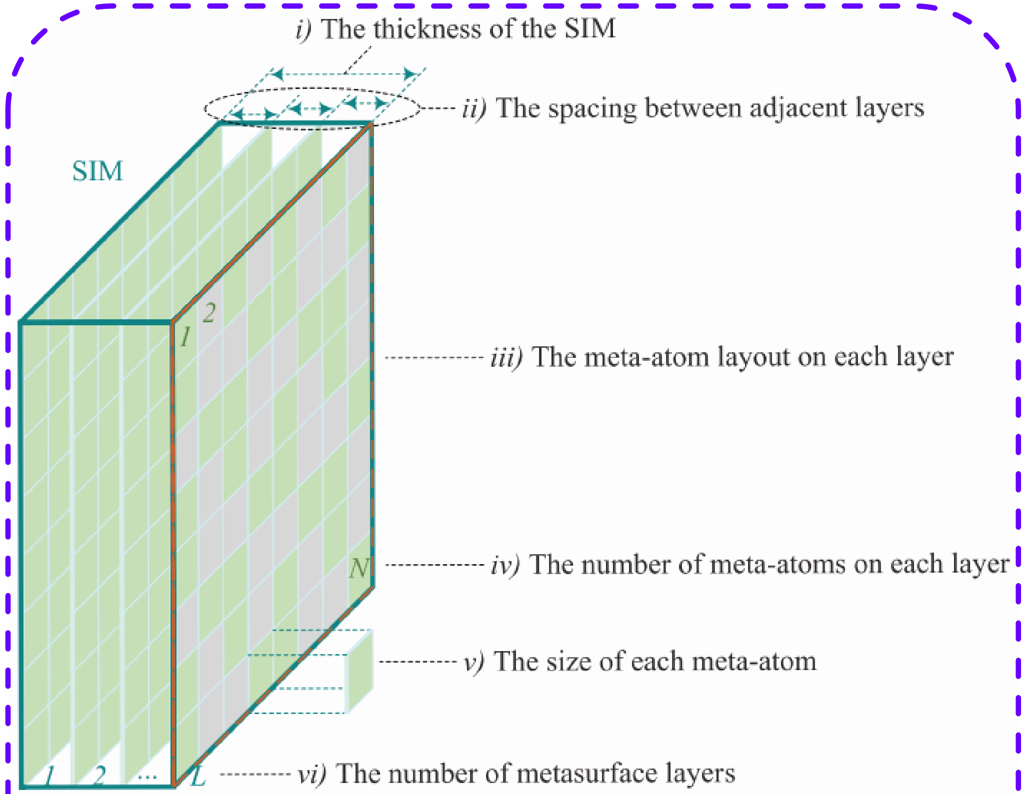

Inter-layer propagation matrix ***W***

- ❑ A very thick SIM → A singular ***W***
- ❑ A very thin SIM → A nearly diagonal ***W***
- ❑ Too much layers → A nearly diagonal ***W***
- ❑ Too few layers → Insufficient design DoF
- ❑ Too much meta-atoms → Unnecessary propagation links
- ❑ Too few meta-atoms → Rank deficiency
- ❑ Large element spacing → A nearly diagonal ***W***
- ❑ Small element spacing → A rank-one ***W***

J. An, C. Yuen, Y. Guan, M. Di Renzo, M. Debbah, H. V. Poor, and L. Hanzo, "Two-dimensional direction-of-arrival estimation using **stacked intelligent metasurfaces**," *IEEE J. Sel. Areas Commun.*, vol. 42, no. 10, pp. 2786-2802, Oct. 2024.

➢ Loss Function versus *L*

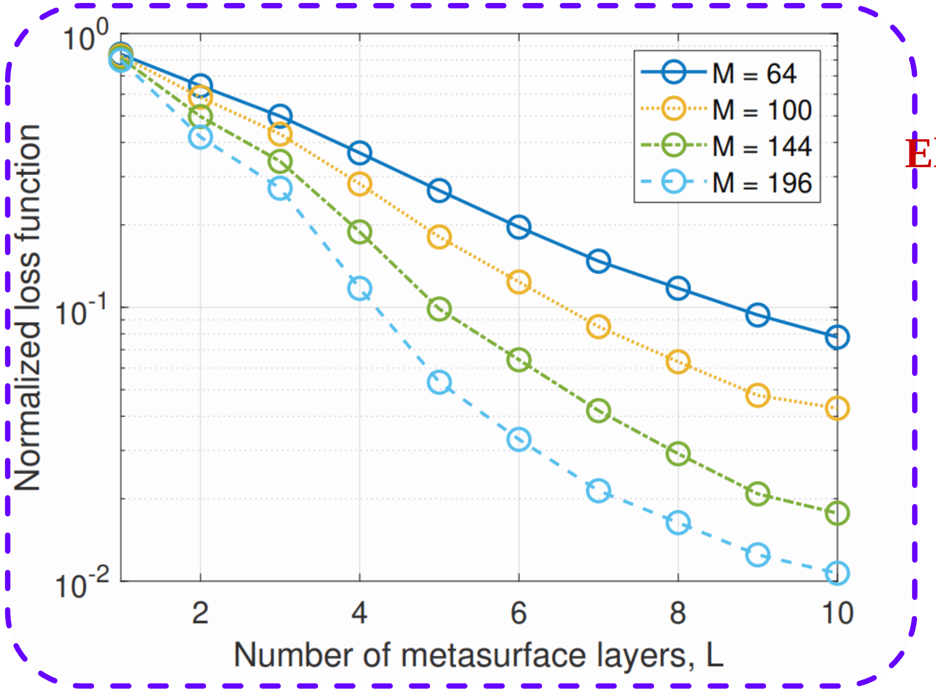

(4, 4) grid points
Layer spacing: λ
Element spacing: $\lambda/2$

➢ MSE versus SNR

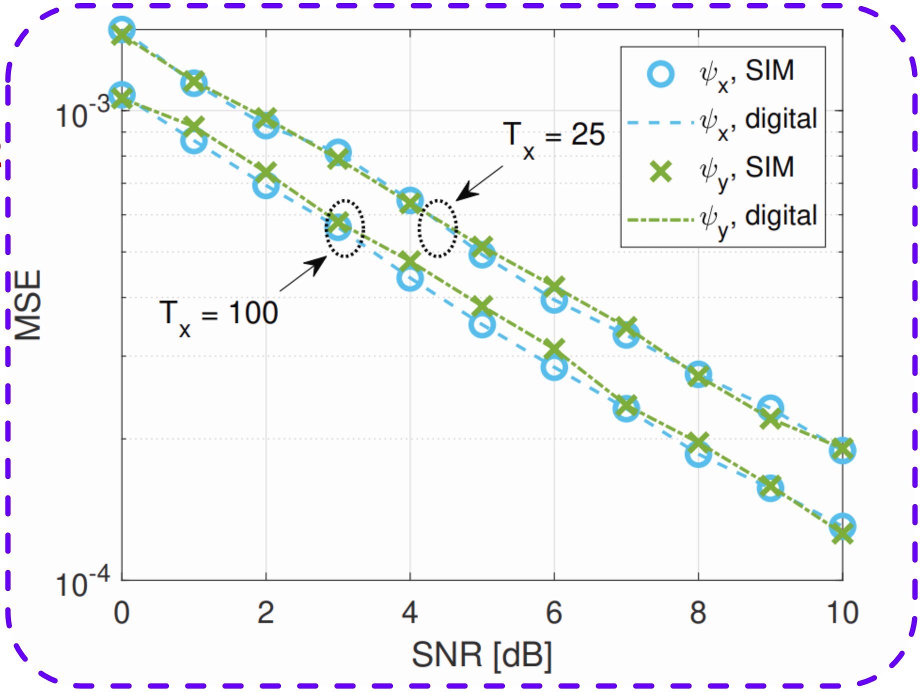

- A SIM having few layers cannot fit the 2D DFT matrix well. Increasing the number of layers succeeds in approximating the 2D DFT in the wave domain.
- The fitting performance also improves with the number of meta-atoms *M* on each layer.
- The MSE improves by 10 dB for every 10 dB increase in SNR.
- Increasing the number of snapshots per block from $T_x = 25$ to $T_x = 100$ provides an extra 2 dB performance gain, thanks to the finer granularity.

J. An, C. Yuen, Y. Guan, M. Di Renzo, M. Debbah, H. V. Poor, and L. Hanzo, "Two-dimensional direction-of-arrival estimation using **stacked intelligent metasurfaces**," *IEEE J. Sel. Areas Commun.*, vol. 42, no. 10, pp. 2786-2802, Oct. 2024.

➢ Angular Spectrum

- ❑ Using a (2 × 2) receiver array

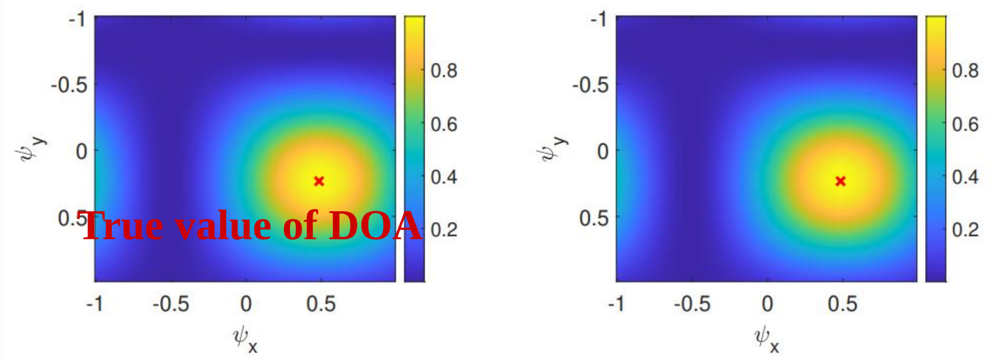

(a) 2D DFT in the wave domain; (b) 2D DFT in the digital domain.

- ❑ Using a (4 × 4) receiver array

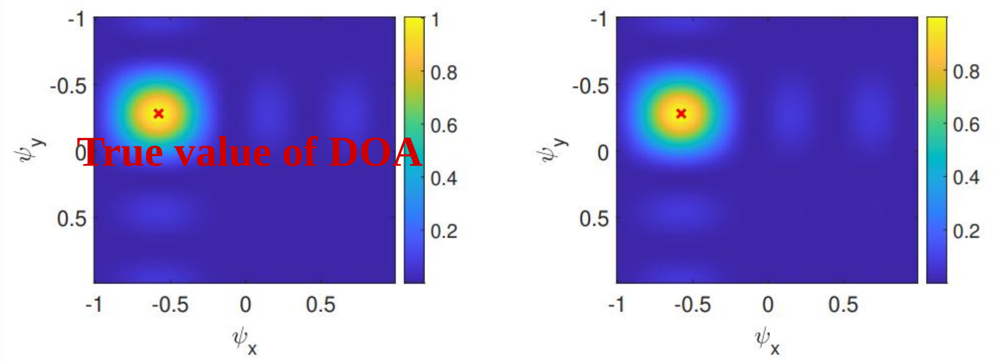

(a) 2D DFT in the wave domain; (b) 2D DFT in the digital domain.

- ❑ The spectrum is obtained by laminating the outputs of 1024 2D DFTs.
- ❑ The energy peak is at the position corresponding to the incident signal's DOA.
- ❑ The SIM outputs almost the same angular spectrum as the 2D digital DFT.
- ❑ A larger array aperture can reduce the leakage.

- ❑ The SIM results in a fundamental DOA estimation paradigm shift by directly observing the angular spectrum instead of the array signal.
- ❑ The computing delay is significantly reduced, and the hardware implementation can be simplified.

J. An, C. Yuen, Y. Guan, M. Di Renzo, M. Debbah, H. V. Poor, and L. Hanzo, "Two-dimensional direction-of-arrival estimation using **stacked intelligent metasurfaces**," *IEEE J. Sel. Areas Commun.*, vol. 42, no. 10, pp. 2786-2802, Oct. 2024.

➢ Conclusions

- We proposed a novel SIM architecture for **estimating the 2D DOA parameters**.
- By appropriately training the SIM to **compute the 2D DFT in the wave domain**, the spatial EM waves can be directly transformed into their spatial frequency domain as they propagate through the SIM.
- We designed a protocol to **generate an angular spectrum with fine granularity** and estimated the DOA by searching for the index having the highest magnitude.
- Simulation results indicate that the proposed SIM-based DOA estimator achieves an MSE of 10^{-4} under moderate conditions, while allowing for **a substantial enhancement in the computation speed at a moderate hardware complexity**.

J. An, C. Yuen, Y. Guan, M. Di Renzo, M. Debbah, H. V. Poor, and L. Hanzo, "Two-dimensional direction-of-arrival estimation using **stacked intelligent metasurfaces**," *IEEE J. Sel. Areas Commun.*, vol. 42, no. 10, pp. 2786-2802, Oct. 2024.

Outline

- Background
- Codebook Solution for RIS-Aided Wireless Systems
- SIM-Enabled Electromagnetic Domain Signal Processing (Q2)
  - MIMO Precoding
  - DOA Estimation
  - **Semantic Encoding**
- FIM-Enhanced Wireless Communication and Sensing
- Future Directions

➢ SIM for Semantic Encoder

- ❑ Image recognition task

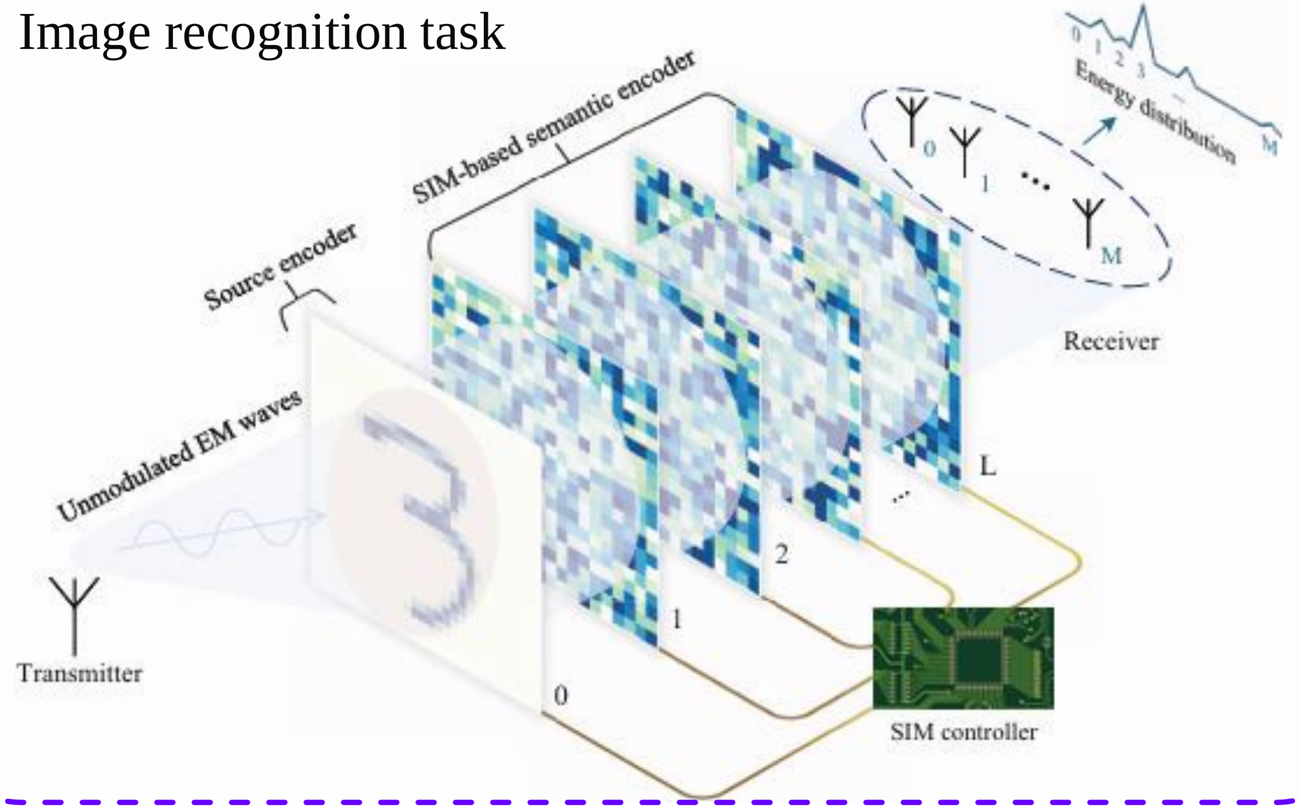

- ❑ A SIM-based DNN transforms the signals passing through the input layer into a unique beam towards a receiving antenna.
- ❑ The image is recognized by probing the signal magnitude across the receiving array.

- ❑ The normalized received power is

$$\tilde{\mathbf{y}} = \mathrm{softmax}(|\mathbf{y}|^2) = [\tilde{y}_1, \tilde{y}_2, \ldots, \tilde{y}_M] \in \mathbb{R}^{M\times 1}$$

- ❑ The expected probability distribution is

$$q_m = \begin{cases} 1, & m \text{ is the class of the source image,} \\ 0, & \text{otherwise.} \end{cases}$$

- ❑ The cross entropy is defined as

$$\mathcal{L}_{\mathrm{CE}}(\mathbf{a}^l, \boldsymbol{\phi}^l) = -\sum_{m=1}^{M} q_m \log(\tilde{y}_m)$$

- ❑ Mini-batch gradient descent
- ❑ Adam optimizer.

G. Huang, **J. An**, Z. Yang, L. Gan, M. Bennis and M. Debbah, "**Stacked intelligent metasurfaces** for task-oriented semantic communications," *IEEE Wireless Commun. Lett.*, vol. 14, no. 2, pp. 310-314, Feb. 2025.

➢ Simulation Results

➢ **Accuracy versus *L***

➢ ***D* = 10λ, *N* = 441, $d_{s,r}$ = 10 m**

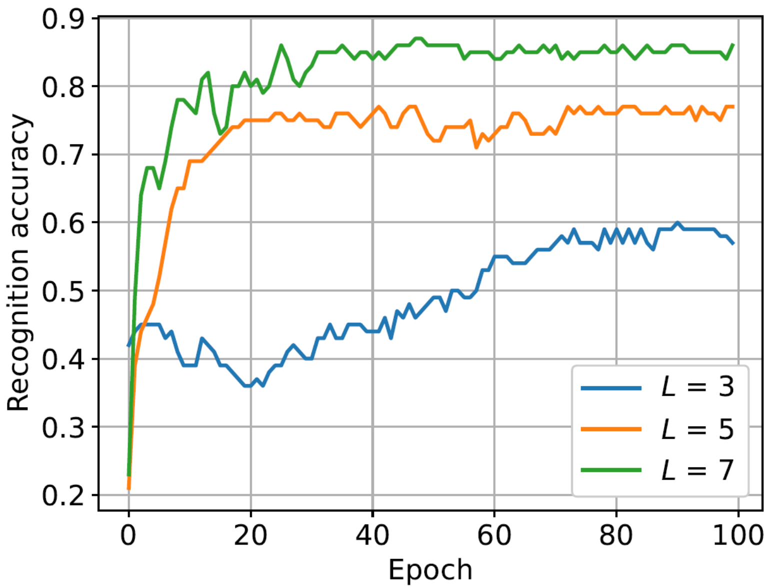

➢ **Accuracy versus $d_{s,r}$**

➢ ***D* = 10λ, *N* = 441, *L* = 7**

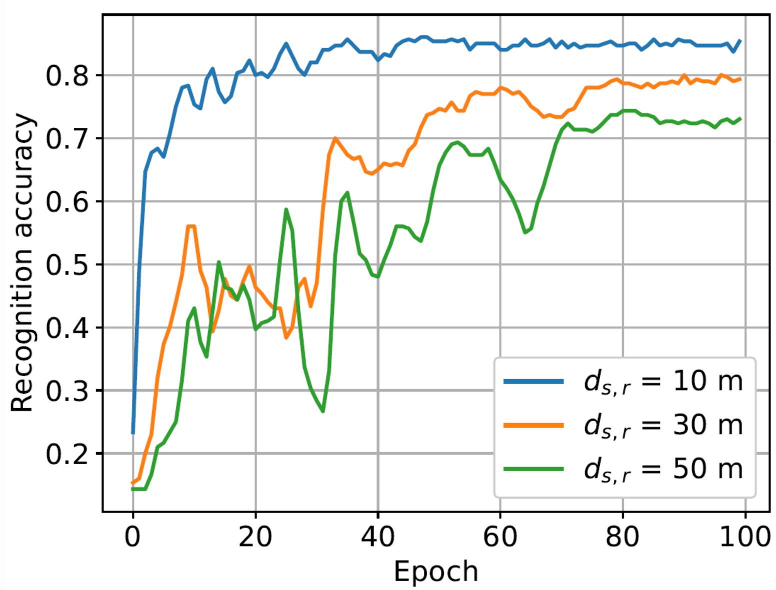

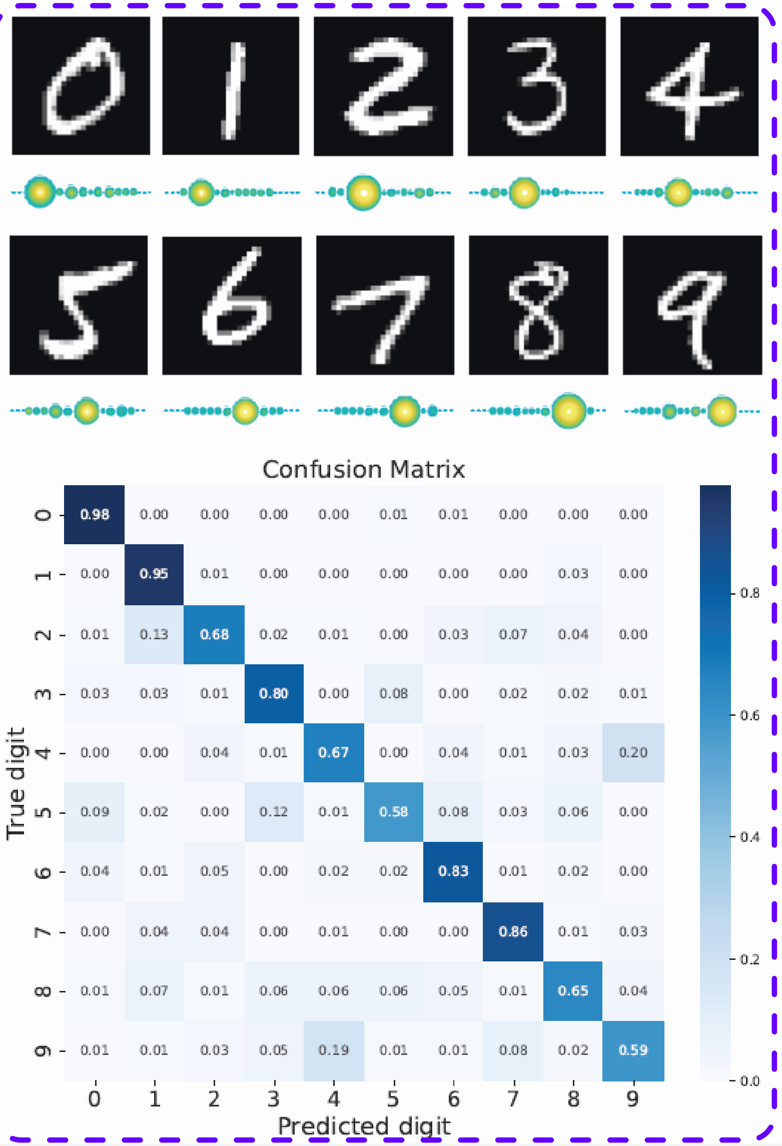

- ❑ The recognition accuracy using the DNN increases with *L*, thanks to the enhanced inference capability of the multi-layer diffractive architecture for achieving more accurate beam steering.
- ❑ A shorter propagation distance would improve the recognition accuracy. (**Less path loss**; & **More distinguishable channels**.)

G. Huang, **J. An**, Z. Yang, L. Gan, M. Bennis and M. Debbah, "**Stacked intelligent metasurfaces** for task-oriented semantic communications," *IEEE Wireless Commun. Lett.*, vol. 14, no. 2, pp. 310-314, Feb. 2025.

Outline

- Background
- Codebook Solution for RIS-Aided Wireless Systems
- SIM-Enabled Electromagnetic Domain Signal Processing
- **FIM-Enhanced Wireless Communication and Sensing (Q3)**
  - Power Reduction
  - MIMO Capacity Enhancement
  - Wireless Sensing
- Future Directions

Q3: Is It Possible to Deploy RIS on Flexible Objects?

➢ Illustration of some existing FIMs

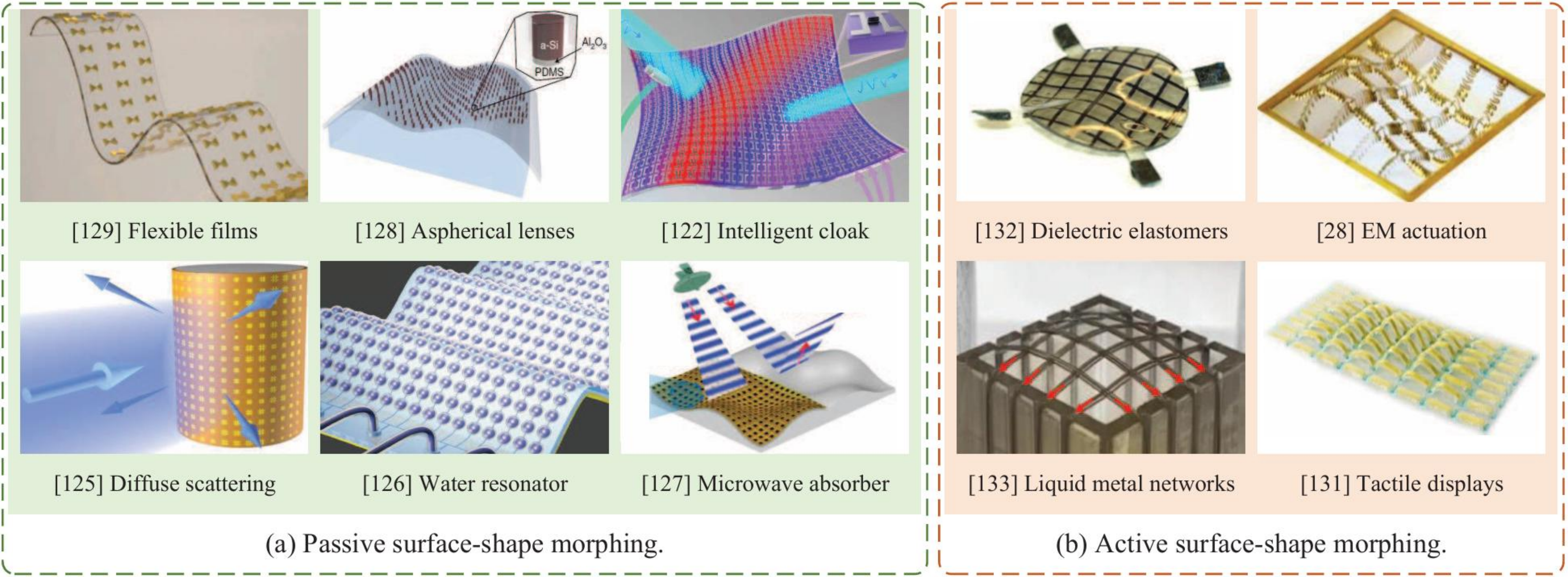

J. An, M. Debbah, T. J. Cui, Z. N. Chen, and C. Yuen, "**Emerging Technologies in Intelligent Metasurfaces: Shaping the Future of Wireless Communications**," *IEEE Trans. Antenna Propag.*, 2025 (***Invited Paper***)

Outline

- Background
- Codebook Solution for RIS-Aided Wireless Systems
- SIM-Enabled Electromagnetic Domain Signal Processing
- FIM-Enhanced Wireless Communication and Sensing (Q3)
  - § **Power Reduction**
  - § MIMO Capacity Enhancement
  - § Wireless Sensing
- Future Directions

➢ FIM-Aided Multiuser MISO System Model

- ❑ An FIM is deployed at the BS
- ❑ Each radiating element can be positioned along the direction perpendicular to the surface

N: The number of transmit antennas;

K: The number of single-antenna users;

L: The number of propagation paths

- ❑ The morphing distance of the *n*-th element

$$y_{\min} \leq y_n \leq y_{\max}, \quad \forall n \in \mathcal{N},$$

- ❑ The FIM surface shape

$$\boldsymbol{y} = [y_1, y_2, \cdots, y_N]^T \in \mathbb{C}^N$$

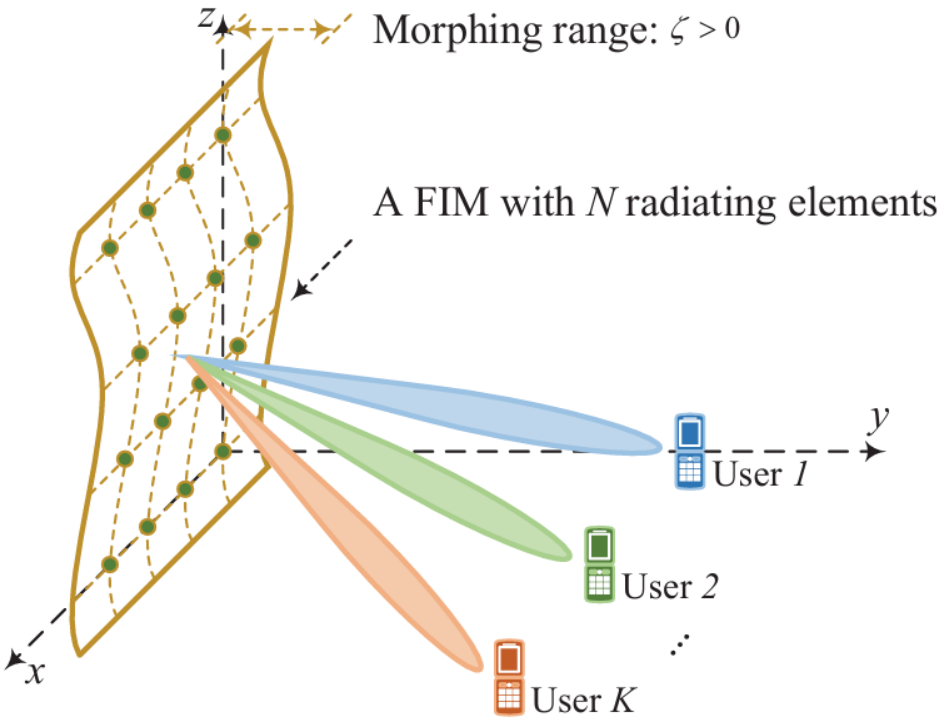

J. An, C. Yuen, M. Di. Renzo, M. Debbah, H. V. Poor, and L. Hanzo, "Downlink multiuser communications relying on **flexible intelligent metasurfaces**," GLOBECOM, 2024.

J. An, C. Yuen, M. Di. Renzo, M. Debbah, H. V. Poor, and L. Hanzo, "**Flexible intelligent metasurfaces** for downlink multiuser MISO communications," *IEEE Trans. Wireless Commun.*, 2025

➢ FIM-Aided Multiuser MISO Channel Model

➢ The array steering vector is

$$\boldsymbol{a}(\boldsymbol{y}, \phi, \theta) = \Big[1, \cdots, e^{j\kappa(x_n \sin\theta\cos\phi + y_n \sin\theta\sin\phi + z_n\cos\theta)}, \cdots, e^{j\kappa(x_N \sin\theta\cos\phi + y_N \sin\theta\sin\phi + z_N\cos\theta)}\Big]^T,$$

➢ The narrowband channel is written as

Channel gain of the *l*-th path

$$\boldsymbol{h}_k(\boldsymbol{y}) = \sum_{\ell=1}^{L} \alpha_{k,\ell}\boldsymbol{a}(\boldsymbol{y}, \phi_\ell, \theta_\ell), \quad \forall k \in \mathcal{K}.$$

➢ The SINR at user *k* is

Beamforming vector of the *k*-th user

$$\text{SINR}_k = \frac{\left|\boldsymbol{h}_k^H(\boldsymbol{y})\boldsymbol{w}_k\right|^2}{\sum_{k'=1,\ k'\neq k}^{K}\left|\boldsymbol{h}_k^H(\boldsymbol{y})\boldsymbol{w}_{k'}\right|^2 + \sigma_k^2}, \quad \forall k \in \mathcal{K}.$$

J. An, C. Yuen, M. Di. Renzo, M. Debbah, H. V. Poor, and L. Hanzo, "Downlink multiuser communications relying on **flexible intelligent metasurfaces**," GLOBECOM, 2024.

J. An, C. Yuen, M. Di. Renzo, M. Debbah, H. V. Poor, and L. Hanzo, "**Flexible intelligent metasurfaces** for downlink multiuser MISO communications," *IEEE Trans. Wireless Commun.*, 2025

➢ Problem Formulation

- Minimize the transmit power at the BS by jointly optimizing the **transmit beamforming vectors** and the **surface shape of the FIM**.
- The optimization problem is formulated as

$$(P_{\mathcal{A}}) \quad \min_{\{\boldsymbol{w}_k\},\boldsymbol{y}} \quad \sum_{k=1}^{K} \|\boldsymbol{w}_k\|^2 \tag{10a}$$

$$\text{s.t.} \quad \frac{\left|\boldsymbol{h}_k^H(\boldsymbol{y})\,\boldsymbol{w}_k\right|^2}{\sum_{k'\neq k}^{K}\left|\boldsymbol{h}_k^H(\boldsymbol{y})\,\boldsymbol{w}_{k'}\right|^2+\sigma_k^2} \geq \gamma_k, \quad \forall k \in \mathcal{K}, \tag{10b}$$

$$0 \leq y_n \leq y_{\max}, \quad \forall n \in \mathcal{N}, \tag{10c}$$

SINR requirement

FIM morphing range

➢ Challenges

- The non-convex SINR constraint;
- The transmit beamforming vectors and the FIM's surface shape are highly coupled.

J. An, C. Yuen, M. Di. Renzo, M. Debbah, H. V. Poor, and L. Hanzo, "Downlink multiuser communications relying on **flexible intelligent metasurfaces**," GLOBECOM, 2024.

J. An, C. Yuen, M. Di. Renzo, M. Debbah, H. V. Poor, and L. Hanzo, "**Flexible intelligent metasurfaces** for downlink multiuser MISO communications," *IEEE Trans. Wireless Commun.*, 2025

➢ Multiuser Scenario – Alternating Optimization

Given the surface-shape vector, the original problem is reduced to

$$(P_{\mathcal{F}}) \quad \min_{\{\boldsymbol{w}_k\}} \sum_{k=1}^{K} \|\boldsymbol{w}_k\|^2 \tag{19a}$$

$$\text{s.t.} \quad \frac{\left|\boldsymbol{h}_k^H(\hat{\boldsymbol{y}})\boldsymbol{w}_k\right|^2}{\sum_{k'\neq k}^{K}\left|\boldsymbol{h}_k^H(\hat{\boldsymbol{y}})\boldsymbol{w}_{k'}\right|^2+\sigma_k^2} \geq \gamma_k, \quad \forall k \in \mathcal{K}. \tag{19b}$$

The optimal solution is the MMSE beamforming, yielding

$$\boldsymbol{w}_k^{\mathrm{o}} = \sqrt{p_k}\underbrace{\frac{\left(\boldsymbol{I}_N + \sum_{k'=1}^{K}\frac{\lambda_{k'}}{\sigma_{k'}^2}\boldsymbol{h}_{k'}(\hat{\boldsymbol{y}})\boldsymbol{h}_{k'}^H(\hat{\boldsymbol{y}})\right)^{-1}\boldsymbol{h}_k(\hat{\boldsymbol{y}})}{\left\|\left(\boldsymbol{I}_N + \sum_{k'=1}^{K}\frac{\lambda_{k'}}{\sigma_{k'}^2}\boldsymbol{h}_{k'}(\hat{\boldsymbol{y}})\boldsymbol{h}_{k'}^H(\hat{\boldsymbol{y}})\right)^{-1}\boldsymbol{h}_k(\hat{\boldsymbol{y}})\right\|}}_{=\tilde{\boldsymbol{w}}_k^{\mathrm{o}},\ \text{transmit beamforming direction}},$$

Obtained by solving fixed-point equations

J. An, C. Yuen, M. Di. Renzo, M. Debbah, H. V. Poor, and L. Hanzo, "Downlink multiuser communications relying on **flexible intelligent metasurfaces**," GLOBECOM, 2024.
J. An, C. Yuen, M. Di. Renzo, M. Debbah, H. V. Poor, and L. Hanzo, "**Flexible intelligent metasurfaces** for downlink multiuser MISO communications," *IEEE Trans. Wireless Commun.*, 2025

➤ Multiuser Scenario – Alternating Optimization

Given the transmit beamforming, the original problem is reduced to

$$(P_{\mathcal{G}}) \quad \text{Find} \quad \boldsymbol{y} \tag{24a}$$

$$\text{s.t.} \quad \frac{\left|\boldsymbol{h}_k^H(\boldsymbol{y})\,\hat{\boldsymbol{w}}_k\right|^2}{\sum_{k'\neq k}^{K}\left|\boldsymbol{h}_k^H(\boldsymbol{y})\,\hat{\boldsymbol{w}}_{k'}\right|^2+\sigma_k^2} \geq \gamma_k, \quad \forall k \in \mathcal{K}, \tag{24b}$$

$$0 \leq y_n \leq y_{\max}, \quad \forall n \in \mathcal{N}. \tag{24c}$$

Auxiliary variable

$$\epsilon_k \triangleq \frac{1}{\gamma_k \sigma_k^2}\left|\boldsymbol{h}_k^H(\boldsymbol{y})\,\hat{\boldsymbol{w}}_k\right|^2 - \frac{1}{\sigma_k^2}\sum_{k'\neq k}^{K}\left|\boldsymbol{h}_k^H(\boldsymbol{y})\,\hat{\boldsymbol{w}}_{k'}\right|^2 - 1,$$

$$(P_{\mathcal{H}}) \quad \max_{\boldsymbol{y}} \quad \epsilon = \sum_{k=1} \epsilon_k$$

$$\text{s.t.} \quad 0 \leq y_n \leq y_{\max}, \quad \forall n \in \mathcal{N},$$

$$\epsilon_k \geq 0, \quad \forall k \in \mathcal{K},$$

Gradient ascent method

Update the surface shape

$$\boldsymbol{y} \leftarrow \boldsymbol{y} + \mu \nabla_{\boldsymbol{y}} \epsilon,$$

Scale the surface shape

$$y_n = \max\left(\min\left(y_n, y_{\max}\right), 0\right), \quad \forall n \in \mathcal{N}.$$

J. An, C. Yuen, M. Di. Renzo, M. Debbah, H. V. Poor, and L. Hanzo, "Downlink multiuser communications relying on **flexible intelligent metasurfaces**," GLOBECOM, 2024.

J. An, C. Yuen, M. Di. Renzo, M. Debbah, H. V. Poor, and L. Hanzo, "**Flexible intelligent metasurfaces** for downlink multiuser MISO communications," *IEEE Trans. Wireless Commun.*, 2025

➢ Simulation Setups

- An FIM having N elements
- Element spacing: Half-wavelength
- Height of the BS: $H_u = 5$ m
- Frequency: 28 GHz
- Noise PSD: - 174 dBm/Hz
- Bandwidth: 100 MHz

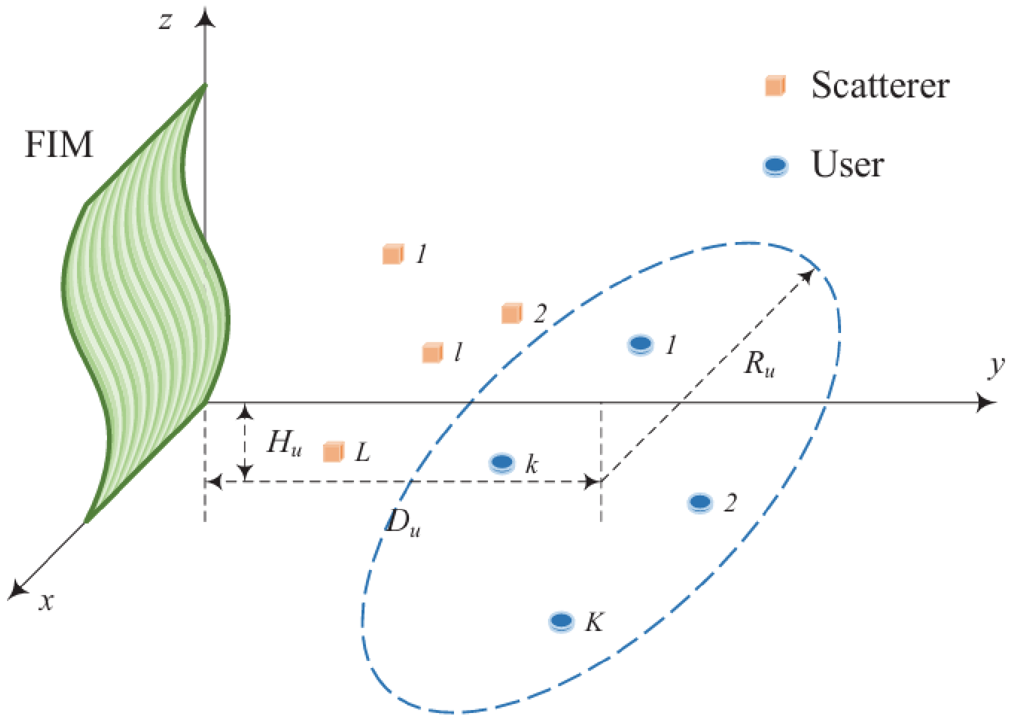

J. An, C. Yuen, M. Di. Renzo, M. Debbah, H. V. Poor, and L. Hanzo, "Downlink multiuser communications relying on **flexible intelligent metasurfaces**," GLOBECOM, 2024.

J. An, C. Yuen, M. Di. Renzo, M. Debbah, H. V. Poor, and L. Hanzo, "**Flexible intelligent metasurfaces** for downlink multiuser MISO communications," *IEEE Trans. Wireless Commun.*, 2025

➢ Morphing Capability of the FIM (A Single User)

$L = 4, \zeta = \lambda/2$

Gain: 11.58 dB

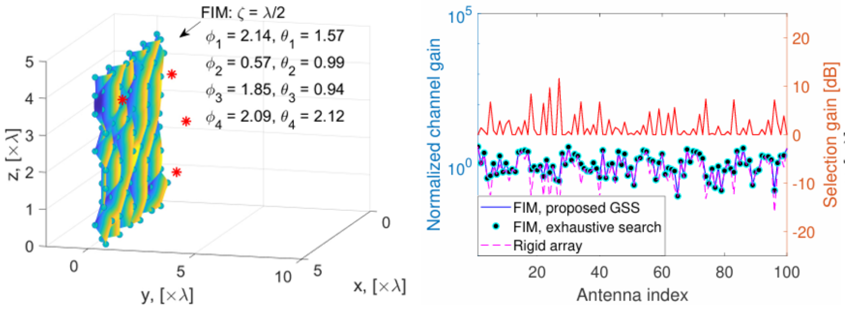

(a) (b)

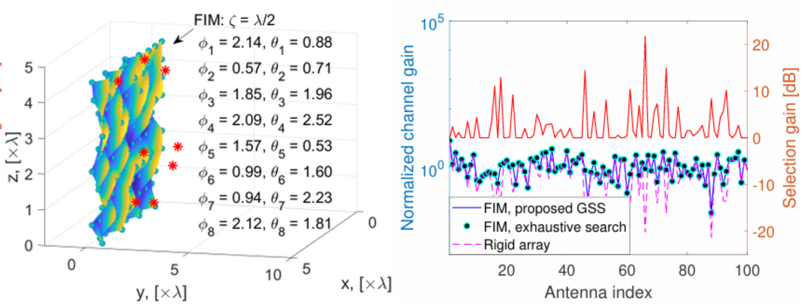

(a) (b)

$L = 8, \zeta = \lambda/2$

Gain: 21.65 dB

$L = 4, \zeta = \lambda$

Gain: 14.52 dB

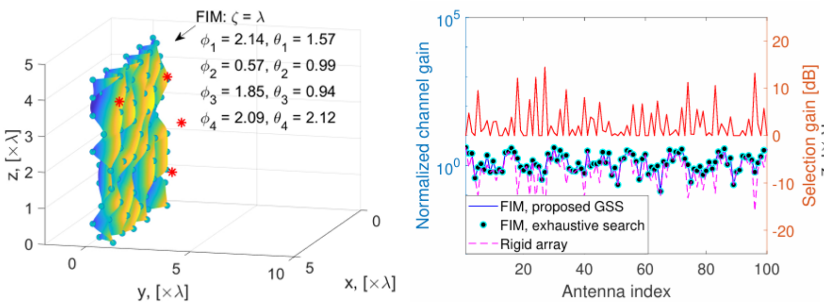

(a) (b)

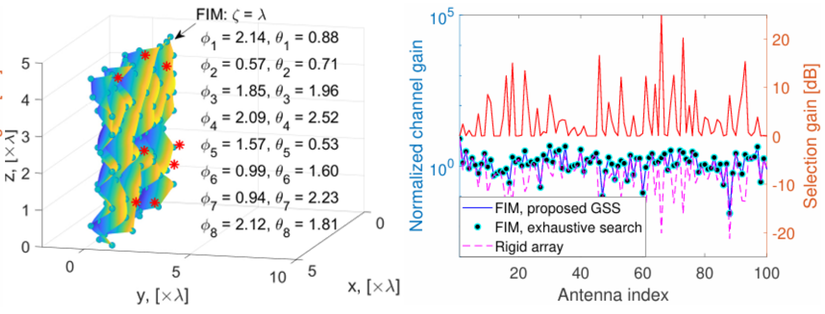

(a) (b)

$L = 8, \zeta = \lambda$

Gain: 24.94 dB

- ❑ FIM can adapt its surface shape by positioning all antenna elements at locations with highest channel gain.
- ❑ The proposed low-complexity GSS approach attains the same surface shape as the exhaustive search method.
- ❑ **The FIM performance gain increases with the morphing range ζ and the number *L* of propagation paths.**

J. An, C. Yuen, M. Di. Renzo, M. Debbah, H. V. Poor, and L. Hanzo, “Downlink multiuser communications relying on **flexible intelligent metasurfaces**,” GLOBECOM, 2024.

J. An, C. Yuen, M. Di. Renzo, M. Debbah, H. V. Poor, and L. Hanzo, “**Flexible intelligent metasurfaces** for downlink multiuser MISO communications,” *IEEE Trans. Wireless Commun.*, 2025

○ Power vs SINR Target $K = 4$ users ○ Power vs Number of Paths

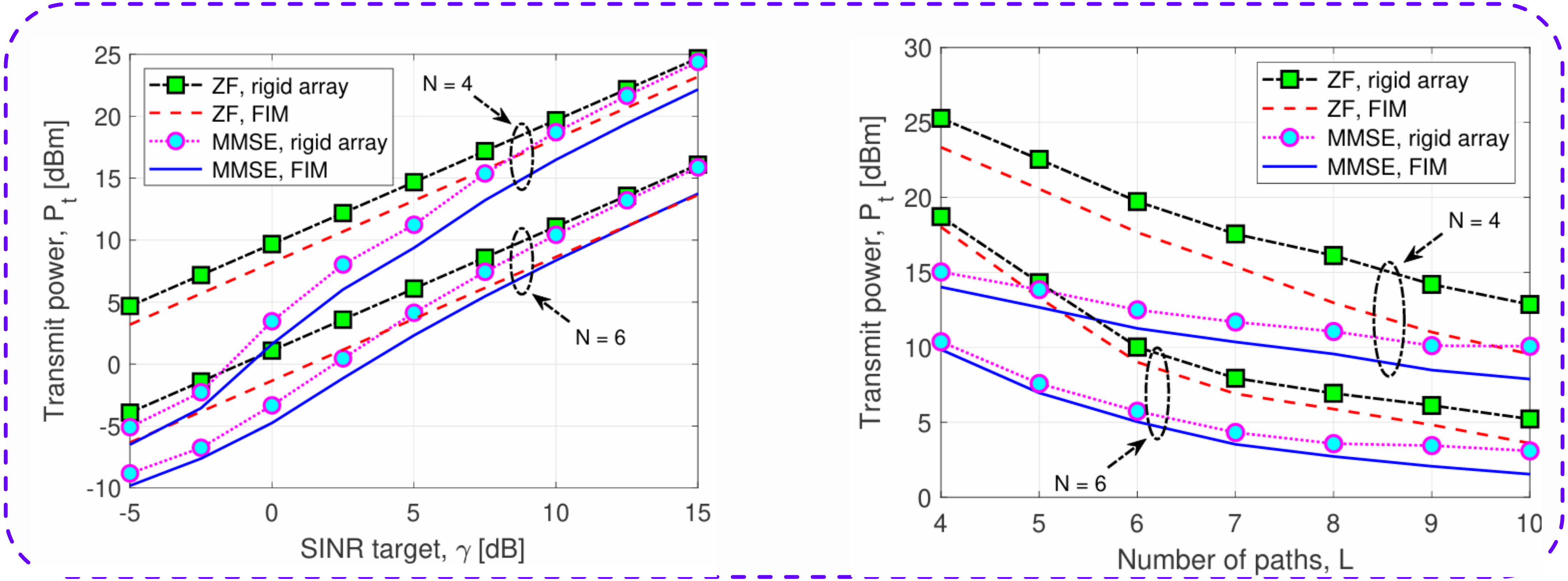

- The FIM provides an additional 3dB SNR gain by morphing its surface shape.
- The performance gain becomes more significant as the number of propagation paths increases.

J. An, C. Yuen, M. Di. Renzo, M. Debbah, H. V. Poor, and L. Hanzo, "Downlink multiuser communications relying on **flexible intelligent metasurfaces**," GLOBECOM, 2024.

J. An, C. Yuen, M. Di. Renzo, M. Debbah, H. V. Poor, and L. Hanzo, "**Flexible intelligent metasurfaces** for downlink multiuser MISO communications," *IEEE Trans. Wireless Commun.*, 2025

○ Power vs the FIM's Morphing Range

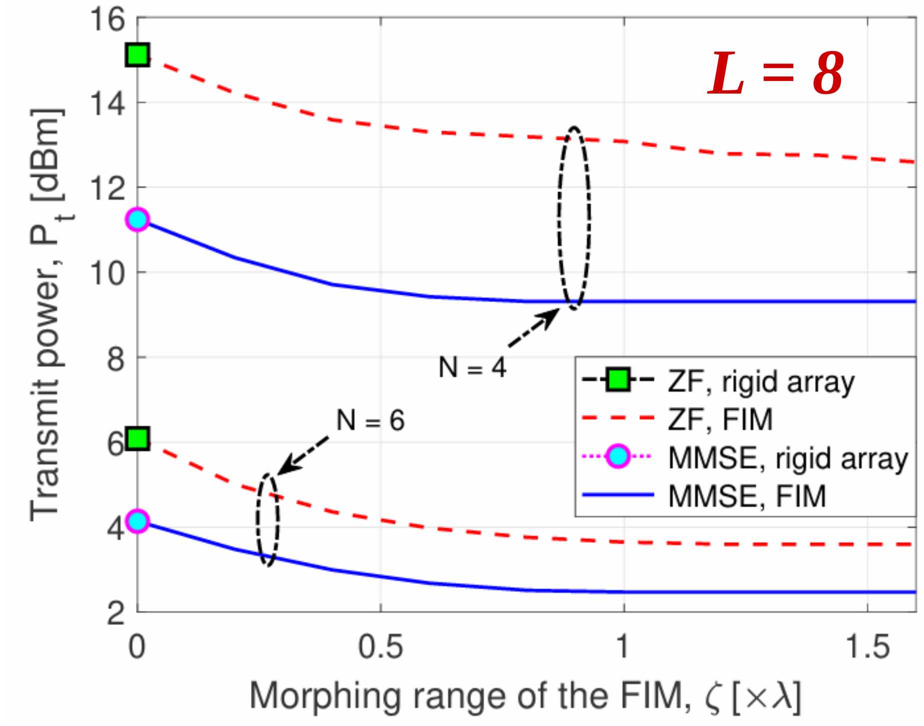

○ Power vs Number of Users

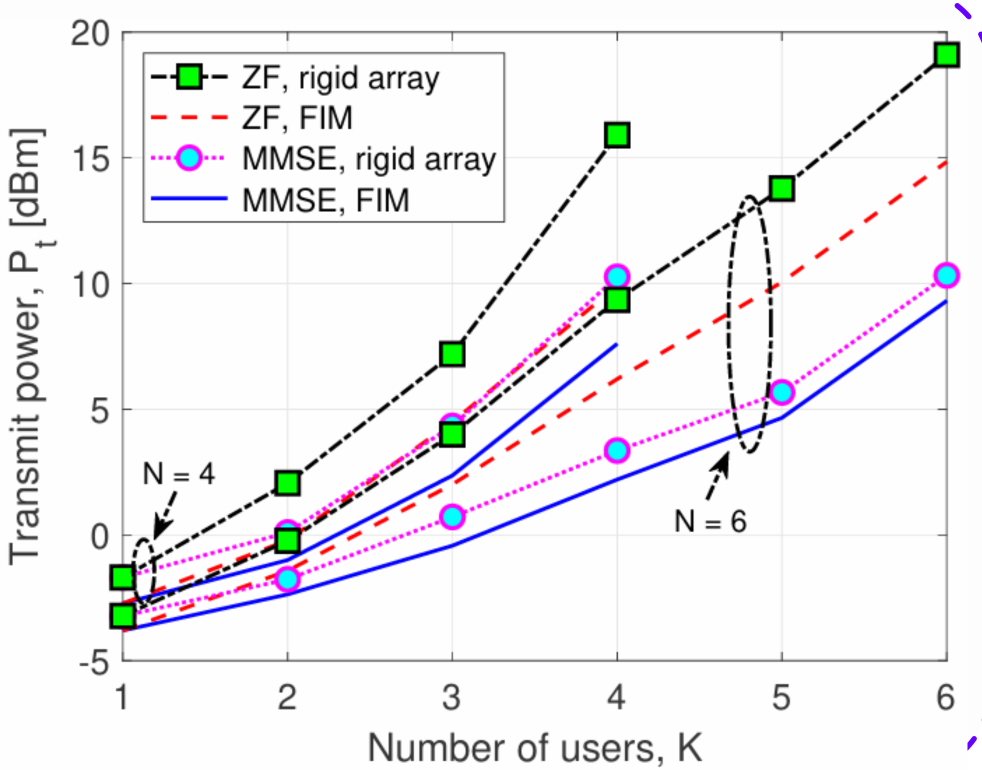

- ❑ As ζ increases, the FIM has more flexibility to adapt its surface shape, gradually reducing the transmit power.
- ❑ The FIM can adapt its surface shape for improving the channel orthogonality among the users as well as each user's channel quality.

J. An, C. Yuen, M. Di. Renzo, M. Debbah, H. V. Poor, and L. Hanzo, "Downlink multiuser communications relying on **flexible intelligent metasurfaces**," GLOBECOM, 2024.

J. An, C. Yuen, M. Di. Renzo, M. Debbah, H. V. Poor, and L. Hanzo, "**Flexible intelligent metasurfaces** for downlink multiuser MISO communications," *IEEE Trans. Wireless Commun.*, 2025

➢ Conclusions

- By morphing its surface shape, we have shown that **an FIM deployed at a BS is capable of significantly reducing the power consumption** in wireless networks, while maintaining the same QoS requirements.
- **For a single-user scenario, each FIM element should adapt its position to maximize the channel gain**. The optimal surface shape is determined by an efficient GSS approach.
- For multiuser scenarios, an efficient alternating optimization method has been customized for iteratively optimizing the FIM's surface shape and the transmit beamformer.
- The numerical results have quantified the performance improvement of using an FIM over conventional rigid 2D arrays. An FIM with a morphing range of one wavelength, which corresponds to10.8 mm at 28 GHz, **results in a power gain of at least 3 dB**.

J. An, C. Yuen, M. Di. Renzo, M. Debbah, H. V. Poor, and L. Hanzo, "Downlink multiuser communications relying on **flexible intelligent metasurfaces**," GLOBECOM, 2024.

J. An, C. Yuen, M. Di. Renzo, M. Debbah, H. V. Poor, and L. Hanzo, "**Flexible intelligent metasurfaces** for downlink multiuser MISO communications," *IEEE Trans. Wireless Commun.*, 2025

Outline

- Background
- Codebook Solution for RIS-Aided Wireless Systems
- SIM-Enabled Electromagnetic Domain Signal Processing
- FIM-Enhanced Wireless Communication and Sensing (Q3)
  - § Power Reduction
  - **§ MIMO Capacity Enhancement**
  - § Wireless Sensing
- Future Directions

➢ FIM-Aided Point-to-Point MIMO System Model

- ❑ An FIM is deployed at the transmitter and another one at the receiver
- ❑ Each radiating element can be positioned along the direction perpendicular to the surface

M: The number of transmitting antennas;

N: The number of receiving antennas;

L: The number of scattering clusters;

G: The number of paths in each cluster.

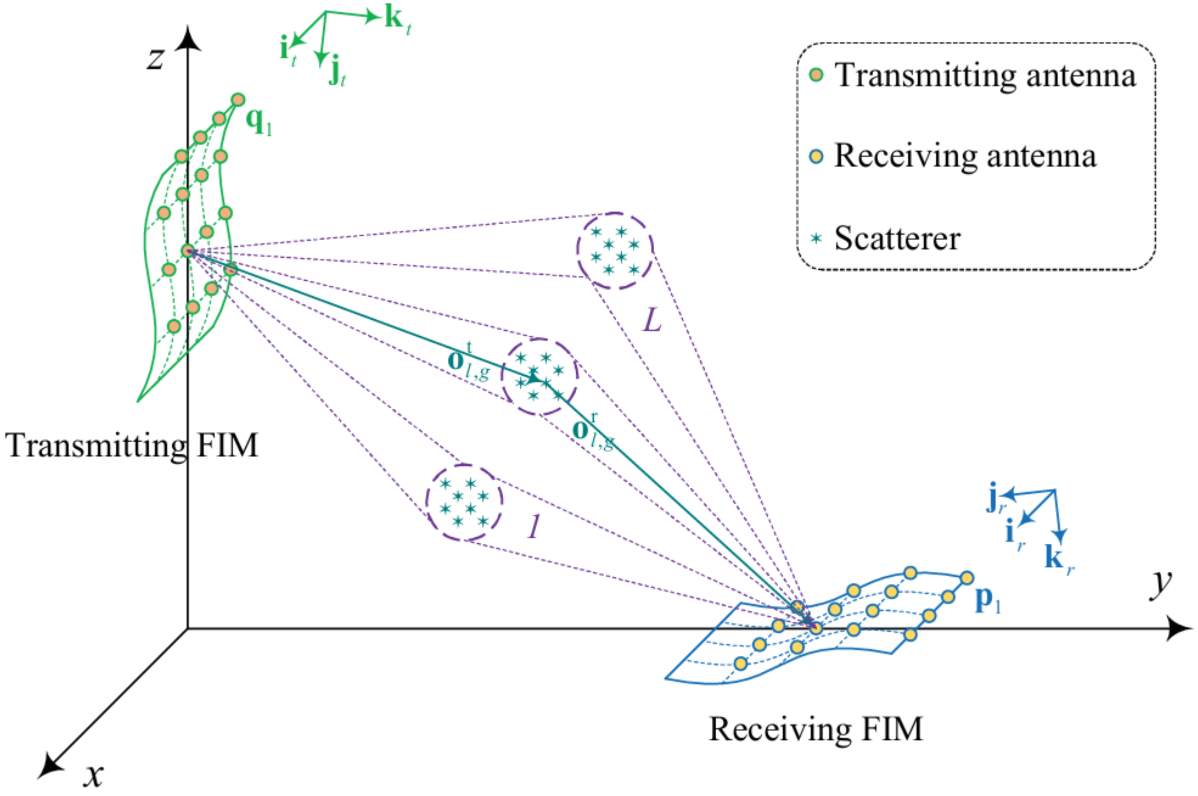

J. An, C. Yuen, M. Debbah and L. Hanzo, "**Flexible intelligent metasurfaces** for enhanced MIMO communications," *IEEE ICC*, 2025.

J. An, Z. Han, D. Niyato, M. Debbah, C. Yuen and L. Hanzo, "**Flexible intelligent metasurfaces** for enhancing MIMO communications," *IEEE Trans. Commun.*, 2025, Early Access.

➢ FIM-Aided Point-to-Point MIMO Channel Model

Channel gain

❑ FIM-aided MIMO channel: $\mathbf{H}(\zeta, \xi) = [\mathbf{A}_{\mathrm{r}} \odot \mathbf{F}_{\mathrm{r}}(\xi)]\, \varsigma\, [\mathbf{A}_{\mathrm{t}} \odot \mathbf{F}_{\mathrm{t}}(\zeta)]^{H}$

Receive array steering vectors of the unmorphed FIM

Extra response component caused by Tx-FIM shape morphing

Extra response component caused by Rx-FIM shape morphing

Transmit array steering vectors of the unmorphed FIM

J. An, C. Yuen, M. Debbah and L. Hanzo, "**Flexible intelligent metasurfaces** for enhanced MIMO communications," *IEEE ICC*, 2025.

J. An, Z. Han, D. Niyato, M. Debbah, C. Yuen and L. Hanzo, "**Flexible intelligent metasurfaces** for enhancing MIMO communications," *IEEE Trans. Commun.*, 2025, Early Access.

➢ Problem Formulation

- Maximize the MIMO channel capacity by jointly optimizing the **transmit covariance matrix** and the **surface shapes of the FIMs**.
- The optimization problem is formulated as

$$
\begin{aligned}
\max_{\mathbf{T},\boldsymbol{\zeta},\boldsymbol{\xi}} \quad & \log_2 \det\left(\mathbf{I}_N + \frac{1}{\sigma^2}\mathbf{H}(\boldsymbol{\zeta},\boldsymbol{\xi})\mathbf{T}\mathbf{H}^H(\boldsymbol{\zeta},\boldsymbol{\xi})\right) \\
\text{s.t.} \quad & \mathrm{tr}(\mathbf{T}) \le P_{\mathrm{t}}, \quad \mathbf{T} \succeq \mathbf{0}, \\
& \boldsymbol{\zeta} = [\zeta_1, \zeta_2, \ldots, \zeta_M]^T, \\
& \boldsymbol{\xi} = [\xi_1, \xi_2, \ldots, \xi_N]^T, \\
& -\tilde{\zeta} \le \zeta_m \le \tilde{\zeta}, \quad m = 1, \ldots, M, \\
& -\tilde{\xi} \le \xi_n \le \tilde{\xi}, \quad n = 1, \ldots, N,
\end{aligned}
$$

Transmit power constraint

Tx-FIM morphing range

Rx-FIM morphing range

➢ Challenges

- The non-concave objective function;
- The transmit covariance matrix and the FIMs' surface shapes are highly coupled.

J. An, C. Yuen, M. Debbah and L. Hanzo, "**Flexible intelligent metasurfaces** for enhanced MIMO communications," *IEEE ICC*, 2025.

J. An, Z. Han, D. Niyato, M. Debbah, C. Yuen and L. Hanzo, "**Flexible intelligent metasurfaces** for enhancing MIMO communications," *IEEE Trans. Commun.*, 2025, Early Access.

➢ Block Coordinate Descent (BCD) – Subproblem I

- ❑ Given the FIM surface-shape vectors, the original problem is reduced to transmit covariance matrix optimization in a conventional MIMO system.

Eigenmode transmission

$$\mathbf{T}^{o} = \mathbf{U}\mathbf{P}^{o}\mathbf{U}^{H}$$

Eigenvectors of $\mathbf{H}\left(\hat{\zeta},\ \hat{\xi}\right)$

Power allocation

Water-filling strategy

$$p_m^o = \max\left(\mu - \sigma^2/\lambda_m^2, 0\right), \quad m = 1, 2, \ldots, M,$$

$$\sum_{m=1}^{M} p_m^o = P_{\mathrm{t}}$$

J. An, C. Yuen, M. Debbah and L. Hanzo, "**Flexible intelligent metasurfaces** for enhanced MIMO communications," *IEEE ICC*, 2025.
J. An, Z. Han, D. Niyato, M. Debbah, C. Yuen and L. Hanzo, "**Flexible intelligent metasurfaces** for enhancing MIMO communications," *IEEE Trans. Commun.*, 2025, Early Access.

➢ Block Coordinate Descent (BCD) – Subproblem II

Given the transmit beamforming, the original problem is reduced to

$$\max_{\boldsymbol{\zeta},\ \boldsymbol{\xi}} \quad \log_2 \det\left(\mathbf{I}_N + \frac{1}{\sigma^2}\mathbf{H}(\boldsymbol{\zeta},\boldsymbol{\xi})\,\hat{\mathbf{T}}\mathbf{H}^H(\boldsymbol{\zeta},\boldsymbol{\xi})\right)$$

$$\text{s.t.} \quad (34c),\ (34d),\ (34e),\ (34f).$$

➢ Gradient Ascent Method

Calculate the gradient

$$\nabla_{\boldsymbol{\xi}} C = -\frac{2}{\ln 2}\mathrm{Diag}\left[\mathbf{B}_{\mathrm{r}}^{-1} \odot \Im\left(\mathbf{S}_{\mathrm{r}}\right)\right]$$

$$\nabla_{\boldsymbol{\zeta}} C = -\frac{2}{\ln 2}\mathrm{Diag}\left[\mathbf{B}_{\mathrm{t}}^{-1} \odot \Im\left(\mathbf{S}_{\mathrm{t}}\right)\right]$$

Update the surface shapes

$$\boldsymbol{\zeta} \leftarrow \boldsymbol{\zeta} + \epsilon\nabla_{\boldsymbol{\zeta}} C$$

$$\boldsymbol{\xi} \leftarrow \boldsymbol{\xi} + \epsilon\nabla_{\boldsymbol{\xi}} C$$

Scale the surface shapes

$$\zeta_m = \max\left(\min\left(\zeta_m, \tilde{\zeta}\right), -\tilde{\zeta}\right)$$

$$\xi_n = \max\left(\min\left(\xi_n, \tilde{\xi}\right), -\tilde{\xi}\right)$$

J. An, C. Yuen, M. Debbah and L. Hanzo, "**Flexible intelligent metasurfaces** for enhanced MIMO communications," *IEEE ICC*, 2025.

J. An, Z. Han, D. Niyato, M. Debbah, C. Yuen and L. Hanzo, "**Flexible intelligent metasurfaces** for enhancing MIMO communications," *IEEE Trans. Commun.*, 2025, Early Access.

➢ Simulation Setups

- Transmitter's location: (0 m, 0 m, 10 m)
- Receiver's location: (0 m, 100 m, 0 m)
- Frequency: 28 GHz
- Noise PSD: - 174 dBm/Hz
- Bandwidth: 100 MHz
- Four schemes:

RAA, WPA	FIM, WPA
RAA, EPA	FIM, EPA

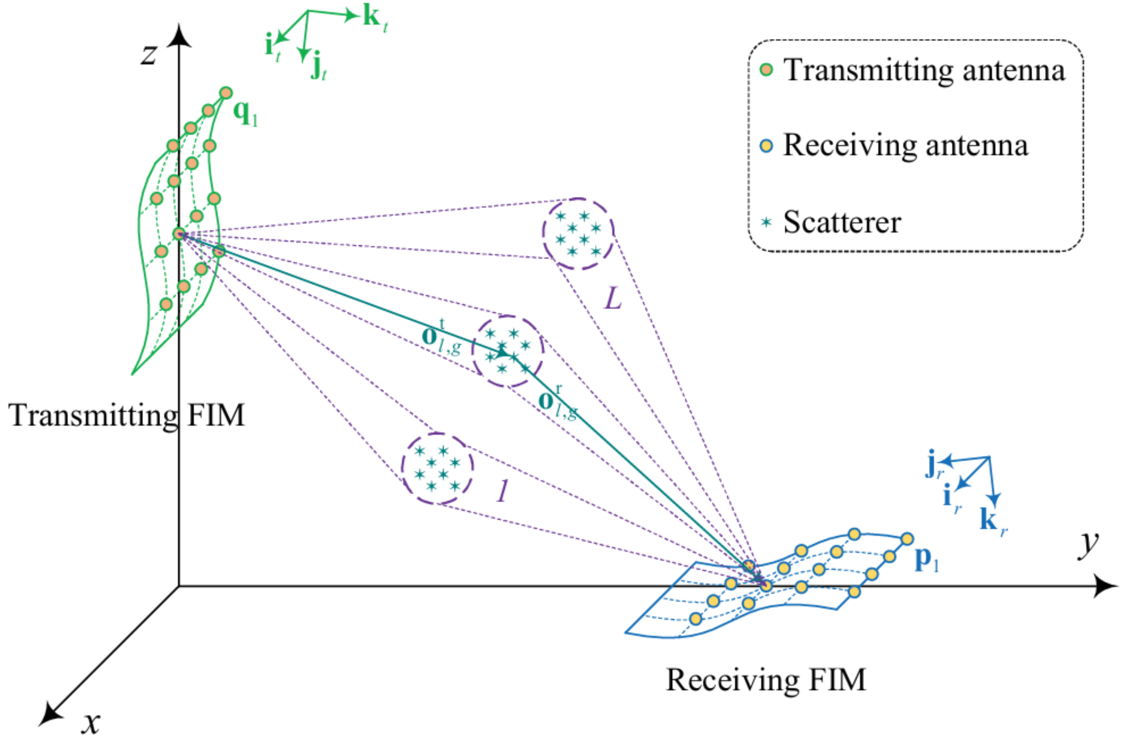

RAA: rigid antenna array; FIM: flexible intelligent metasurface

EPA: equal power allocation WPA: water-filling power allocation

J. An, C. Yuen, M. Debbah and L. Hanzo, "**Flexible intelligent metasurfaces** for enhanced MIMO communications," *IEEE ICC*, 2025.

J. An, Z. Han, D. Niyato, M. Debbah, C. Yuen and L. Hanzo, "**Flexible intelligent metasurfaces** for enhancing MIMO communications," *IEEE Trans. Commun.*, 2025, Early Access.

○ Capacity vs Number of Antennas

○ Capacity vs Number of Clusters

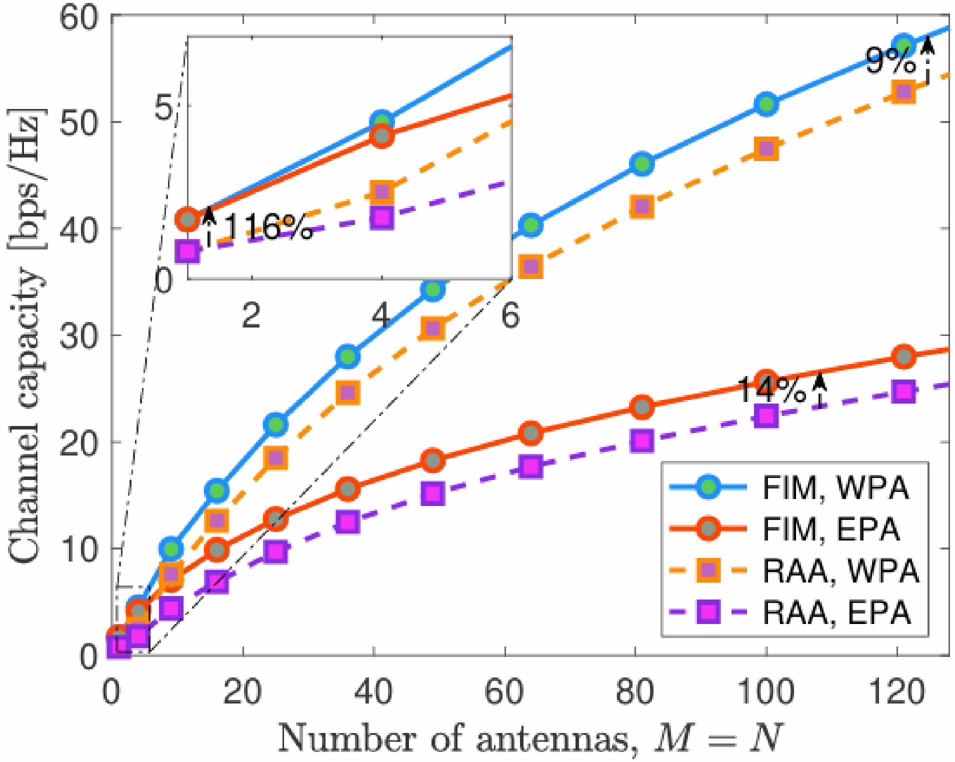

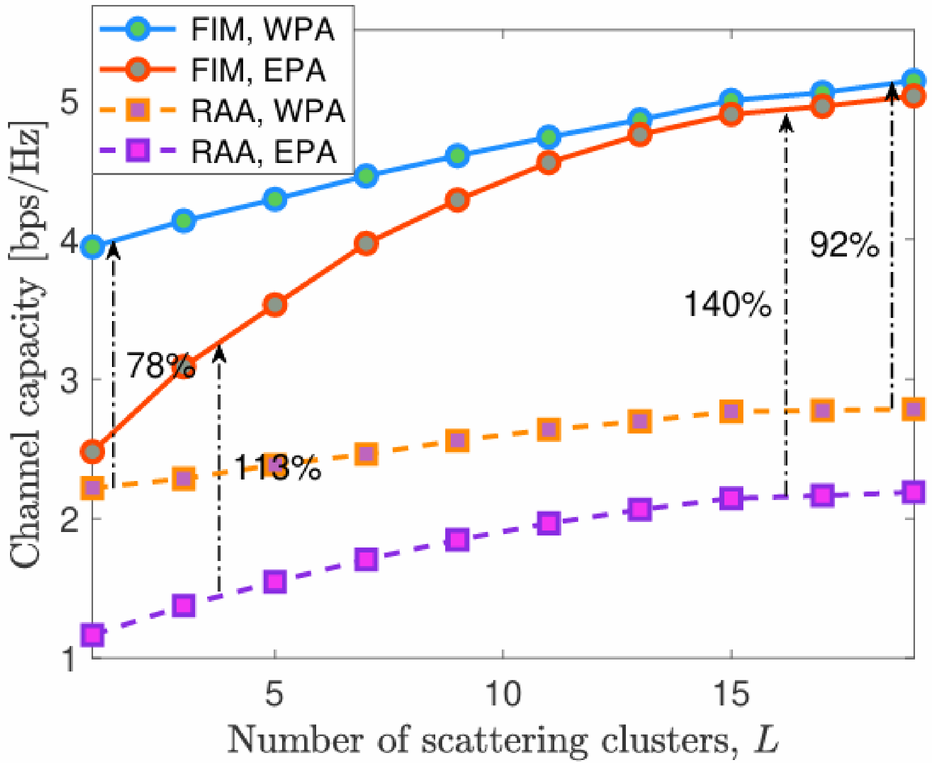

- ❑ FIMs consistently outperform the conventional benchmark schemes, with at least a 9% capacity improvement being observed.
- ❑ The performance gain becomes more significant as the number of clusters increases.

J. An, C. Yuen, M. Debbah and L. Hanzo, "**Flexible intelligent metasurfaces** for enhanced MIMO communications," *IEEE ICC*, 2025.

J. An, Z. Han, D. Niyato, M. Debbah, C. Yuen and L. Hanzo, "**Flexible intelligent metasurfaces** for enhancing MIMO communications," *IEEE Trans. Commun.*, 2025, Early Access.

○ Capacity vs morphing range

○ Capacity vs morphing range

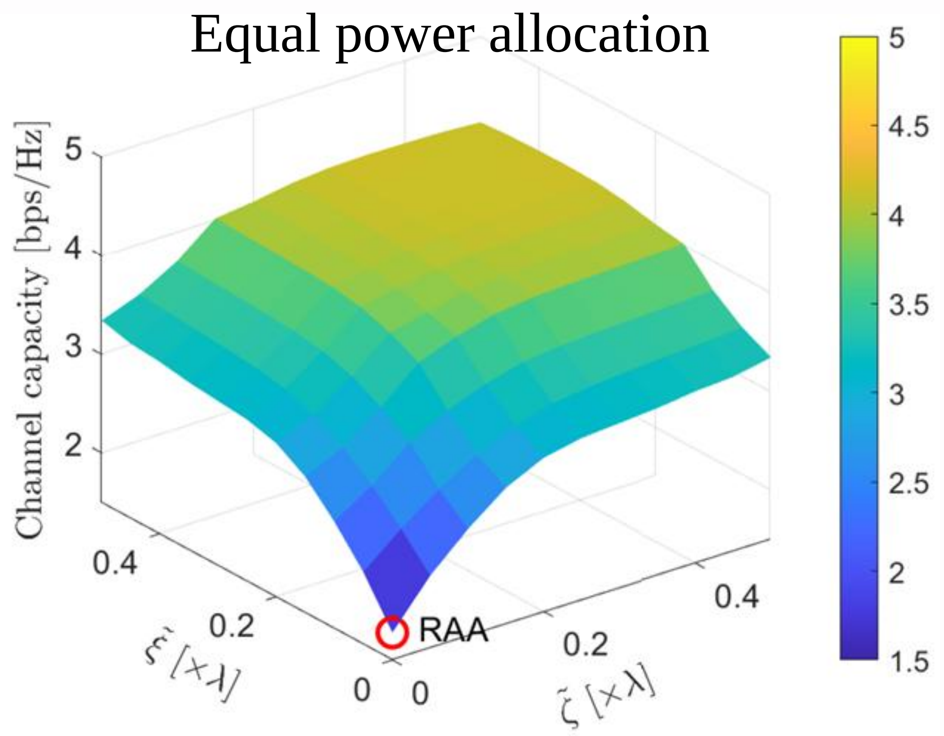

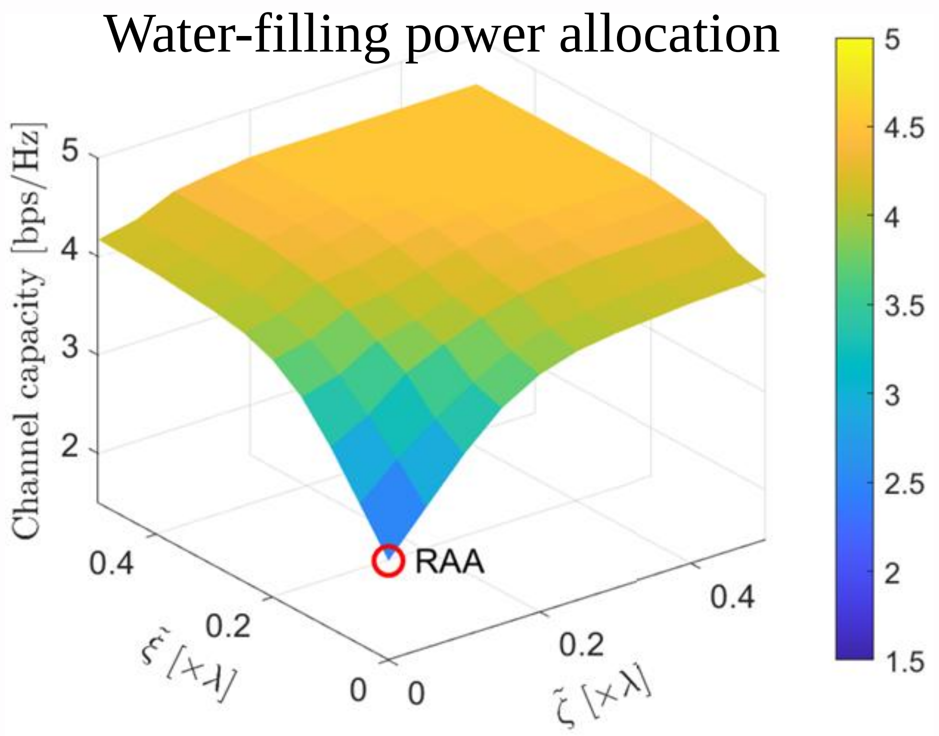

- ❑ As ξ and ζ increases, the transmitting and receiving FIMs have more flexibility to adapt their surface shapes, gradually increasing the channel capacity.
- ❑ Diminishing returns exist as the morphing range increases.

J. An, C. Yuen, M. Debbah and L. Hanzo, "**Flexible intelligent metasurfaces** for enhanced MIMO communications," *IEEE ICC*, 2025.

J. An, Z. Han, D. Niyato, M. Debbah, C. Yuen and L. Hanzo, "**Flexible intelligent metasurfaces** for enhancing MIMO communications," *IEEE Trans. Commun.*, 2025, Early Access.

○ Channel Gain under Different FIM Surface Shapes

FIM Surface Shapes
Morphing range: 0.1λ

FIM Surface Shapes
Morphing range: 0.5λ

Channel Gain

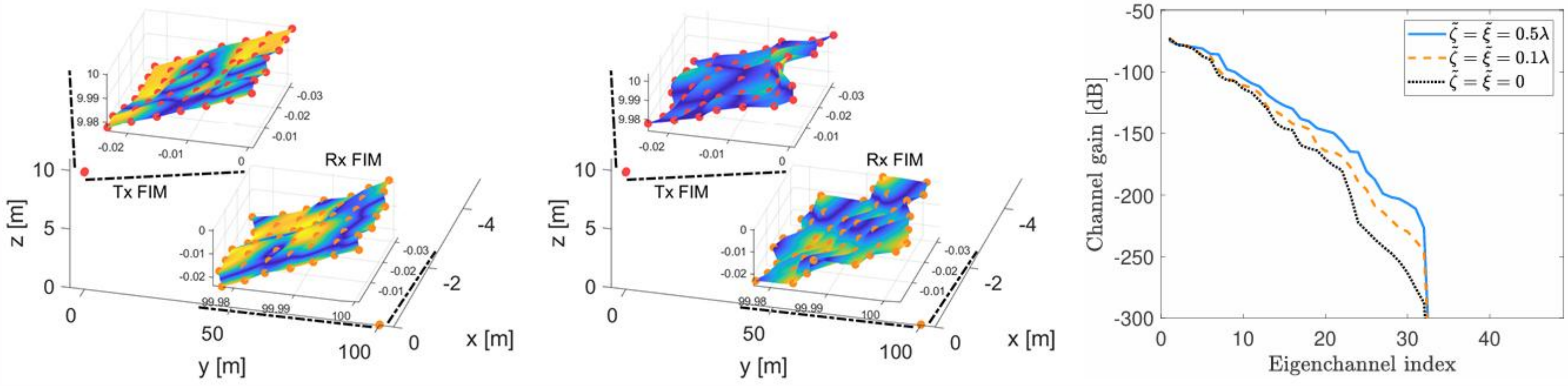

- ❑ When the maximum morphing range is 0.1λ, the gain of weak eigenchannels is improved by 40 dB.
- ❑ When the maximum morphing range increases to 0.5λ, the gain of weak eigenchannels is further improved by 20 dB.

J. An, C. Yuen, M. Debbah and L. Hanzo, "**Flexible intelligent metasurfaces** for enhanced MIMO communications," *IEEE ICC*, 2025.

J. An, Z. Han, D. Niyato, M. Debbah, C. Yuen and L. Hanzo, "**Flexible intelligent metasurfaces** for enhancing MIMO communications," *IEEE Trans. Commun.*, 2025, Early Access.

Conclusions

- By morphing their surface shapes, we have shown that **a pair of FIMs deployed at the transmitter and receiver are capable of significantly improving the MIMO channel capacity**.
- An efficient block coordinate descent method has been customized for iteratively optimizing the FIMs' surface shapes and the transmit covariance matrix.
- The numerical results have quantified the performance improvement of using FIMs over conventional rigid 2D arrays. Two FIMs with a morphing range of half wavelength, which corresponds to 5.4 mm at 28 GHz, **results in a capacity improvement of 70%**.

J. An, C. Yuen, M. Debbah and L. Hanzo, "**Flexible intelligent metasurfaces** for enhanced MIMO communications," *IEEE ICC*, 2025.

J. An, Z. Han, D. Niyato, M. Debbah, C. Yuen and L. Hanzo, "**Flexible intelligent metasurfaces** for enhancing MIMO communications," *IEEE Trans. Commun.*, 2025, Early Access.

Outline

- Background
- Codebook Solution for RIS-Aided Wireless Systems
- SIM-Enabled Electromagnetic Domain Signal Processing
- FIM-Enhanced Wireless Communication and Sensing (Q3)
    - Power Reduction
    - MIMO Capacity Enhancement
    - **Wireless Sensing**
- Future Directions

➢ Wireless Sensing

❑ FIM-aided Wireless Sensing

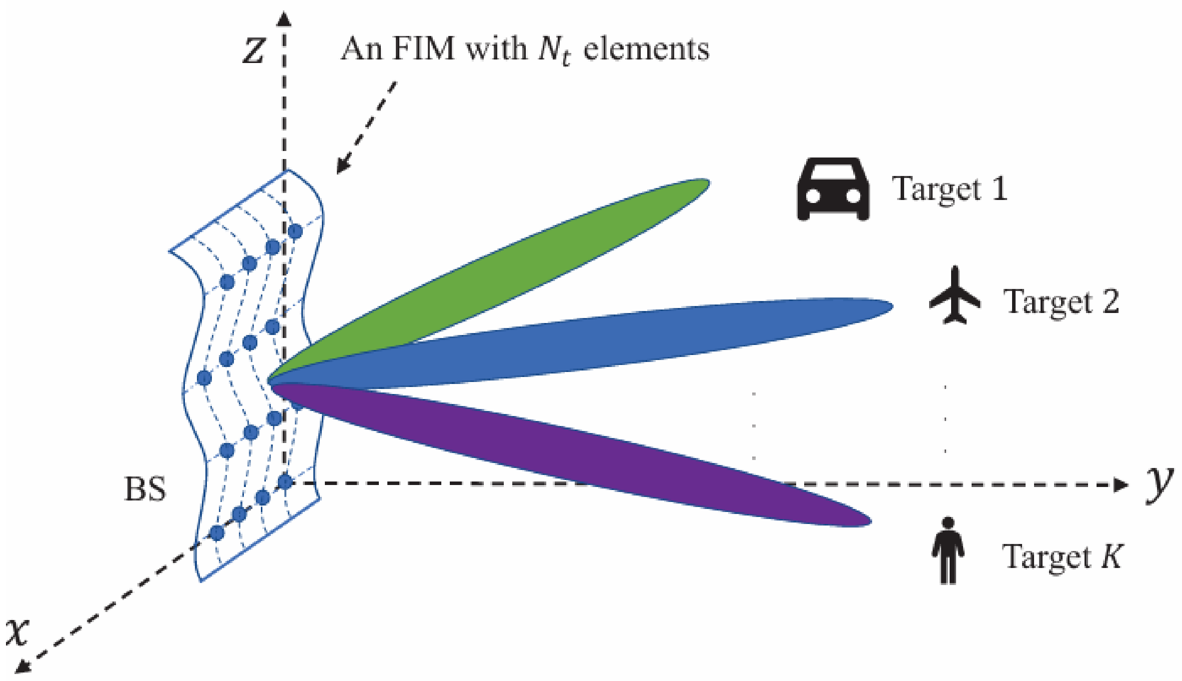

Conventional Rigid Array

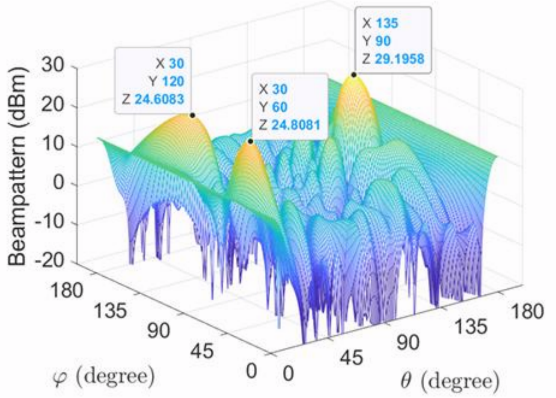

FIM

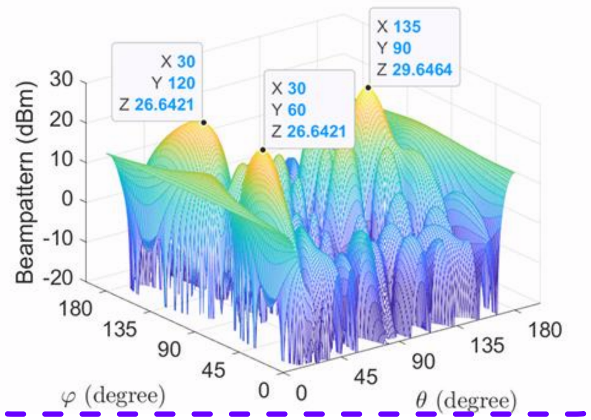

Z. Teng, J. An, L. Gan, N. Al-Dhahir, and Z. Han, "**Flexible Intelligent Metasurface** for Enhancing Multi-Target Wireless Sensing," *IEEE Trans. Veh. Technol.*, Under Review.

Outline

- Background
- Codebook Solution for RIS-Aided Wireless Systems
- SIM-Enabled Electromagnetic Domain Signal Processing
- FIM-Enhanced Wireless Communication and Sensing
- **Future Directions**

➢ Future Research Opportunities

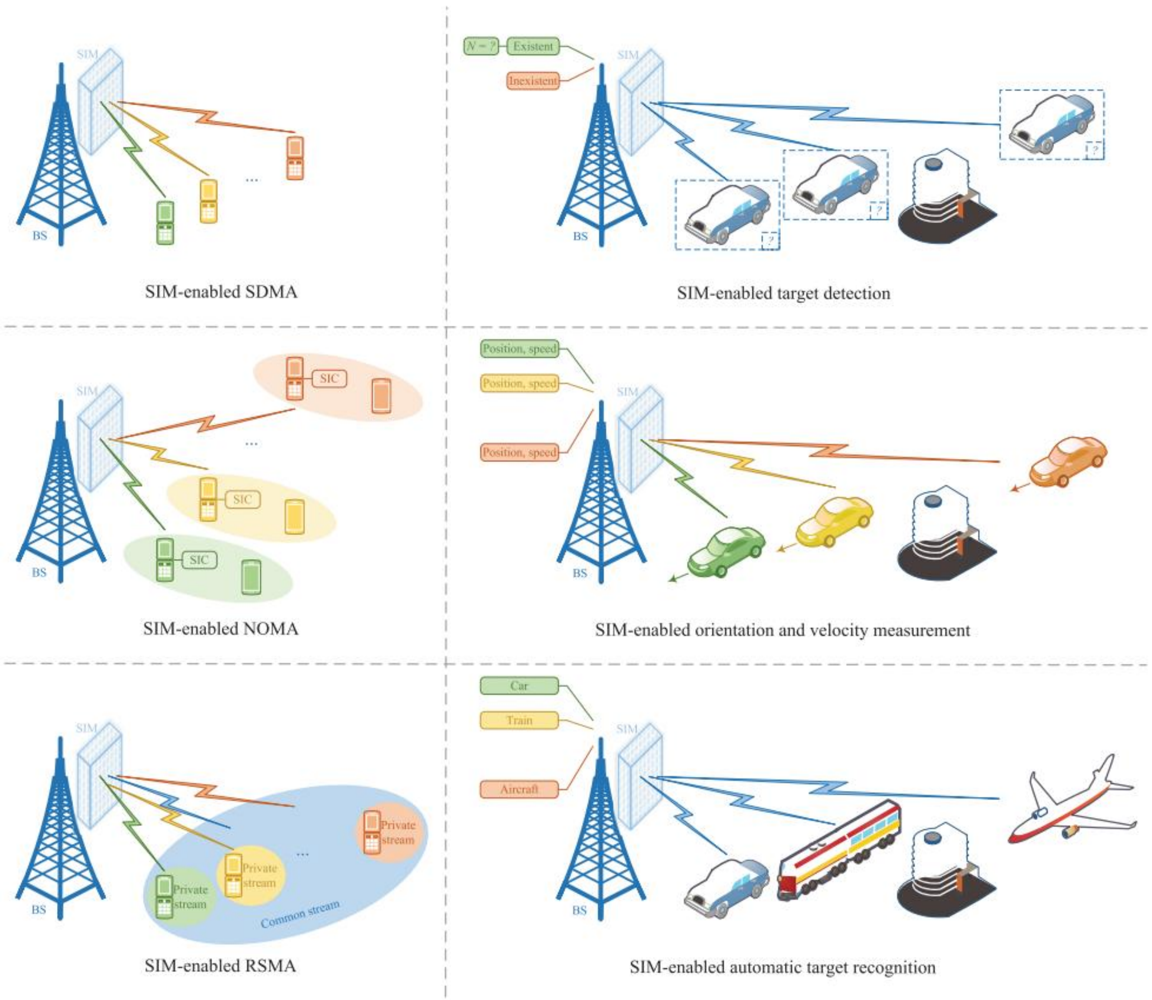

Wireless Communication

- ❑ NOMA/RSMA
- ❑ OFDM/OTFS
- ❑ CoMP/Cell-free networks
- ❑ Near-field communications/Holographic MIMO

Wireless Sensing

- ❑ Target detection
- ❑ Parameter estimation
- ❑ Target recognition
- ❑ Integrated sensing and communications

J. An, C. Yuen, C. Xu, H. Li, D. W. K. Ng, M. Di Renzo, M. Debbah, and L. Hanzo, "**Stacked intelligent metasurface**-aided MIMO transceiver design," *IEEE Wireless Commun.*, vol. 31, no. 4, pp. 123-131, Aug. 2024. (**Highly Cited Paper**)

➢ The Trend of Intelligent Metasurfaces

Q1: Codebook

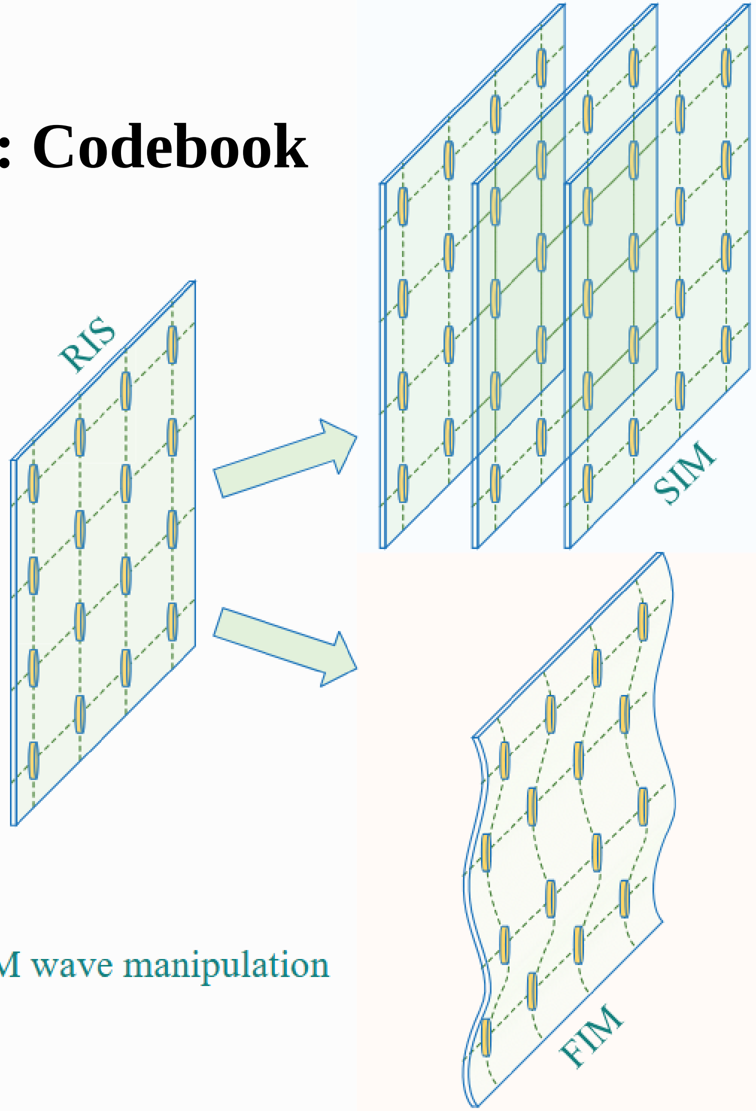

- EM wave manipulation

Q2: SIM

- Stacked Intelligent Metasurface
- Enhanced EM wave tunability
- Diffractive neural network

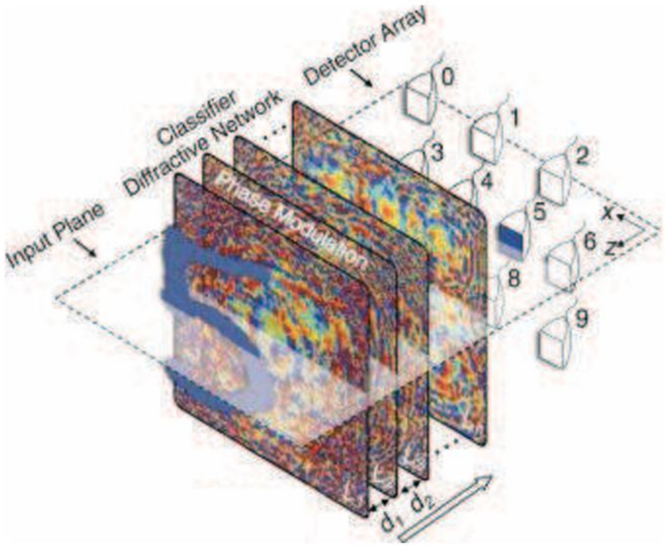

Q3: FIM

- Flexible Intelligent Metasurface
- Conformal deployment
- Surface-shape morphing capability

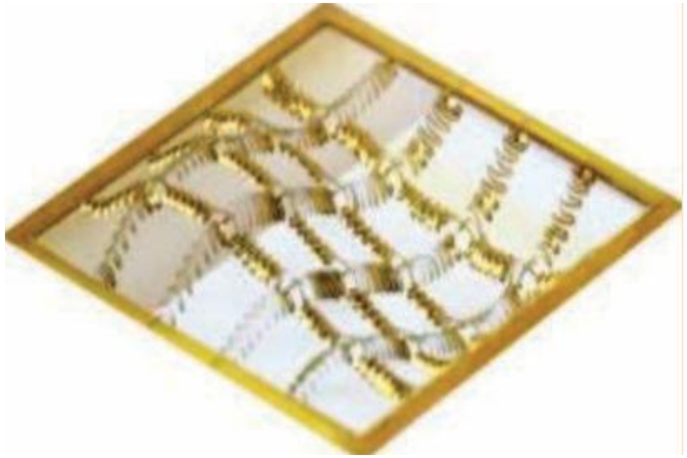

J. An, M. Debbah, T. J. Cui, Z. N. Chen, and C. Yuen, "**Emerging Technologies in Intelligent Metasurfaces: Shaping the Future of Wireless Communications**," *IEEE Trans. Antenna Propag.*, 2025 (***Invited Paper***)

Information

- Code: https://jiancheng-an.github.io/

References

[R1] J. An, C. Xu, Q. Wu, D. W. K. Ng, M. Di Renzo, C. Yuen, and L. Hanzo, “Codebook-Based Solutions for Reconfigurable Intelligent Surfaces and Their Open Challenges,” *IEEE Wireless Commun.*, vol. 31, no. 2, pp. 134-141, April 2024. (**Highly Cited Paper**)

[R2] J. An, et al., “Low-complexity channel estimation and passive beamforming for RIS-assisted MIMO systems relying on discrete phase shifts,” *IEEE Trans. Commun.*, vol. 70, no. 2, pp. 1245-1260, Feb. 2022. (**Highly Cited Paper**)

[R3] Z. Yu, J. An, E. Basar, L. Gan and C. Yuen, “Environment-Aware Codebook Design for RIS-Assisted MU-MISO Communications: Implementation and Performance Analysis,” *IEEE Trans. Commun.*, vol. 72, no. 12, pp. 7466-7479, Dec. 2024.

[R4] Z. Yu, J. An, L. Gan, H. Li and S. Chatzinotas, “Weighted Codebook Scheme for RIS-Assisted Point-to-Point MIMO Communications,” *IEEE Wireless Commun. Lett.*, vol. 14, no. 5, pp. 1571-1575, May 2025.

[R5] **J. An** et al., “**Stacked intelligent metasurfaces** for efficient holographic MIMO communications in 6G,” IEEE J. Sel. Areas Commun., vol. 41, no. 8, pp. 2380–2396, Aug. 2023. (**Highly Cited Paper**)

[R6] **J. An**, M. Di Renzo, M. Debbah, and C. Yuen, “**Stacked intelligent metasurfaces** for multiuser beamforming in the wave domain,” Proc. IEEE Int. Conf. Commun. (ICC), Rome, Italy, May 2023, pp. 2834 – 2839. **(ICC 2023 Best Paper Award)**

[R7] **J. An**, M. Di Renzo, M. Debbah, H. V. Poor, and C. Yuen. “**Stacked intelligent metasurfaces** for multiuser downlink beamforming in the wave domain,” *IEEE Trans. Wireless. Commun.*, 2025, Early Access.

[R8] **J. An**, C. Yuen, C. Xu, H. Li, D. W. K. Ng, M. Di Renzo, M. Debbah, and L. Hanzo, “**Stacked intelligent metasurface**-aided MIMO transceiver design,” *IEEE Wireless Commun.*, vol. 31, no. 4, pp. 123-131, Aug. 2024. (**Highly Cited Paper**)

[R9] **J. An**, C. Yuen, Y. Guan, M. Di Renzo, M. Debbah, H. V. Poor, and L. Hanzo, “Two-dimensional direction-of-arrival estimation using **stacked intelligent metasurfaces**,” *IEEE J. Sel. Areas Commun.*, vol. 42, no. 10, pp. 2786-2802, Oct. 2024.

[R10] G. Huang, **J. An**, Z. Yang, L. Gan, M. Bennis and M. Debbah, “**Stacked intelligent metasurfaces** for task-oriented semantic communications,” *IEEE Wireless Commun. Lett.*, vol. 14, no. 2, pp. 310-314, Feb. 2025.

References

[R11] J. An, M. Debbah, T. J. Cui, Z. N. Chen, and C. Yuen, "**Emerging Technologies in Intelligent Metasurfaces: Shaping the Future of Wireless Communications**," *IEEE Trans. Antenna Propag.*, 2025 (***Invited Paper***)

[R12] J. An, C. Yuen, M. Di. Renzo, M. Debbah, H. V. Poor, and L. Hanzo, "Downlink multiuser communications relying on **flexible intelligent metasurfaces**," GLOBECOM, 2024.

[R13] J. An, C. Yuen, M. Di. Renzo, M. Debbah, H. V. Poor, and L. Hanzo, "**Flexible intelligent metasurfaces** for downlink multiuser MISO communications," *IEEE Trans. Wireless Commun.*, 2025

[R15] J. An, C. Yuen, M. Debbah and L. Hanzo, "**Flexible intelligent metasurfaces** for enhanced MIMO communications," *IEEE ICC*, 2025.

[R16] J. An, Z. Han, D. Niyato, M. Debbah, C. Yuen and L. Hanzo, "**Flexible intelligent metasurfaces** for enhancing MIMO communications," *IEEE Trans. Commun.*, 2025, Early Access.

[R17] Z. Teng, J. An, L. Gan, N. Al-Dhahir, and Z. Han, "**Flexible Intelligent Metasurface** for Enhancing Multi-Target Wireless Sensing," *IEEE Trans. Veh. Technol.*, Under Review.

Many thanks!

Q & A